

MSc thesis in Civil Engineering

Single Reservoir Pumped Hydro Storage with Seawater: A Big Battery for Big Problems

Widana Bayu Nugraha
2023



Thesis Report

Single Reservoir Pumped Hydro Storage with Seawater: A Big Battery for Big Problems

by

Widana Bayu Nugraha

to obtain the degree of Master of Science
at the Delft University of Technology

Student number: 5377854

Thesis committee: dr. ir. Maurits Ertsen, TU Delft, supervisor
dr. ir. Olivier Hoes, TU Delft, supervisor
dr. ir. Juan Aguilar-Lopez, TU Delft, supervisor

An electronic version of this thesis is available at <http://repository.tudelft.nl/>.



Preface

I stand at the culmination of an extraordinary journey – the completion of my thesis – and I write these words with a profound sense of gratitude. Without the unwavering support, encouragement, and understanding of those who have been my pillars of fortitude, this journey would not have been possible.

First and foremost, I would like to express my deepest gratitude to my family, who have always been there for me, believing in me, and encouraging me throughout the various chapters of my academic endeavour. Thank you for your understanding and patience throughout this journey. To my wife, whose love and support have been my constant motivation, and to my daughter, who brings me unbounded pleasure every day. To my parents for their unwavering support, my elder brother for the inspiration, and my younger sister for her steadfast support.

I would like to acknowledge the invaluable guidance, wisdom, and support provided by my graduation committee. Dr. ir. Maurits Ertsen, your perceptive feedback, valuable counsel, and dedicated time to this endeavour have been fundamental in shaping this research. Dr. ir. Olivier Hoes, I extend my profound gratitude to you for your unwavering guidance and insightful feedback that has motivated me to finish my research. Dr. ir. Juan Aguilar-Lopez, your deep insights and expertise in hydropower have significantly enriched my understanding.

I would also like to thank my classmates and Indonesian peers, who have provided me with companionship and support throughout this journey.

I am grateful to everyone who has contributed to my academic journey through a deed, a word of encouragement, or a shared experience. Due to these combined efforts and unwavering support, I have reached this educational milestone in my voyage.

*With heartfelt gratitude,
Widana Bayu Nugraha
Delft, November 2023*

Abstract

Indonesia faces the challenge of attaining renewable energy goals and reducing carbon emissions by 29% by 2030. Despite a renewable energy goal of 23% of the national energy mix by 2025, only 14% of electricity production is projected to be generated from renewable sources by 2023. Accelerated deployment of renewable energy solutions is required to achieve these goals.

Indonesia has abundant renewable energy sources, such as hydropower, solar, and wind. Yet, a challenge arises from the difference between the electricity demand and supply patterns of these sources, which do not match throughout the day. Fluctuating energy supply patterns and variable energy demand necessitate using efficient Energy Storage Systems (ESS) to bridge the gap.

With its extensive coastline, Indonesia can potentially explore single reservoir Seawater Pumped Hydro Storage (SPHS), a variant of Pumped Hydro Energy Storage (PHES), as an alternative to solve these challenges. Similar to an enormous rechargeable battery, the reservoir in an SPHS system functions as an energy storage system. The system works by pumping up the seawater to the reservoir to store surplus energy during periods of ample supply and discharging it to generate electricity through a hydropower plant during periods of high electricity demand. This research aims to identify the ideal locations for SPHS systems in coastal areas of Indonesia. A Python GIS algorithm was developed to automate the selection process. The identified SPHS sites are then evaluated economically to ascertain their viability. The study concludes by comparing the carbon reduction potential of these systems to Indonesia's carbon emission reduction goals.

The research reveals 609 potential SPHS sites across Indonesia, with a total peak power that can be regenerated of technically potential sites of 29 Gigawatt-peak (GWp). Among these, 297 locations are deemed economically feasible, contributing a potential peak power that can be regenerated of 15 GWp. The peak electricity demand in Indonesia is approximately 44 GW, typically occurring at 8 p.m. The technical potential of SPHS promises an 11% reduction in carbon emissions from the energy sector, while the economically feasible sites could achieve a 6% reduction in carbon emissions projected in 2030.

Keywords: Seawater Pumped Hydro Storage (SPHS), renewable energy, Indonesia, QGIS, Energy Storage Systems (ESS).

Contents

Preface	i
Summary	ii
Acronyms	ix
1 Introduction	1
1.1 Background	1
1.2 Introduction to Pumped Hydro Energy Storage (PHES)	2
1.3 Problem Definition	3
1.4 Research Objectives	4
1.5 Relevance	4
1.6 Report Outline	4
2 State of The Art	6
2.1 Indonesia Energy Demand	6
2.2 Indonesia Energy Sources	8
2.3 Potential of Renewable Energy Sources in Indonesia	8
2.4 Necessity of Energy Storage Systems (ESS) for Supporting Renewable Energy Sources	10
2.5 Pumped Hydro Energy Storage	11
2.6 Seawater PHES	14
2.7 Pumped Hydro Storage in Indonesia	15
3 Methodology	17
3.1 Data and Software	17
3.1.1 Digital Elevation Model (DEM)	17
3.1.2 GIS Software	18
3.1.3 Tools and Features	19
3.2 Identification of Potential SPHS Sites	19
3.2.1 GIS-based Model (DEM Analysis)	20
3.2.2 Hydropower Calculation	25
3.2.3 Distance from The Electricity Grid	29
3.2.4 Penstock Line Topography	29
3.2.5 Levelised Cost of Storage (LCOS)	29
3.3 Carbon Emission Reduction Calculation	32

4	Site Rank and Classification Criteria	33
4.1	Selection Criteria	33
4.2	Ranking The Feasible Sites	34
4.3	Classification	35
5	Technical and Economical Potential of Seawater Pumped Hydro Storage	36
5.1	Technical Potential	36
5.1.1	SPHS Potential on National and Grid System Level	37
5.1.2	Classification of The Potential SPHS Sites	39
5.2	Economical Potential	46
5.2.1	Levelised Cost of Storage (LCOS)	46
5.2.2	Economical Feasibility	49
5.2.3	Comparison with Other Energy Storage System	51
5.2.4	Sensitivity Analysis	52
6	Environmental Impact	54
6.1	Carbon Emission Reduction	54
6.2	Local Environment Impact	57
7	Conclusion and Recommendations	59
7.1	Conclusion	59
7.2	Limitations of The Research	60
7.3	Recommendations	61
	References	62
A	SPHS Sites Properties	69
B	SPHS Classification	76
C	Preprocessing Python Script	84
D	Main Processing Python Script	92

List of Figures

1.1	Schematic of Pumped Hydro Energy Storage (PHES) [10].	2
1.2	Okinawa seawater-pumped hydro storage [13].	3
2.1	Evolution of Indonesian daily load curve between 2010 and 2030 [18].	7
2.2	Electricity demand projection [21].	7
2.3	Power plant installed capacity and generation projection [1] [2].	8
2.4	Comparison between renewable energy potential and installed capacity.	9
2.5	Illustration of energy storage systems according to their storage capacity and discharge duration within power system utilisation [36].	11
2.6	Components of pumped hydro energy storage [15].	12
2.7	Pumped-back pumped hydro energy storage [44].	13
2.8	Open loop pumped hydro energy storage [45].	14
2.9	Closed loop pumped hydro energy storage [46].	14
2.10	SPHS system in Ludington, Michigan [49].	15
3.1	Satellite view vs. DEMNAS.	18
3.2	The methodology flow chart of the research.	20
3.3	Preprocessing flowchart.	22
3.4	3D Visualization of identified SPHS site: algorithm-generated potential location for SPHS	23
3.5	Longitudinal (a) and cross-sectional (b) profile of the reservoir.	24
3.6	Main processing flowchart.	25
3.7	Daily electricity demand pattern vs solar energy availability [18] [52]	26
3.8	Daily SPHS generation phase pattern.	26
3.9	Indonesia’s electric transmission lines map [55]	29
5.1	Distribution of 609 identified SPHS sites in Indonesia.	37
5.2	Distribution of SPHS sites per peak power classification.	38
5.3	Electricity demand and SPHS power production per electrical grid.	39
5.4	Example of the SPHS sites	40
5.5	Distribution of class 1 SPHS sites.	41
5.6	Distribution of class 2 SPHS sites.	41
5.7	Distribution of class 3 SPHS sites.	42
5.8	Distribution of class 4 SPHS sites.	42

5.9	Distribution of class 5 SPHS sites.	43
5.10	Distribution of class 6 SPHS sites.	43
5.11	Distribution of class 7 SPHS sites.	44
5.12	Distribution of class 8 SPHS sites.	44
5.13	Distribution of class 9 SPHS sites.	45
5.14	Distribution of class 10 SPHS sites.	45
5.15	LCOS statistics.	47
5.16	Distribution of LCOS per region.	47
5.17	Average investment per site.	48
5.18	Map of SHPS' LCOS.	49
5.19	Economically feasible location of SPHS in Indonesia.	50
5.20	Comparison between technical and economical potential	51
5.21	Sensitivity analysis of LCOS	52
5.22	Sensitivity analysis of potential sites	52
6.1	Carbon emission of various electricity generation	54
6.2	The reduction of carbon emission production per year based on the SHPS technical potential in every electrical grid.	56
6.3	The reduction of carbon emission production per year based on the SHPS economical potential in every electrical grid.	56
6.4	Example of geomembrane installation in a reservoir [72]	58

List of Tables

- 4.1 Weights of selected criteria for the TOPSIS analysis 33
- 4.2 Classification criteria 35

- 5.1 Comparison of annual energy and daily peak power between demand and SPHS 38
- 5.2 SPHS peak power production on each electrical grid system per class 40
- 5.3 Power and energy provided by identified SPHS systems 46
- 5.4 Comparison between electricity ceiling price and total LCOE/LCOS per region 50
- 5.5 Comparison of LCOS Values - This Study vs. Previous Studies 51

- 6.1 Carbon reduction per year 55

Acronyms

AHP Analytic Hierarchy Process 33, 34, 39

BIG Badan Informasi Geospasial 18, 19

CAPEX Capital Expenditure 19, 29, 30, 32, 46, 52, 53, 61

DEM Digital Elevation Model 4, 17, 19, 21, 23, 60

DEMNAS DEM Nasional 18, 60

ESS Energy storage systems 10, 12

GIS Geographic Information System 4, 17–19

GRP Glass Reinforced Plastic 27, 58

GW Gigawatt 6, 9, 10

GWp Gigawatt-peak 38, 49, 51, 52, 59, 60

kWh kilowatt-hours 8, 29, 46, 49, 52, 60

LCOE Levelised Cost of Electricity 46, 49, 50, 60

LCOS Levelised Cost of Storage 19, 29, 30, 33, 36, 46–53, 60, 61

MW Megawatt 9, 15, 19, 28, 37

MWh Megawatt-hours 7, 24

MWp Megawatt-peak 3, 25, 37, 39, 60

OPEX Operational Expenditure 19, 29, 30, 32, 46, 52, 53, 61

PHES Pumped Hydro Energy Storage 1, 2, 4, 11–16, 27, 29, 30, 34, 35, 51

PyQGIS Python QGIS 22, 24, 59

QGIS Quantum Geographic Information System 4, 17–19, 29

SPHS Seawater-Pumped Hydro Storage 2–5, 14, 15, 17–25, 27–30, 32–40, 45–61

TOPSIS Technique for Order of Preference by Similarity to Ideal Solution 33–35, 39, 40

TWh Terawatt-hours 7, 38, 55, 60

Introduction

1.1. Background

The growing recognition of climate change and the global commitment to reduce greenhouse gas emissions have increased the emphasis on transitioning towards renewable energy sources. As a rapidly developing nation with a significant reliance on fossil fuels for its energy needs, Indonesia faces the challenge of mitigating its carbon footprint while ensuring a sustainable energy supply to meet the demands of its expanding population and growing economy [1]. The motivation behind developing renewable energy solutions in Indonesia lies in saving the planet, addressing environmental concerns, achieving energy security, and fostering economic growth in a socially responsible manner.

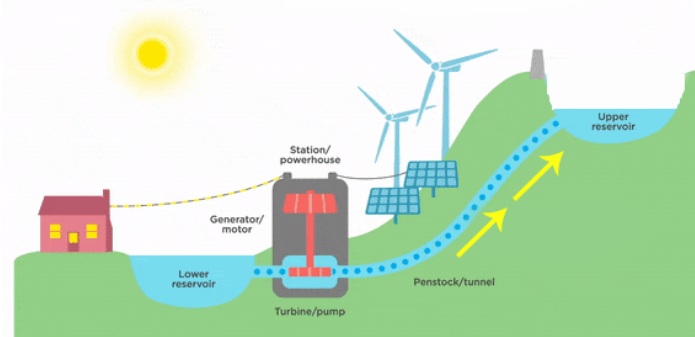
As an effort to answer the climate issue, Indonesia has a renewable energy target of 23% of the national energy mix by 2025. This policy, combined with Indonesia’s commitment to reduce carbon emissions by 29% by 2030, is a clear move towards a cleaner energy system and sustainability [1]. However, only 14% of electricity production in Indonesia generated from renewable energy projected in 2023 [2]. So far, Indonesia’s energy plan has prioritised the use of domestic coal to satisfy its needs [3], with a longer-term transition away from this resource [4].

Hydropower plants, a grid-connected solution to the need for clean energy sources, have been adopted in Indonesia to generate electricity. However, the system has high seasonal variability due to the supply of water discharge [5]. Hydropower plants need large reservoirs to reduce this limitation, resulting in significant investment costs and lengthy construction times [6]. Solar and wind are two other clean energy alternatives. Yet, solar and wind energy are daily intermittent renewable energy sources, which means their availability varies over a short period [7].

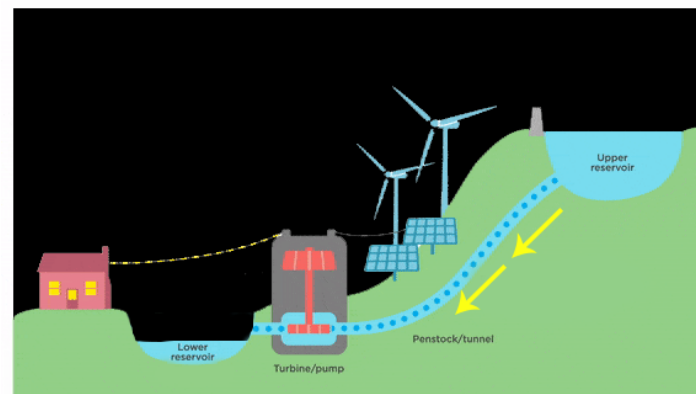
As a result, an energy storage system, such as a battery or a Pumped Hydro Energy Storage (PHES) system, becomes an excellent addition to a system in which variable sources account for a significant source supply energy portion of the energy system. This system facilitates flexibility by keeping operations to an optimum output. When the system’s electricity production exceeds the required demand, energy is stored; when demand exceeds production, stored energy is discharged to generate the power. Appropriate storage implementation of wind and solar power allows consistent energy output and increases flexibility.

1.2. Introduction to Pumped Hydro Energy Storage (PHES)

PHES operates on the principle of storing excess energy for later use, similar to other energy storage systems like batteries. It stores surplus energy during periods of low demand and releases it when electricity is required. PHES works by pumping water from a lower reservoir to an upper reservoir when excess electricity is available and releasing it by flowing downhill to generate power when needed for storing energy to maintain stability [8]. PHES is recognised as a technique for storing energy, maintaining the stability of power grids and controlling periods of high energy use [9]. PHES is often combined with intermittent energy sources like solar power to store excess electricity. During periods characterised by an overabundance of energy generation, for instance, occurring during off-peak hours and sunny periods, surplus electricity facilitates water transfer from a lower reservoir to an upper reservoir. This action increases the potential energy of the water, storing the electrical energy in the form of gravitational potential. Figure 1.1 shows the schematic of PHES.



(a) Pumping phase.



(b) Generation phase.

Figure 1.1: Schematic of Pumped Hydro Energy Storage (PHES) [10].

Seawater-Pumped Hydro Storage (SPHS)

Technically, Seawater-Pumped Hydro Storage (SPHS) resembles common PHES, which uses reversible pump turbine units to facilitate energy conversion. The system utilises seawater as the working fluid and eliminates the need for a lower artificial reservoir, using the ocean as the substitute, which is the primary distinction to the common PHES. To minimise head losses and reduce overall investment costs, SPHS facilities must be located close to the coast. Coastal topography, elevation differences, and distance

from the coastline are crucial factors in determining the viability of SPHS installations [11]. An example of SPHS implemented in the real world can be found in Okinawa, Japan, as seen in Figure 1.2. This SPHS system was finished in 1999. Built to address Okinawa's energy needs, this facility includes a reservoir that stores 564 thousand m^3 of seawater. The power generation capacity of this SPHS installation is 30 Megawatt-peak (MWp) [12].



Figure 1.2: Okinawa seawater-pumped hydro storage [13].

1.3. Problem Definition

Renewable energy sources, such as solar, wind, and hydroelectric power, offer a cleaner and more sustainable alternative to conventional fossil fuels, such as coals, gas and diesel. However, their intermittent nature poses a challenge to the stability and reliability of the national power grid. Integrating energy storage systems is crucial to effectively harness the potential of renewable energy and ensure a consistent energy supply. Energy storage systems store excess energy during periods of high generation and release it during peak demand or when renewable sources are unavailable. This balancing act enhances grid stability, reduces curtailment of renewable energy generation, and improves the overall efficiency of the energy system.

Indonesia has a long coastline of more than 80,000 km, indicating that many possible SPHS potentials can be developed in the coastal area using seawater. In this context, SPHS emerges as a promising solution to address the energy storage challenges. Indonesia's extensive coastline, abundant seawater resources, and topographical diversity make SPHS a viable option to bridge the gap between intermittent renewable energy generation and fluctuating energy demand. By effectively storing surplus energy during periods of high renewable generation and releasing it during peak demand hours, SPHS can contribute to grid stability, energy security, and the successful integration of renewable energy sources into the national energy mix.

Site selection is an essential step in the life cycle of SPHS plants because it is the first step in project implementation [11]. The process is challenging due to the interplay of topographical, economic, and

environmental factors. As these factors vary across different regions, a robust and systematic approach is essential to ensure the accuracy and reliability of site selection.

1.4. Research Objectives

Research objective

The study aims to identify the potential locations for seawater-pumped hydro storage in coastal areas of Indonesia.

Research questions

Based on this objective, the main research question can be formulated as follows: “What is the potential for seawater pumped hydro storage in coastal areas of Indonesia?” To achieve the research objective, the following research questions must be answered:

1. Where are the potential sites for seawater-pumped hydro storage in Indonesia?
2. What is the technical potential of seawater-pumped hydro storage in Indonesia?
3. What is the economical potential of seawater-pumped hydro storage in Indonesia?
4. How much carbon reduction can be achieved by developing seawater-pumped hydro storage in Indonesia?

1.5. Relevance

Numerous studies have identified suitable locations for PHES [14] [15] [16]. Using topographic data, these studies evaluate the viability of various sites for energy storage applications. Mainly, Digital Elevation Model (DEM) data has been instrumental in analysing the topography of potential sites. Geographic Information System (GIS) software, specifically Quantum Geographic Information System (QGIS), has been used to process and visualise topographic data and derive valuable insights. By integrating DEM data with GIS software, researchers identified optimal locations for gravity-driven energy storage, facilitating grid stability and renewable energy integration.

Using GIS, Ghorbani et al. (2019) identified a potential site for PHES in Iran [14]. Jimenez Capilla et al. (2016) determine the optimal potential location for the upper reservoir for pumped-back PHES using DEM data in Spain. Along with that, Pradhan et al. (2021) locate the potential location for SPHS in Curacao using DEM data and automate the process using QGIS features [16].

Meanwhile, there is a lack of research on identifying prospective sites for PHES, especially focusing on seawater pumped hydro storage using DEM data in Indonesia. This research marks a pioneering effort to uncover the PHES potential within Indonesia, exploring uncharted territory. By utilising DEM data to evaluate the topography of potential SPHS sites in Indonesia, this study aims to provide novel insights and substantially contribute to understanding SPHS feasibility in a country rich in coastal areas and ripe for sustainable energy solutions. Consequently, this research provides a perspective separate from previous studies, contributing to the corpus of knowledge in energy storage systems and sustainable development in Indonesia.

1.6. Report Outline

This study is structured into seven chapters. In Chapter 1, the study sets the stage by introducing the background, research problem, objectives, and questions. It provides an overview of the study’s scope

and purpose, outlining the context for the subsequent chapters. Chapter 2 delves into the literature relevant to the research topic. It reviews prior studies, theories, and practices related to SPHS, renewable energy, and energy demand in Indonesia. This chapter helps establish the theoretical and empirical foundation for the research. Chapter 3 outlines the research methodology employed in the study. It details the data sources, software, tools, and techniques for data collection, analysis, and modelling to identify Indonesia's feasible SPHS site.

Chapter 4 is dedicated to elucidating the methodology employed for ranking and classifying the identified SPHS sites based on pertinent technical parameters. The primary objective of this chapter is to establish an order that reflects the varying degrees of the suitability of these sites, ranging from those exhibiting the most favourable conditions to those facing more challenging circumstances. Chapter 5 presents the research results in the technical and economical potential for SPHS in Indonesia. It highlights key findings, identifies suitable sites based on technical and economic aspects, and discusses the implications of these findings for sustainable energy development.

Chapter 6 focuses on the environmental impact of SPHS development, assessing its implications for carbon reduction efforts and localised environmental concerns, including corrosion and seawater intrusion. The concluding chapter, Chapter 7, draws conclusions based on the research findings. In addition, recommendations for policymakers, stakeholders, and future research directions are provided.

State of The Art

This chapter explores the relationship between increasing electricity demand, the current energy generation sources, and the untapped potential of renewable resources in a country with vast renewable energy sources. Furthermore, this study aims to analyse the potential transformational capabilities associated with pumped hydro storage technologies, emphasising single reservoir seawater pumped hydro storage.

2.1. Indonesia Energy Demand

Indonesia is characterised by rapid development and demographic growth. The country has significant implications for its electricity demand. With a population of 281 million people and an expected rise to 350 million by 2050 [17], the nation faces a notable surge in energy requirements. Within Indonesia's energy landscape of 2020, the average peak electricity demand approximates 44 Gigawatt (GW), reflecting the integral role of electricity in sustaining diverse sectors and daily activities [18]. Projections for the near future project a significant surge in peak demand, with expectations of reaching approximately 77 GW by 2030. This surge predominantly occurs during evening hours, from 7 to 10 p.m., driven by varied activities requiring electricity consumption [18]. Figure 2.1 shows the average hourly demand pattern in Indonesia. Residential end uses, led by appliances such as air conditioners, lighting, refrigerators, and televisions, significantly contribute to over half of the nation's peak demand [18]. As Indonesia navigates this evolving energy landscape, insights into peak electricity demand and its composition underscore the urgency of energy efficiency measures, sustainable energy integration, and the adoption of intelligent energy storage technologies to ensure a resilient and sustainable energy future.

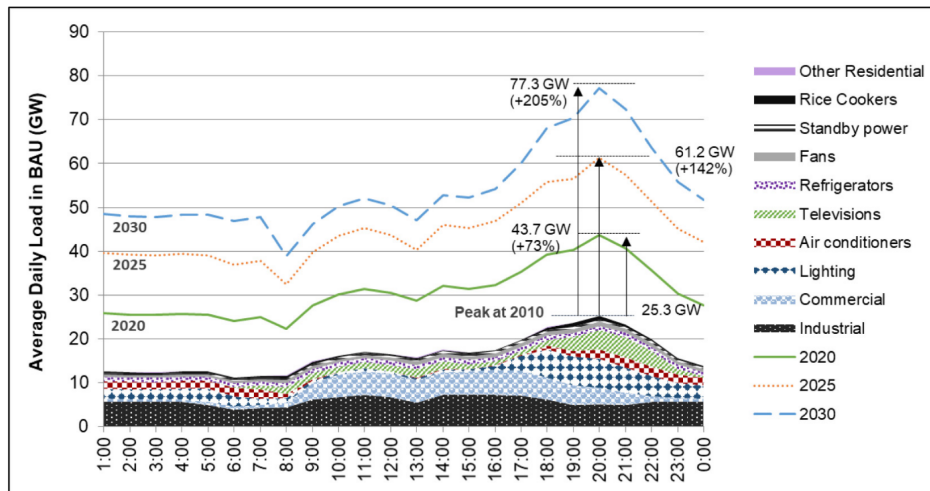


Figure 2.1: Evolution of Indonesian daily load curve between 2010 and 2030 [18].

The growth in energy needs experienced by Indonesia is explained by population expansion and economic development, intensifying the electricity demand. Presently at 1.2 Megawatt-hours (MWh) per capita annually, electricity demand is forecasted to reach 4.5 MWh per capita within the next two decades [19]. The nation's power consumption has a consistent upward momentum due to urbanisation, industrialisation, and societal improvements. Addressing the challenges posed by this escalating electricity demand is pivotal for sustaining reliable energy access [20].

Indonesia's electricity demand currently stands at around 310 Terawatt-hours (TWh) per year, indicative of the growing necessity for energy to facilitate economic progress and population growth [1]. Projections reveal a substantial surge in electricity demand, reaching an estimated 1400 TWh by 2050 [21]. This remarkable escalation underscores the imperative of robust energy policies, sustainable energy integration, and energy efficiency enhancements to secure a dependable and adaptable energy supply [3].

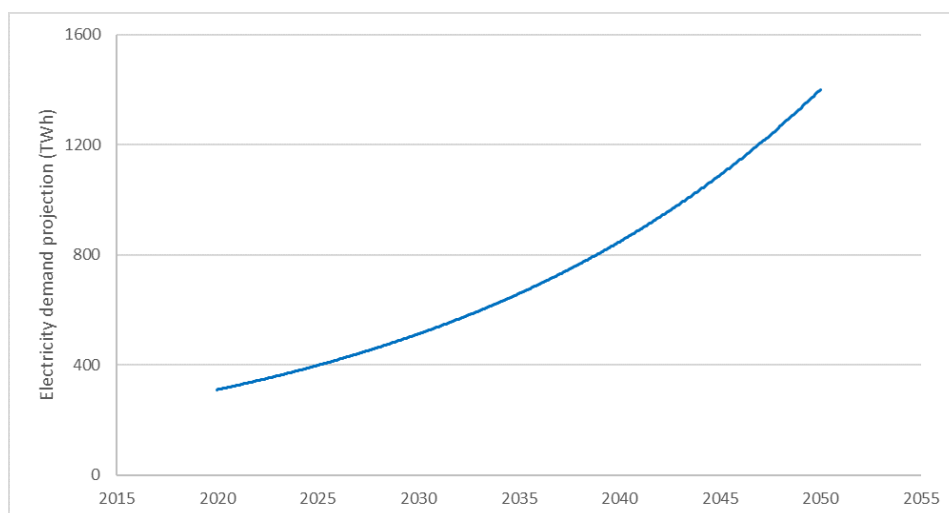


Figure 2.2: Electricity demand projection [21].

In response to the increasing demand, Indonesia has primarily relied on common energy sources, such as coal and natural gas, for electricity generation [22]. Nevertheless, renewable energy sources,

including solar, wind, hydro, and geothermal, have garnered attention as viable options for diversifying the energy portfolio and addressing the environmental consequences associated with fossil fuel energy sources [19].

2.2. Indonesia Energy Sources

A diverse mix of energy sources characterises Indonesia's energy landscape, each playing a distinct role in meeting the nation's growing energy demand. Historically, the country has heavily relied on fossil fuels, primarily coal, for its energy generation [21]. Coal maintains its position as the prevailing energy source, constituting a significant proportion of Indonesia's energy generation, amounting to 61% [22]. The nation is recognised as a prominent global producer and exporter of coal, hence establishing coal-fired power plants as a substantial source of its energy provision. Nevertheless, the environmental ramifications of coal combustion, such as releasing greenhouse gases and air contamination, where carbon emissions associated with coal-fired power plants are estimated to be around 820 grams of CO₂ per kilowatt-hour (gCO₂/kWh) of electricity produced [23].

Natural gas also holds a significant share in Indonesia's energy mix (21%), providing a cleaner alternative to coal and oil [1]. The country's substantial natural gas reserves make it a valuable resource for electricity generation and industrial processes. Natural gas power plants are relatively efficient and emit fewer pollutants per kilowatt-hours (kWh) than coal-fired plants, with 490 gCO₂/kWh [24]. Figure 2.3 shows Indonesia's share of electricity generation sources projection until 2030.

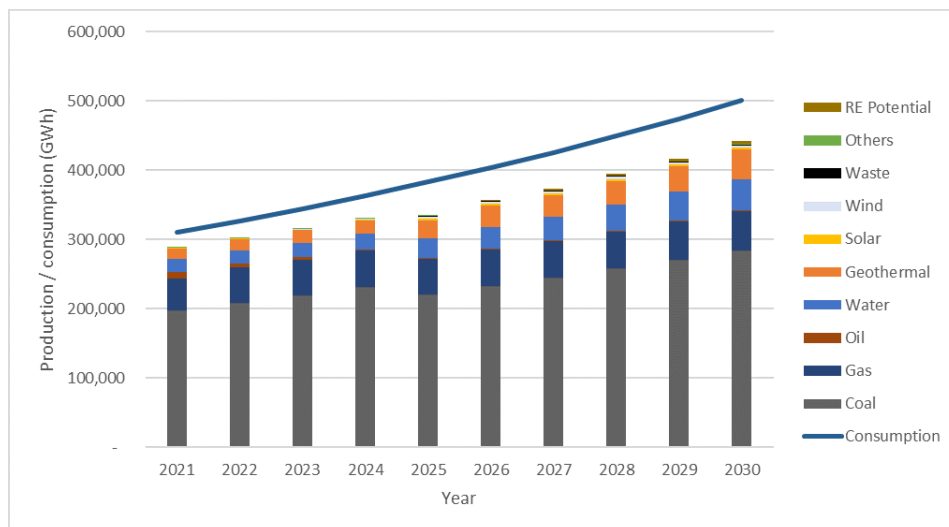


Figure 2.3: Power plant installed capacity and generation projection [1] [2].

Currently, renewable energy sources, including hydropower, geothermal, solar, wind, and biomass, collectively contribute 14% to the country's electricity production [2]. Despite the dominant role of fossil fuel energy sources in Indonesia's current energy supply, there is a strong governmental commitment and determination to diversify the energy mix by promoting and establishing more renewable energy sources [2].

2.3. Potential of Renewable Energy Sources in Indonesia

As a nation rich in natural resources and diverse geographical features, Indonesia holds significant potential for harnessing clean energy sources. Figure 2.4 compares renewable energy potential, current

installed capacity and 2050 projection in Indonesia.

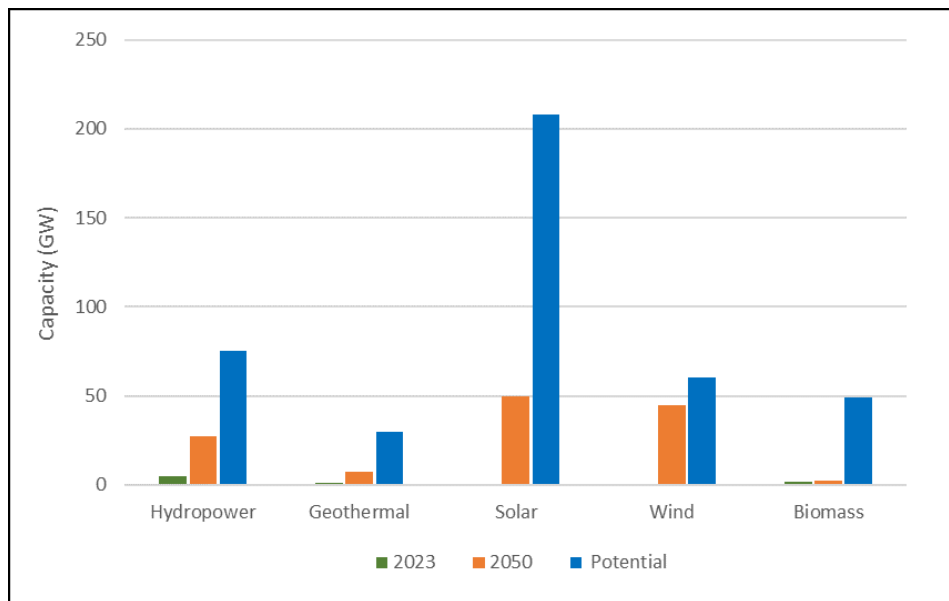


Figure 2.4: Comparison between renewable energy potential and installed capacity.

Hydropower

Endowed with numerous rivers and water bodies, Indonesia possesses considerable hydropower potential. Hydropower presents an opportunity for sustainably meeting the nation's energy needs, with an estimated range between 550 TWh to 700 TWh and an associated capacity of 63 GW to 80 GW [25]. Despite the substantial potential for hydropower in Indonesia, the installed capacity of hydropower plants remains relatively modest, standing at just 5 GW [2].

Geothermal energy

Sitting within the Pacific Ring of Fire, Indonesia boasts abundant geothermal resources, making it one of the world's top geothermal energy producers. The geothermal energy potential in the country is nearly 40% of the global geothermal energy potential, roughly equivalent to 29 GW [26]. However, the current utilisation of this capacity for power generation within the country is a modest 1.4 GW [2].

Solar energy

Indonesia's equatorial location positions it advantageously for harnessing solar energy. With abundant sunlight throughout the year, solar energy presents a viable and sustainable option for electricity generation. Previous studies have constantly emphasised the considerable capacity of Indonesia's land for the utilisation of solar energy [27][28][29]. A range of solar irradiation values, ranging from 4.6 kWh/m² to 7.2 kWh/m², has been observed, equivalent to a capacity of 207 GW nationwide. However, the current installed capacity of solar panels in Indonesia only provides 78 Megawatt (MW) [2].

Wind energy

Indonesia has ventured into the realm of utility-scale wind power, evident through the establishment two noteworthy wind power plants: Tolo 1, with a capacity of 72 MW, which commenced operations in 2019, and Sidrap, with a capacity of 75 MW, operational since 2018. The projected objective for wind power is to achieve a capacity of 850 MW by 2025, with an additional 597 MW of capacity anticipated to be added by 2030 [2]. At the national level, the country possesses an estimated potential of 61 GW [30].

Bioenergy

Indonesia's agrarian landscape provides ample opportunities for bioenergy production. Biomass, biogas, and biofuels derived from organic materials hold the potential to contribute to the energy mix [31]. The expansive geographical landscape of Indonesia calls for the revitalisation of regions to strategically reposition the potential of biomass resources [32]. The estimated biomass resource potential in Indonesia, which is obtained from plants and garbage, is approximately 49 GW nationwide [32]. Currently, the installed capacity of bioenergy sources in Indonesia is approximately 1.7 GW [2].

2.4. Necessity of Energy Storage Systems (ESS) for Supporting Renewable Energy Sources

Incorporating intermittent renewable energy sources, such as solar and wind energy, into the power grid offers significant potential for advancing sustainable energy generation. Nevertheless, the fluctuating nature of these sources requires a methodical approach to guarantee a consistent and dependable energy provision. Energy storage systems (ESS) becomes an essential element of this strategy, providing a solution to address the disparity between energy production and consumption [33]. Some common examples of ESS include battery storage, pumped hydro storage, and flywheel systems.

Intermittent Energy Sources and their Challenges

Intermittent energy sources are non-consistent or fluctuating energy sources. These sources typically depend on external factors, such as weather or natural conditions, and their power output may not be constant [34]. Solar and wind power are examples of intermittent energy sources.

The fluctuation of solar power generation is influenced by factors such as cloud cover, meteorological conditions, and the onset of night, necessitating the implementation of energy storage technologies to store surplus energy for utilisation during periods of reduced sunshine [35].

Wind energy generation is contingent upon the impact of varying wind velocities and patterns, leading to erratic power generation. The presence of sudden fluctuations in wind velocity introduces an element of uncertainty in the power system, necessitating the implementation of technologies to manage these variations and avert any potential disruptions [34].

Role of Energy Storage Systems

Energy storage technology encompasses diverse solutions, each uniquely designed to cater to specific power needs, efficiency requirements, and the pattern to capture and release energy during peak and off-peak demand periods [36]. Within power system contexts, energy storage serves various purposes, including daily equilibrium operation, peak load reduction, enhancement of power quality, and the exploitation of energy price disparities for consumers [36]. Energy storage methods within power systems are frequently categorised into three primary classifications: electrical, thermal, and mechanical. These distinct categories encapsulate various techniques utilised to store and manage energy resources within power infrastructure effectively [35].

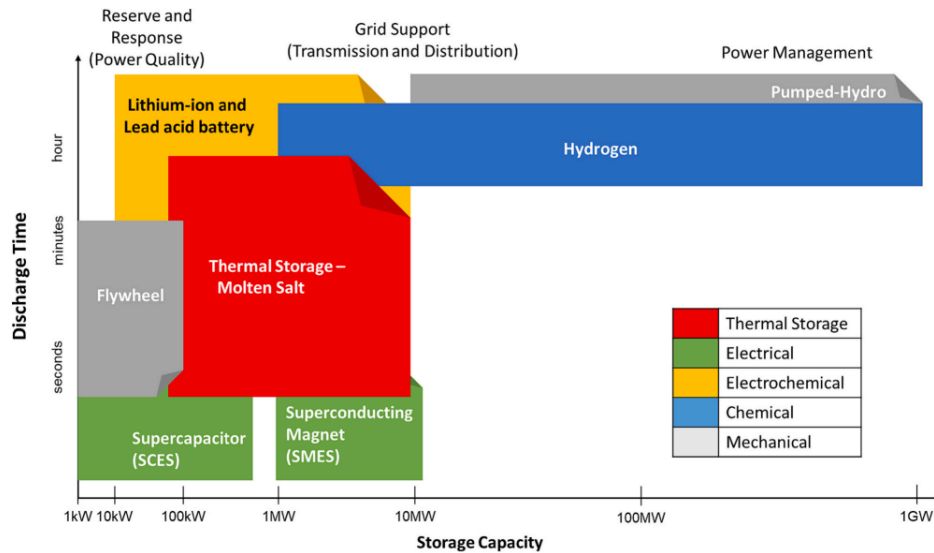


Figure 2.5: Illustration of energy storage systems according to their storage capacity and discharge duration within power system utilisation [36].

Battery technologies, such as lithium-ion and advanced lead-acid batteries, offer minutes to hours duration scale energy storage solutions that rapidly respond to demand fluctuations [33]. They store surplus energy during periods of high generation and discharge it during peak demand, ensuring grid stability [33]. Pumped hydro storage facilitates large-scale energy storage and is sustained for hours or even up to a day, depending on the size and capacity of the system. [37]. This ability makes PHES well-suited for applications requiring longer duration and bigger scale energy storage than batteries [36]. Flywheel systems store energy in rotational motion and release it by converting kinetic energy back into electricity. They offer rapid response times and high cycling efficiency [35]. The duration of the flywheel system's generation phase is relatively shorter than batteries and PHES [35].

2.5. Pumped Hydro Energy Storage

Blakers et al.(2021) explain that PHES transfers the stored water from the higher reservoir to the lower reservoir whenever there is a rise in energy demand or a decline in renewable energy production. When the water travels downward, it passes through turbines now functioning as generators to produce power from the potential energy. The stored energy is converted back into electrical energy through this process, which may then be delivered to the grid to satisfy rising demand [8]. Figure 2.6 shows the components of PHES.

PHES's capacity to react quickly to shifts in energy demand gives it its efficiency. PHES stands out from many other energy storage options due to its long-duration storage capability. PHES facilities are beneficial for meeting energy demands for extended periods since they can store energy for long periods, ranging from hours to even days.

PHES projects need appropriate topography considering the storage capacity and the elevation differential between the higher and lower reservoirs [11]. Typically, the building process entails the engineering of dams, tunnels, and penstocks and the setting up of turbines and generators [11]. Despite the original investment in infrastructure, PHES is renowned for having very cheap operational and maintenance costs over its prolonged working lifespan [36].

PHES has been successfully implemented in several nations worldwide as a mature technology, making a substantial contribution to grid stability, renewable energy integration, and energy storage

capacity [38]. PHES stands apart from other energy storage systems thanks to several compelling characteristics, including:

1. **High Efficiency:** PHES has one of the greatest energy conversion efficiencies among energy storage devices. It is a very efficient way to store and release energy, with round-trip efficiencies topping 70% to 87% [39].
2. **Long Duration Storage:** Depending on reservoir capacities, PHES can store energy for long periods, extending from hours to days. This capacity addresses short-term fluctuations and long-term energy management requirements [40].
3. **Large-Scale Capacity:** PHES facilities have a large amount of storage space that allows them to store gigawatt-hours of energy and deliver steady power for a long time [38].
4. **Low Environmental Impact:** Because PHES systems use water as the energy storage medium, their environmental impact is negligible. Compared to other storage options, they have a modest operational footprint [41].

Compared to other ESS, PHES exhibits definite advantages, including:

1. **Battery Energy Storage Systems (BESS):** PHES offers improved long-duration storage capabilities and longer lifespans, making it suitable for handling prolonged energy demand periods. BESS systems deliver high power output and quick response times [42].
2. **Flywheel systems:** PHES frequently have greater storage capacity, enabling them to hold and release more energy for extended periods. Compared to flywheel systems, PHES is typically more cost-effective regarding initial investment and ongoing operating costs [43].
3. **Thermal Energy Storage (TES):** Because TES systems store energy as heat, their flexibility for producing electricity is constrained. PHES offers a more versatile means of converting potential energy into kinetic energy [43].

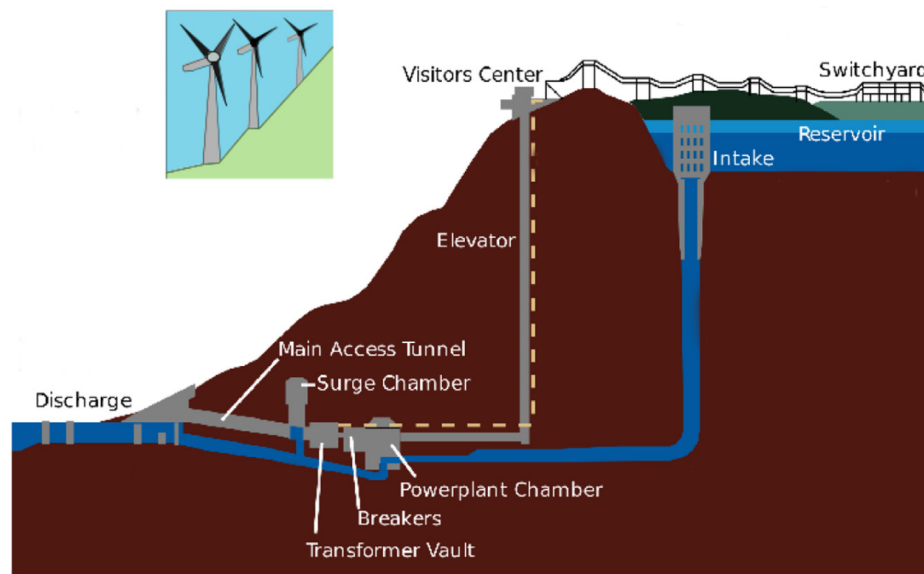


Figure 2.6: Components of pumped hydro energy storage [15].

PHES encompasses several distinct types based on the characteristics of the reservoirs' location, including pumped-back, open-loop, and closed-loop systems. When selecting the type of PHES, several

factors must be considered. These factors include technical, environmental, regulatory, and economic considerations to ensure that the chosen system fulfils the requirements and objectives of the project [9]. The site's physical characteristics, such as elevation differences, natural water bodies, and available land, are crucial in determining which PHES type is feasible [11]. The availability and sustainability of water sources have a significant bearing on the choice of PHES. Open-loop and pumped-back PHES systems rely on natural water bodies, whereas closed-loop PHES systems require artificial reservoirs.

Pumped-back Pumped Hydro Storage (PBPHS)

The same river acts as both the upper and lower reservoirs. However, when energy storage is required, this PHES form acts as a pumped storage system backed by potential energy in the higher reservoir. In normal circumstances, it functions as a traditional hydropower plant [9].



Figure 2.7: Pumped-back pumped hydro energy storage [44].

Open Loop Pumped Hydro Storage

The primary distinction between open-loop PHES and other types of PHES resides in the water sources used and the characteristics of those water sources. In an open-loop PHES system, the reservoirs are connected to a natural water body, typically a river or lake, providing continuous water discharge. The water used for energy storage and conversion is replenished naturally and is part of the extant water cycle [9]. Open-loop pumped hydro storage systems necessitate cautious water management to ensure a consistent and sustainable water supply.



Figure 2.8: Open loop pumped hydro energy storage [45].

Closed Loop Pumped Hydro Storage

The distinction between closed-loop pumped hydro storage and other types of PHES resides in their methods of utilising water sources and the properties of those sources. In a typical closed-loop PHES system, the water source consists of reservoirs that have been artificially created and are located at various elevations. These reservoirs contain water dedicated solely to the energy storage process and not a component of the natural water cycle [9]. Figure 2.9 illustrates a closed-loop PHES system. In this configuration, both reservoirs are isolated and not connected to a natural water body, such as a river or lake.

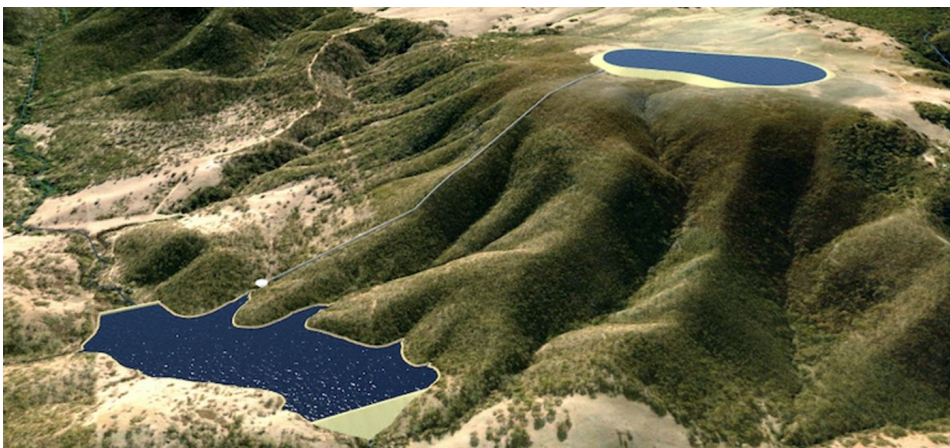


Figure 2.9: Closed loop pumped hydro energy storage [46].

2.6. Seawater PHES

Both Seawater Pumped Hydro Storage (SPHS) and Pumped Hydro Energy Storage (PHES) are types of hydropower-based energy storage, but there are differences between them. SPHS is a variant of PHES whose working fluid is seawater. Instead of constructing two reservoirs, SPHS systems are typically constructed near the coast, with the sea as the lower reservoir [47]. During periods of excess

energy, seawater is pumped to a reservoir at a higher altitude or further inland. When electricity is needed, seawater is released from the reservoir and flows through turbines back into the ocean to generate electricity. One advantage of SPHS is that it doesn't compete with freshwater resources used for drinking, irrigation, tourism, and other purposes.

Due to the enormous quantity of available seawater, the SPHS possesses the potential for large-scale energy storage. The seawater serves as one of the reservoirs, thereby reducing the infrastructure requirements and environmental considerations associated with reservoir construction [48]. Figure 2.10 shows an example of an upper reservoir for a SPHS system in Ludington, Michigan, located next to the coastline.

Indonesia's extensive shoreline offers ample access to seawater, which can be utilised for energy storage. This abundant coastal resource is a reason for research to examine the potential of SPHS in Indonesia.



Figure 2.10: SPHS system in Ludington, Michigan [49].

2.7. Pumped Hydro Storage in Indonesia

In Indonesia, PHES seems to have great potential for facilitating the integration of intermittent renewable energy sources. Its advantages and difficulties are integral to pursuing a sustainable energy future. With PHES, Indonesia's extensive solar, wind, and hydroelectric power potential can be utilised more efficiently, which allows for storing excess renewable energy, mitigating the intermittent nature of sources such as solar and wind. PHES enables efficient energy balancing by storing extra energy during low-demand hours and delivering it when required, thereby reducing reliance on fossil fuels and enhancing energy security. By maximising the utilisation of renewable energy sources, PHES can contribute to Indonesia's climate goals by substantially reducing greenhouse gas emissions.

The first PHES project in Indonesia is the Upper Cisokan pumped storage hydropower plant, set to be located in West Java, which is planned to commence in 2022. With an expected capacity of 1,040 MW, this project aims to address the growing electricity demand during peak periods and provide substantial energy storage capabilities to facilitate the integration of renewable energy sources. As a result, it will contribute to a more environmentally sustainable and dependable electricity supply, benefiting consumers in the densely populated regions of Java and Bali [50].

To navigate the development of PHES in Indonesia, it is crucial to consider its prospective benefits

and significant implementation obstacles. The construction of PHES facilities may have environmental repercussions, such as habitat destruction, water consumption, and alterations to the natural river flow. Identifying sites with the necessary topography and water resources, particularly in densely populated areas, can take time and effort. Furthermore, It is essential to balance land use and environmental concerns. The initial investment required for PHES development can be sizable, where financing and investment models must be established to attract private and public funding. Moreover, successful PHES projects must involve local communities and resolve their concerns regarding land use, environmental impacts, and potential disruptions.

Methodology

Chapter 3 provides a detailed insight into the methodology employed to identify potential SPHS sites in Indonesia. This chapter outlines the data sources, software tools, and systematic procedures utilised to assess the technical and economic feasibility of SPHS across the nation. Furthermore, it explains the method for collecting technical site attributes.

3.1. Data and Software

Identifying potential sites for SPHS is contingent upon the availability and utilisation of data sources, specialised software, and analytical tools. In the analysis and decision-making processes, DEM, software platforms, and geospatial tools are indispensable.

Geographic Information System (GIS) is a technology used to capture, store, analyse, and present spatial and geographical data [14]. In this study, GIS is utilised to process the DEM data. GIS platforms, such as QGIS and ArcGIS, enable the integration, visualisation, and analysis of numerous geospatial datasets stored in DEM data. These software packages enable researchers and engineers to generate topographic maps, contour lines, and 3D visualisations, which facilitates identifying and evaluating suitable SPHS locations.

In addition, specialised geospatial tools, such as SAGA and PCRaster, frequently incorporated into GIS software, enable professionals to conduct comprehensive analyses. These instruments facilitate the calculation of slope angles, drainage patterns, and flow direction, thereby facilitating the selection of upper and lower reservoir sites. Incorporating hydrological data to evaluate water availability and flow dynamics ensures a comprehensive evaluation of site viability.

3.1.1. Digital Elevation Model (DEM)

Analysing the topography is crucial in locating sites suitable for SPHS. DEM data has emerged as an indispensable resource for this endeavour, providing a complete depiction of a region's terrain. DEM data, typically derived from satellite or airborne surveys, provides a detailed elevation profile of the land surface, including altitude and slope variations.

DEM data facilitates the construction of topographic maps, contour lines, and three-dimensional visualisations, thereby facilitating the visualisation of potential SPHS sites. These maps and models provide a comprehensive view of elevation changes, allowing for the identification of prospective upper reservoir locations and the evaluation of their hydraulic viability.

To identify potential sites for SPHS in Indonesia, selecting the optimal DEM data source is crucial.

DEM Nasional (DEMNAS), a comprehensive dataset provided by Badan Informasi Geospasial (BIG) of Indonesia, was utilised for this research. DEMNAS has a spatial resolution of 8.25 meters (0.27-arcsecond), a notable feature. This level of detail enables us to depict Indonesia's diverse terrain's intricate nuances precisely. The higher resolution of DEMNAS relative to other alternatives, such as the Shuttle Radar Topography Mission (SRTM) data, enables us to discern elevation variations and subtle topographical features that may be essential for determining SPHS suitability.

DEMNAS gathering method

DEMNAS was constructed from multiple Digital Terrain Models (DTM) and Digital Surface Model (DSM) data sources, such as IFSAR data (5m resolution), TERRASAR-X (5m resampling resolution from the original 5-10 m resolution), and ALOS PALSAR (11.25 m resolution) [51]. Due to the use of DSM, the provided data may be canopy elevation rather than terrain elevation.

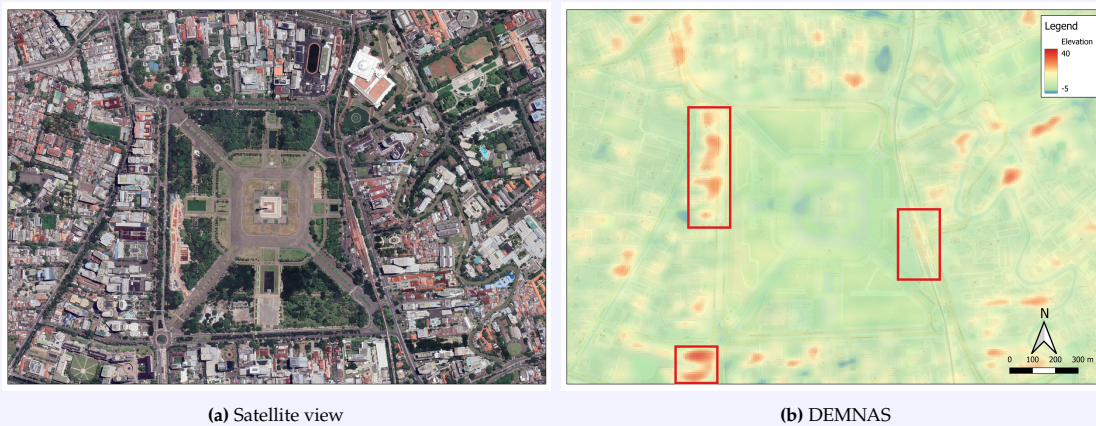


Figure 3.1: Satellite view vs. DEMNAS.

Figure 3.1 (highlighted in red) illustrates that the data obtained from DEMNAS pertains to land cover elevation rather than terrain elevation.

While it is possible that DEMNAS provides data related to the elevation of land cover, it can still be effectively utilised in this study. This is primarily because the study area predominantly encompasses rural regions with extensive vegetation cover. In these areas, the specific elevation of natural features and terrain details may not be as critical as obtaining a general understanding of the terrain's broader characteristics.

3.1.2. GIS Software

QGIS has been selected as the GIS software for this study. QGIS is an open-source program, which makes it readily available to researchers and professionals. This accessibility aligns with the dedication to accessibility and transparency in the research endeavours. In contrast to proprietary GIS software such as ArcGIS, QGIS eliminates licensing fees and restrictions, ensuring the analysis is not constrained by financial constraints. This accessibility democratises geospatial analysis, enabling a larger audience to interact with and benefit from our research findings.

One of the most notable features of GIS to support this study is its robust support for Python scripting for customisation and automation. Python, a versatile and widely used programming language, enables the automation of complex geospatial duties. Creating Python programs that facilitate the analysis of

DEM data makes the workflow significantly more streamlined and repeatable. The compatibility of QGIS with Python demonstrates its adaptability and versatility in meeting our research's specific needs.

3.1.3. Tools and Features

In the research, the QGIS plugin known as PCRaster played a role in the geospatial analysis, which included streamflow identification to identify the valleys, catchment delineation, and inundation calculation. With an emphasis on objective and reproducible analysis, these key functionalities were utilised to evaluate potential sites for SPHS in Indonesia.

Stream identification using the PCRaster plugin identifies and delineates the geographical features associated with valleys where SPHS systems might be potentially constructed. Catchment delineation utilised DEM data and PCRaster's capabilities to identify watershed boundaries and define catchment areas associated with particular valleys. The third feature, inundation calculation, enabled estimating areas impacted by submersion or inundation during reservoir construction.

3.2. Identification of Potential SPHS Sites

The study evaluates power generation potential, head loss, investment requirements, and penstock line topography. It was initiated by collecting data, including DEM data from BIG. Using GIS tools, streamflows were identified within the DEM data, aiding in the recognition of locations with valleys suitable for SPHS. The primary objective of this study is to identify potential SPHS locations in Indonesia that possess significant energy potential, surpassing the qualifications for medium-scale hydropower generation, which is typically defined as having an energy capacity exceeding 15 MW. By emphasising this threshold, the objective is to distinguish sites with the ability to generate a considerable amount of power, thereby maximising the investment efficiency. This approach helps ensure that the identified locations are not only numerous but also possess the necessary power generation capabilities to make them economically viable and environmentally beneficial for the development of SPHS systems.

The economic assessment carried out in this study aims to calculate the Levelised Cost of Storage (LCOS) for each identified site. This calculation considers various factors, including Capital Expenditure (CAPEX), Operational Expenditure (OPEX), and other relevant parameters. Once the LCOS for each site is determined, it is compared with the ceiling price of electricity in the respective region. This comparison is essential to assess the economic viability of each site, as it determines whether the potential SPHS system can generate electricity at a cost lower than the prevailing electricity price ceiling in its designated area. The detailed information about LCOS calculation is explained in Subsection 3.2.5.

Environmental impact assessment focuses predominantly on carbon reduction. The transition from fossil energy generation to renewable energy sources represents a fundamental shift toward sustainable and environmentally responsible energy practices, making this evaluation essential. This study highlights the environmental benefits associated with developing SPHS in Indonesia by quantifying the reduction in carbon emissions resulting from this transition.

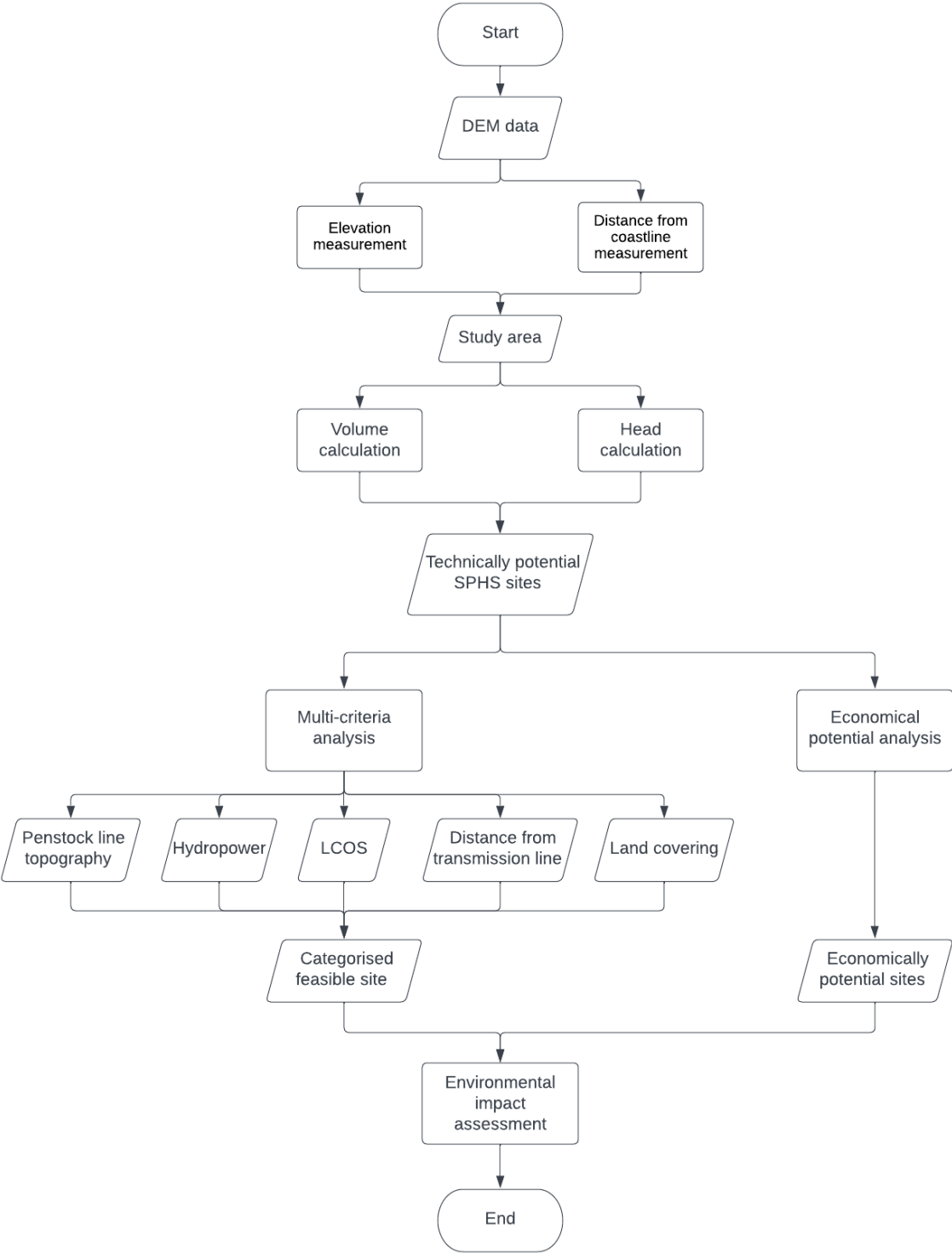


Figure 3.2: The methodology flow chart of the research.

3.2.1. GIS-based Model (DEM Analysis)

The primary focus of this study is the development of a Python script to automate the process of identifying potential SPHS locations. Automating the processes with a Python script is crucial in

streamlining the SPHS site selection process.

Identifying valleys and inundation areas is a feature of the script. These characteristics are necessary for evaluating the topographical suitability of potential SPHS sites. By outsourcing the extraction and delineation of these geographical elements, the Python script ensures consistency and efficiency while reducing the time and effort required for analysis.

The development of the Python script represents a significant development in the research, as it enables the study to expand its analysis to encompass a broader range of potential SPHS sites. In addition, the automation of the script ensures the reproducibility and transparency of the research methodology, allowing others in the field to replicate and validate the findings.

Preprocessing

This study's initial analysis phase involves merging the acquired DEM files. This process is necessary due to the limited size of the downloaded DEM datasets, which typically cover an area of approximately 770 square kilometres for each file. Due to Indonesia's immense and diverse geography, which spans numerous islands and coastal regions, it is necessary to combine these individual datasets to represent the nation's topography. With 38 provinces in Indonesia, 37 of which have coastlines, the study is designed to strategically conduct analyses on a provincial level.

In the following analysis stage, a buffer zone is established 8 kilometres inland from the coast. This buffer zone is set at an 8-kilometre distance from the shoreline because SPHS site suitability is typically enhanced by proximity to the coast. To ensure that the selected locations within the buffer zone are suitable for SPHS, the analysis also imposes an elevation criterion, requiring that the land within this area be at least 200 meters above sea level. This elevation threshold is set to fulfil specific requirements related to the water storage volume and the inundation area necessary to store a minimum amount of energy efficiently.

After defining the buffer zone with the specified elevation threshold, the analysis focuses on this particular study area. This concentrated study area is selected because it is more likely to contain suitable topographical characteristics for SPHS development, such as the necessary elevation differentials and proximity to marine sources.

After defining the focus area, the next stage is clipping the DEM data to this focus area. This process isolates and extracts the topographical data within the focus area from the broader DEM dataset. By isolating this specific region, the study can evaluate the terrain's suitability for potential SPHS sites, considering elevation, storage volume, and other topographical parameters essential for determining SPHS feasibility.

The next step is creating a dataset of local drain directions using the PCRaster plugin, followed by the delineation of streamflows to identify the valleys, constituting the subsequent phase in the analysis. local drain directions dataset contains vital information regarding water flow direction across the study area's terrain. It depicts how water naturally travels and drains across the landscape by identifying its paths. This directional information is indispensable for the subsequent analysis processes.

After generating a dataset of local drain directions, the study defines streamflows. Streamflows represent various levels or magnitudes of river flow, each illustrating a distinct flow scenario. These streamflows aid in evaluating the hydrological characteristics of the terrain, enabling the evaluation of how water travels through the landscape under different conditions. By delineating streamflows at multiple levels, the study ensures a thorough examination of the topographical suitability of the study area. This approach identifies optimal SPHS locations that align with specific valleys represented by streamflows. This study categorises the streamflows used for analysis based on their stream order,

focusing mainly on streams with a Strahler order of 5. The selection of Strahler Order 5 in this study is based on a thorough evaluation of various Strahler orders. Strahler Order 5 is deemed the most suitable for identifying valleys and river networks that align with the requirements of SPHS systems. This choice was made after a series of trial-and-error processes.

The preprocessing phase has been meticulously described and encapsulated in the Python QGIS (PyQGIS) script, which is available for reference in Appendix C or as "01.preprocessing.py" within the supplementary files. This script encapsulates the precise sequence of operations carried out during the preparatory phase, such as data merging, buffer area creation, local drain direction generation, and streamflow delineation.

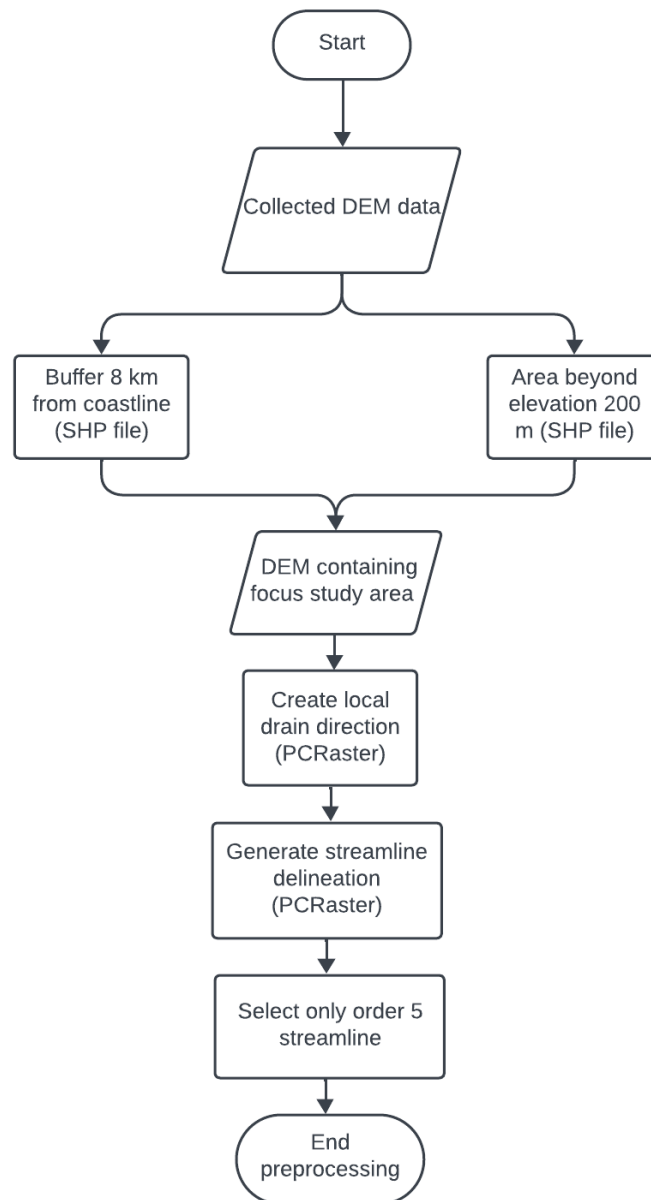


Figure 3.3: Preprocessing flowchart.

Main Process

Identifying prospective SPHS sites requires evaluating each candidate location via a series of steps. First, for each valley represented by a branch of streamflow with a Strahler order of 5, the analysis identifies the lowest elevation along that branch to determine the outflow point. This essential stage pinpoints the ideal location within the stream network for potential SPHS development.

Subsequently, the calculation of catchment areas is carried out using the "catchment" algorithm available in the PCRaster software. This algorithm aids in delineating the catchment boundaries associated with each selected streamflow branch. These catchment areas serve as the foundation for further analysis.

After defining the catchment areas, the analysis simulates the installation of a 15-meter-tall dam at the outflow of each catchment. In this study, Indonesian regulatory considerations primarily influenced limiting the dam's height to 15 meters. Dams exceeding 15 meters in height are considered "large dams" under Indonesian regulations. This classification necessitates more intricate and stringent design and safety procedures, which can significantly impact the planning and implementation of a hydropower project. Figure 3.4 illustrates the 3D visualisation of the simulation result.

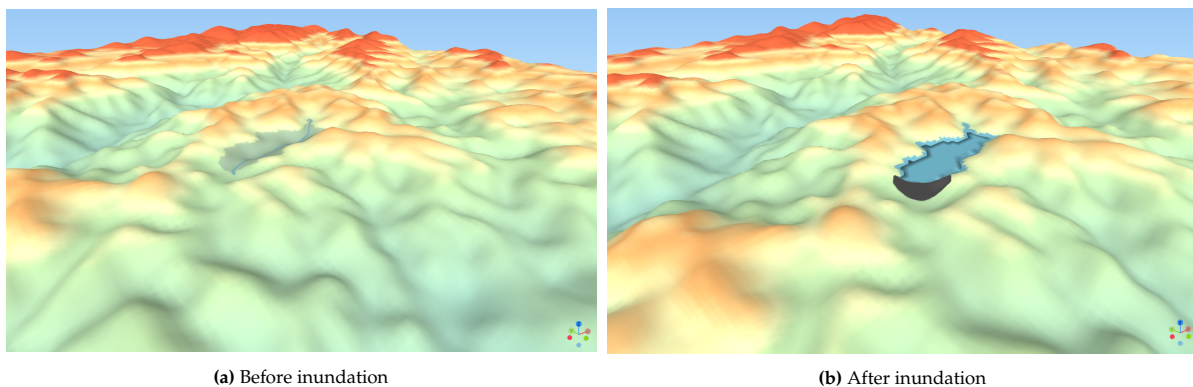


Figure 3.4: 3D Visualization of identified SPHS site: algorithm-generated potential location for SPHS

The dam replicates the structure used in an SPHS system and enables the identification of inundation zones within the catchment. The study obtains insight into the available energy potential by calculating the water-impounding volume resulting from this flooding. This analysis uses a cell-by-cell approach to estimate the inundation volume. This indicates that the analysis quantifies the volume of water for each DEM cell or pixel. To achieve this, the following formula is applied to each cell.

$$V = \sum_{i=1}^n h_i * gridsize^2 \quad (3.1)$$

The volume calculation formula considers several variables, including the DEM elevation data and the area represented by each cell. It calculates the volume of water that would occupy the space defined by the difference elevation between the water level in the reservoir with the related ground level (h_i) and the area of the cell. The analysis systematically evaluates the entire dam-formed reservoir by executing this calculation for every DEM cell.

The resolution of the DEM data is an essential factor to consider in this procedure. The resolution of a dataset refers to the measurement of each cell or pixel. A DEM dataset with a higher resolution contains smaller, more numerous cells that provide precise topographic detail. In contrast, a DEM dataset with a lower resolution incorporates larger cells and provides coarser topographical information.

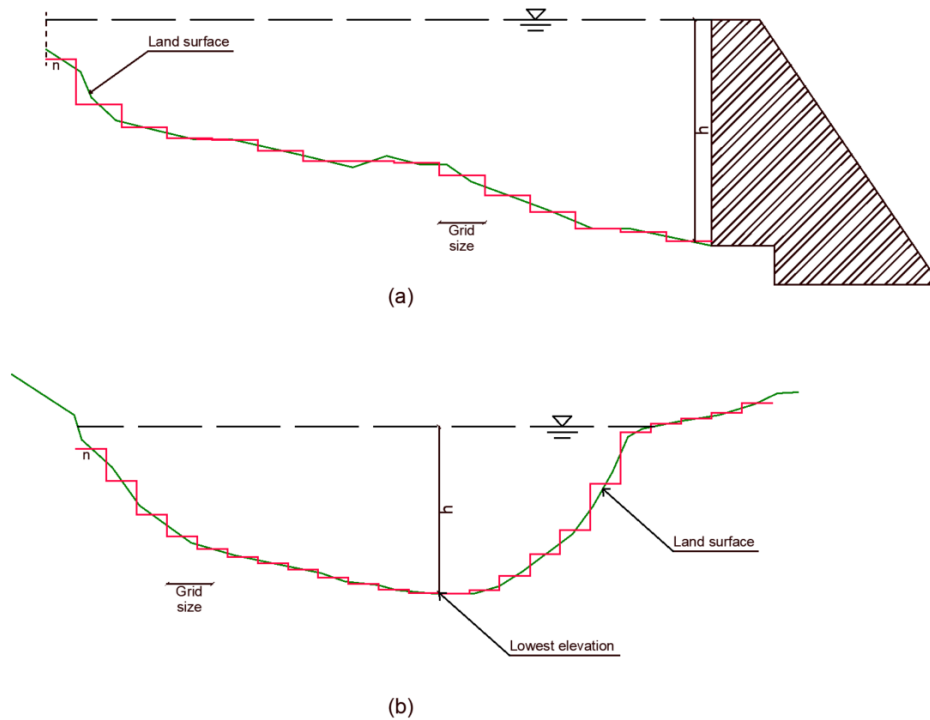


Figure 3.5: Longitudinal (a) and cross-sectional (b) profile of the reservoir.

The calculation of potential energy considers the dam-created reservoir's inundation volume and elevation. This calculation helps estimate the energy production capacity of each identified location. If the calculated potential energy exceeds a predetermined threshold value, in this study 120 MWh, the analysis continues to generate additional vital data. The following formula calculates the potential energy stored in the reservoir.

$$E = \frac{\eta * \rho * g * V * H}{3600} \quad (3.2)$$

Where E is potential energy stored in the reservoir in watt-hour (Wh), η is the efficiency of the system, in this study, the efficiency is determined to be 80%, V is the volume of the reservoir in m^3 , and H is the head in meters.

For locations that meet the energy threshold, the analysis further characterises the site by determining its exact distance from the nearest coastline. In addition, the calculation evaluates the penstock slope, which is essential for effectively transferring water between the upper and lower reservoirs during the generation phase of SPHS operation. The study also quantifies the potential power that can be generated during this generation phase.

By following these steps, the analysis systematically evaluates potential SPHS sites, considering multiple factors and criteria to identify locations that offer the most promising prospects for efficient and sustainable energy storage in the coastal regions of Indonesia.

As shown in Figure 3.6, the outlined stages have been incorporated into a PyQGIS script, automating each streamflow branch's evaluation. This report's Appendix D for the detailed script entitled "02. main-process.py" can be used as a reference for the process. This scripted method streamlines the analysis, allowing for an accurate and reproducible evaluation of prospective SPHS sites across Indonesia's coastal regions.

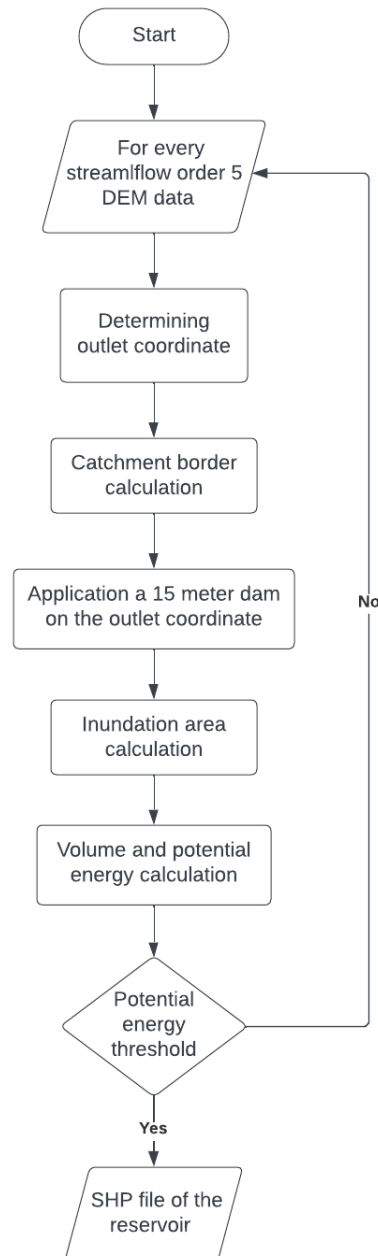


Figure 3.6: Main processing flowchart.

3.2.2. Hydropower Calculation

In this study, the hydropower calculation aligns with the typical daily energy consumption pattern, reflecting the gradual increase in electricity demand. This pattern is observable from 4 p.m. onwards, with the peak power demand occurring at 8 p.m., as illustrated in Figure 3.7. Consequently, the SPHS system design considers this energy consumption curve and aims to provide power over an 8-hour duration, commencing at 4 p.m. and concluding at 12 a.m., where the hourly power generation distribution can be seen in Figure 3.8. The power production potential of SPHS is determined by evaluating the peak power generation capacity, measured in MW_p, representing the maximum power produced in one generation phase.

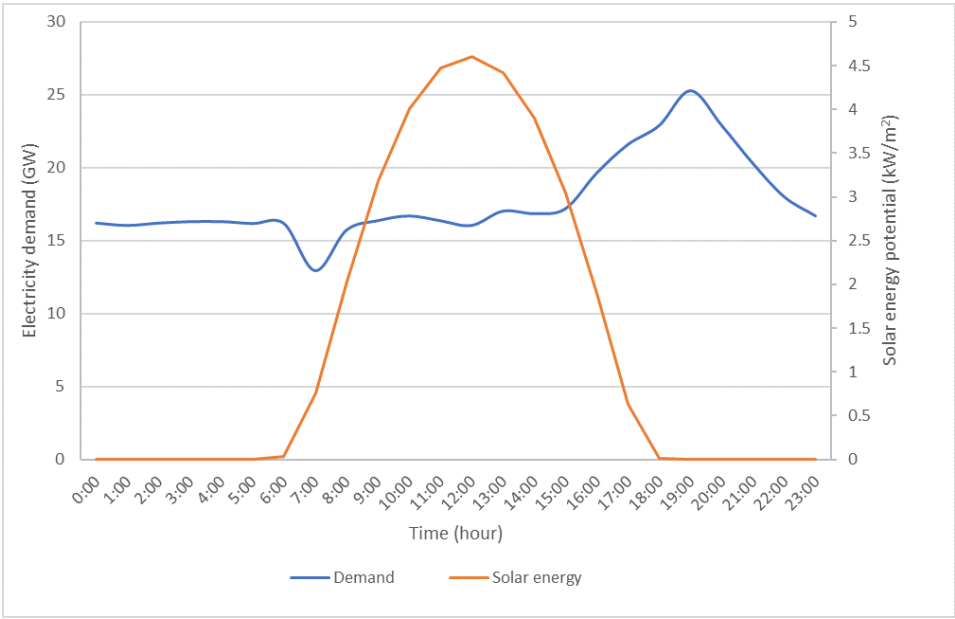


Figure 3.7: Daily electricity demand pattern vs solar energy availability [18] [52]

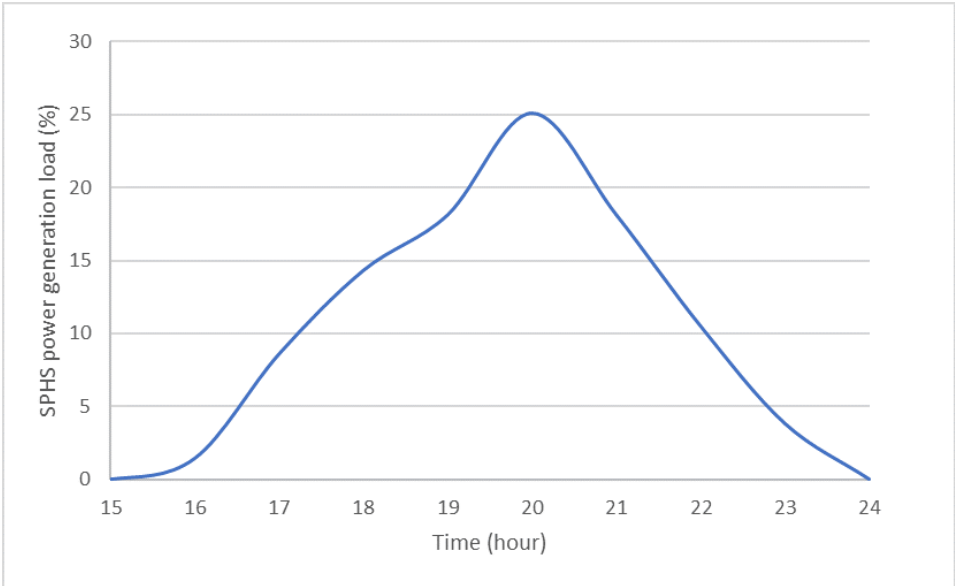


Figure 3.8: Daily SPHS generation phase pattern.

As water flows through various components of the hydropower system, such as penstocks, frictional losses occur. Mainly, roughness-induced losses and localised losses due to changes in the cross-section of the direction of the flow are influenced by variables such as flow velocity, penstock dimension, roughness, and fluid viscosity. Frictional losses directly impact the system’s efficiency and, consequently, the amount of energy that can be harnessed.

On the other hand, local losses occur at specific points in the system where the flow is interrupted or redirected. Abrupt changes in the geometry of the conduit, such as bends, junctions, or sudden expansions or contractions, frequently cause these losses. Local losses can significantly impact the overall system efficiency and must be accounted for in hydropower potential calculation.

Head Loss Calculation

Calculating head loss for PHES necessitates careful consideration of several factors to ensure accurate and reliable results. The system's hydraulic characteristics must be specified first, including the penstock's length and dimensions. In addition, the choice of materials and surface texture of the hydraulic components significantly impact head loss calculations. Flow rates, fluid characteristics, and environmental conditions such as temperature and pressure also play crucial roles. In addition, the system must account for the effects of friction, turbulence, and any connectors or valves. Lastly, it is imperative to account for any losses caused by the pump turbine. To accurately estimate head loss and maximise the efficiency of PHES systems, it is necessary to conduct a comprehensive analysis of these factors. The following formula can describe the total head losses (ΔH_{ea}).

$$\Delta H_{ea} = \Delta H_f + \Sigma \Delta H_s \quad (3.3)$$

Where ΔH_f is friction loss in penstock and ΔH_s is local losses produced by valve, pipe bend, trash rack and other parts of the hydropower.

1. **Friction Loss in Penstock:** The calculation of friction loss (ΔH_f) within the Seawater Pumped Hydro Storage (SPHS) system involves a systematic series of steps to ensure efficiency and accuracy. To begin, the peak discharge is determined based on the system's operational requirements. This discharge value is crucial for further calculations. Subsequently, an initial velocity of 4 m/s is set as a starting point, serving as a reference for the dimension of the penstock required. The discharge is then divided by this initial velocity to establish the penstock's preliminary dimensions.

To align with practical market availability, these dimensions are rounded up to match readily accessible sizes. However, this is not the final step, as the velocity must be evaluated to fall within the optimal range of 2-5 m/s. The friction loss itself is determined using the Hazen-Williams formula, considering the hydraulic slope (S). The hydraulic slope is calculated using a specific formula, as can be seen in Equation 3.4.

$$S = \frac{Q^{1.85}}{0.08905 * C^{1.85} * D^{4.87}} \quad (3.4)$$

The parameter "C" represents the roughness coefficient, which describes the inner surface of the pipe used for the SPHS penstock. This coefficient measures the resistance to water flow within the penstock and is affected by the pipe's surface roughness.

Glass Reinforced Plastic (GRP) pipe has been selected for the penstock. The selection of GRP pipes is based on their specific properties, which make them suitable for this application. Corrosion resistance is one of the primary advantages of using GRP pipes in the SPHS system. Given that the system operates with seawater, which can be extremely corrosive to many materials, it is crucial to choose a corrosion-resistant material such as GRP. This decision helps ensure the penstock's long-term durability, avoiding potential problems associated with corrosion-induced damage. The roughness coefficient (C) for GRP is 150. Q and D are discharge in m^3/s and penstock diameter in meters respectively.

The study considers the operational pressure within the penstock, which is the pipeline or channel used to transport water in a pumped hydro storage system. This operational pressure must meet certain standards of the American Society for Testing and Materials (ASTM) and the manufacturer's specifications [53].

Finally, the friction loss is subsequently computed by multiplying this hydraulic slope by the length of the penstock, as can be seen in Equation 3.5. Moreover, the penstock length (L) is determined by the vertical distance between the lowest elevation of the reservoir and sea level (h) and the distance between the reservoir outlet and the coastline (l). The shortest horizontal distance between the reservoir outlet and the coastline (l) must be multiplied by a factor to consider the topography condition between the reservoir and the coastline and the delta condition requiring a longer distance. The multiplying factor was assumed to be 1.5 in this study.

$$\begin{aligned}\Delta H_f &= S * L \\ L &= \sqrt{l^2 + h^2}\end{aligned}\tag{3.5}$$

2. **Local losses:** Local losses (ΔH_s) in head loss calculations encompass a variety of hydraulic factors that can influence the system's overall effectiveness. These elements include bends in the penstock, the design and configuration of trash racks, the characteristics of intake and outlet structures, and other components. These local losses (ΔH_s) must be considered because they impact the hydropower system's overall performance. This study uses the simplified estimation of local losses by attributing them to approximately 50% of the estimated friction losses experienced along the penstock. This simplification permits a reasonable approximation of local losses while maintaining a practical and computationally manageable approach to the head loss calculation, particularly when dealing with complex systems such as SPHS.

Pump-Turbine

The selection of an appropriate pump-turbine for a hydropower system is contingent on several crucial factors, including head, discharge, and generated power. The head, the vertical distance between the water source and the turbine, is the most critical factor. It directly impacts the available energy for conversion and dictates the type of pump-turbine required. The volume of water passing through the turbine per unit of time is determined by the discharge or water flow rate. This, along with the head, defines the system's hydraulic conditions and power potential. The ultimate objective is to generate power, which is contingent upon the combination of head and discharge, as well as the efficacy of the chosen pump turbine.

In this study, the selection of Francis turbines for the hydropower system is influenced by specific factors, such as the desire to generate more than 15 MW of electricity. The Francis turbine is renowned for its adaptability to various hydraulic conditions, making it an ideal choice for situations involving variable flow rates and head levels.

The efficiency of a Francis turbine can vary based on several variables but typically falls between 80% and 95% [54]. In this particular study, an 85% pump turbine efficiency ($\eta_{turbine}$) has been assumed. This assumption allows a conservative estimate of the system's performance based on a reasonable assumption to be made. Although actual efficiency may vary depending on the design, operation, and environmental conditions of the turbine, a 85% efficiency assumption provides a practical and widely accepted baseline for the calculations.

Finally, the power generated by the system (P) can be estimated using Equation 3.6.

$$P = \eta_{turbine} * \rho * g * Q * (H - \Delta H_{ea})\tag{3.6}$$

Where ρ is the density of the seawater in kg/m^3 , Q is the flow discharge, calculated by dividing the reservoir volume (m^3) by the operational phase duration (hours converted to seconds), and H is the

elevation different between the reservoir and the sea level in meters.

3.2.3. Distance from The Electricity Grid

The distance between each SPHS system and the closest electric grid must be computed to evaluate the system's integration into the electrical infrastructure. This calculation is based on estimating the distance between the SPHS installations and the nearest 500 kV or 150 kV transmission line. To accomplish this, the Indonesian Ministry of Energy and Mineral Resources provides a specific map from which the transmission lines are extracted. This map is a trustworthy and authoritative source of information regarding the locations of transmission lines, enabling accurate distance calculations.



Figure 3.9: Indonesia's electric transmission lines map [55]

In addition to optimising electrical infrastructure planning, this distance measurement will be a crucial factor in the multi-criteria analysis of the potential sites. Considering the proximity distance of each PHES system to the grid and the associated electrical infrastructure, the costs associated with connecting these systems to the grid and transmitting the generated energy can be estimated.

3.2.4. Penstock Line Topography

The topography of the penstock line is evaluated by calculating the standard deviation of the slope for each cell that the penstock traverses. This assessment uses the "terrain profile" plugin in QGIS. When the standard deviation of the slope in each cell is lower, it indicates that the topography of that area is more favourable for supporting SPHS project. In other words, a lower standard deviation of the penstock line slope suggests a more even and suitable terrain for developing the SPHS system.

3.2.5. Levelised Cost of Storage (LCOS)

LCOS calculation formula comprises several key components, each contributing to the overall assessment of the cost of energy storage over its operational lifetime. These components include CAPEX, representing the installation and construction costs associated with the energy storage system. It comprises equipment, infrastructure, land, permits, and installation expenditures. Typically, CAPEX is expressed as a cost per unit, such as euros per kWh of storage capacity. Secondly, OPEX consists of the ongoing expenses associated with operating and maintaining the energy storage system over its lifetime. This includes

routine maintenance, labour, monitoring, insurance, and any other recurring operational expenses. Typically, OPEX is expressed as an annual cost. LCOS is also dependent on the revenue produced by the energy storage system (E_{out}). It represents the revenue earned from selling stored energy to the grid or participating in energy markets. Typically, the revenue is determined by the system's energy output and the prevailing electricity market prices.

In LCOS calculations, both the discount rate (i) and the system's operational lifetime (t) are considered. The discount rate is an essential parameter to adjust future costs and benefits to their present value. It considers that the value of money declines over time due to inflation and the opportunity cost of committing capital to the project. A 6% discount rate has been selected for this study. This means that future costs and benefits are converted to their equivalent value in today's currency, considering the expected inflation rate. The operational lifetime of the energy storage system is the number of years the system is expected to function efficiently and effectively before requiring significant maintenance or replacement. In this study, the system lifetime is set to 50 years, indicating that the analysis considers the costs and benefits of the energy storage system over 50 years.

$$LCOS = \frac{CAPEX + \sum_{t=1}^n \frac{OPEX}{1+i^t}}{\sum_{t=1}^n \frac{E_{out}}{1+i^t}} \quad (3.7)$$

In this study, the LCOS is calculated using a method developed by Al Zohbi in 2022, as documented in the Encyclopedia of Energy Storage [56]. The work of Al Zohbi (2022) is an important contribution to the field of energy storage economics. His approach simplifies the LCOS estimation procedure, making it more accessible and applicable to PHES project stakeholders.

Al Zohbi's method is intended to provide a simple and user-friendly method for evaluating the economic viability of PHES systems. Using his methodology, project developers, investors, and policymakers can gain valuable insight into the financial aspects of PHES projects. This method simplifies the LCOS calculation, making it easier to make well-informed decisions regarding the implementation and funding of PHES technology.

Capital Expenditure (CAPEX)

In this study, the calculation of CAPEX for SPHS system considers several investment factors. These components include the electro-mechanical equipment, which includes the cost of required machinery, electrical components, and associated technologies for the storage system to function. In addition, CAPEX accounts for civil works, which include the costs associated with the construction of infrastructure, such as the reservoir, penstock, and other structures essential to the system's operation. In addition, indirect costs such as permitting, engineering, project management, and other associated overheads necessary to successfully implement the energy storage project are included in CAPEX. This study aims to provide a comprehensive assessment of the capital expenditure required to establish the energy storage system, thereby contributing to a more accurate evaluation of its economic viability and long-term cost-effectiveness.

1. **Cost of electro-mechanical equipment:** In the context of hydropower plants, the cost of electro-mechanical equipment typically comprises between 30% and 40% of the total project cost. This cost allocation is affected by several factors, including the head, the discharge, and the power generated by the hydro-power system. To accurately estimate the cost of electro-mechanical equipment, it is necessary to have a thorough understanding of these factors. In a recent study published in 2022 by Al Zohbi [56], an attempt was made to consolidate the calculation method by drawing on the work developed by Cavazzini et al. in 2016 [57] and Al Zohbi in 2018 [58]. Equation 3.8 shows

a simplified formula for estimating the cost of electro-mechanical equipment for hydropower systems (C_{EM}) employing Francis Turbines.

$$C_{EM} = 190.37H_m^{1.27963} + 1441610.56 * Q_{ls}^{0.03064} + 9.62402P_{kW}^{1.28487} - 162157.28 \quad (3.8)$$

2. **Cost of civil works:** Due to the dependence on the site's particular layout, estimating civil works costs is complex. Civil construction cost is estimated using unit prices and parameters such as excavation volume in cubic meters. Expenses associated with excavating the reservoir and piping, backfilling, lining, constructing waterways, the powerhouse, and installing electrical lines and piping fall under this category.

The expense associated with constructing a reservoir (C_{res}) varies depending on the type of reservoir and several key parameters. These factors encompass excavation costs, land acquisition expenses (C_{land}), coating expenditures (C_{coat}), and spillway outlays ($C_{spillway}$). Notably, in the case of valley dam types, the excavation cost is typically disregarded. To estimate these costs, the following expressions can be employed:

$$\begin{aligned} C_{land} &= \alpha * S_{tank} \\ C_{coating} &= \delta * S_{coat} \\ C_{spillway} &= \sigma * C_{land} + C_{coating} \\ C_{res} &= C_{land} + C_{coating} + C_{spillway} \end{aligned} \quad (3.9)$$

where S_{tank} is the surface of the reservoir (m^2), S_{coat} is the surface needed to be coated (m^2), α is the cost of 1 m^2 of land ($\text{€}/m^2$), and δ is the cost of coating of 1 m^2 ($\text{€}/m^2$).

The cost associated with the penstock (C_{pens}) is calculated by combining several components, including the thickness of the penstock (t_{pens}) [59], excavation expenses ($C_{pens,exc}$), penstock material costs ($C_{pens,mat}$), and the cost of concrete work ($C_{pens,conc}$) [60]. Equation 3.10 shows the estimation for the penstock expenditure formula.

$$\begin{aligned} t_{pens} &= \frac{0.1 * H * D_{opt}}{2\sigma} \\ C_{pens,exc} &= 1.39 * D_{opt}^2 * C_e * L_{pens} \\ C_{pens,mat} &= t_{pens} * \rho * L_{pens} * C_m \\ C_{pens,conc} &= 0.6 * D_{opt}^2 * L_{pens} * C_c \\ C_{pens} &= C_{pens,exc} + C_{pens,mat} + C_{pens,conc} \end{aligned} \quad (3.10)$$

where σ is the allowable stress for the material of the penstock.

The powerhouse refers to the building that houses the majority of the electrical and mechanical equipment required for power generation. This power plant can be underground or on the ground's surface. Using a formula developed by Signal et al. (2008) [61], the construction cost of the powerhouse (C_{PH}) is determined by factors such as the head (H) and the power output (P) of the hydroelectric system.

$$C_{PH} = 30421.22P^{-0.238} H^{-0.0602} \quad (3.11)$$

The cost associated with the investment in transmission line infrastructure is derived from Midcontinent Independent System Operator (MISO) guidelines [62]. These guidelines consider

the costs associated with land acquisition and securing the right-of-way for transmission lines, construction structures and their foundations, professional services and overhead, and the conductor (the wire that carries the electricity) and shield wire (used for safety and grounding purposes). These factors estimate the total investment required for power line transmission (C_{trans}).

3. **Indirect cost:** In this context, indirect costs include a variety of engineering-related expenses, such as project management, taxes, costs associated with potential risks and unforeseen events, and project monitoring expenses. By the methodology proposed by Zhang et al. (2012), these indirect costs are equal to 50% of the direct costs, which include the combined costs of electromechanical equipment and civil work [59]. Indirect costs are supplementary expenditures necessary for the successful planning, execution, and oversight of the hydroelectric project but not directly related to the physical construction of equipment or infrastructure.

Operational Expenditure (OPEX)

The OPEX costs are the expenses associated with the ongoing operation and maintenance of the hydroelectric system's various components. These elements include the electrical infrastructure, hydro-mechanical components (such as turbines and generators), and the civil engineering framework (including dams and other structures). Numerous studies have evaluated OPEX costs, and the method of calculation can vary [63] [64]. It is typically expressed as a percentage of the initial CAPEX or as an annual cost per kilowatt (cost/kW) of installed capacity.

In this study, the approach used for estimating OPEX costs aligns with research conducted by De Jager et al. (2011). Their research suggests that, for large hydropower installations, the average OPEX cost is approximately \$42 per kilowatt per year [63]. This figure provides a valuable benchmark for assessing the ongoing expenses associated with operating and maintaining a hydropower plant, in this case, SPHS, helping to ensure the project's economic feasibility and sustainability over time.

3.3. Carbon Emission Reduction Calculation

The study uses the technical and economic potential of SPHS to calculate the carbon emission reduction. This strategy entails scenarios predicated on these potentials, in which SPHS systems are presumed to generate substantial electricity. This electricity generation is a direct replacement for Indonesia's primary source of carbon emissions, coal-fired power production. The method necessitates determining the difference in CO₂ emissions between electricity generated by coal-fired power plants and SPHS systems. The calculated difference represents the quantifiable reduction in carbon emissions that can be realised by implementing SPHS technology.

Site Rank and Classification Criteria

This chapter delves into the methodology used to rank and classify the identified SPHS sites based on their priority and feasibility. This chapter explains the criteria and parameters for assessing and differentiating these sites.

4.1. Selection Criteria

This study uses a hybrid method known as Analytic Hierarchy Process-Technique for Order of Preference by Similarity to Ideal Solution (AHP-TOPSIS) to classify potential SPHS sites based on multiple criteria [65]. Using the Analytic Hierarchy Process (AHP) method, weights are assigned to various evaluation criteria based on their relative importance [66]. Once the criteria are weighted, the Technique for Order of Preference by Similarity to Ideal Solution (TOPSIS) method is applied to classify and rank the potential SPHS sites based on their overall performance against the established criteria, using the weights assigned to each criterion [15]. This combined approach offers a robust and systematic way to assess and classify potential SPHS locations, ensuring that the most suitable sites are identified for development.

These analysis parameters included the topography of the penstock line, the potential power that could be harnessed at each site, the site’s distance from the electrical grid, the type of land covering the area, the site’s proximity to the coastline, the LCOS, and the site’s total inundation area. The achieved consistency ratio (CR) from AHP analysis is 0.058, which is comfortably below the required threshold of 0.1, validating the consistency of the AHP results. These weighting factors were subsequently used in the TOPSIS analysis, allowing for a comprehensive and systematic classification of the potential SPHS sites based on their weighted criteria, as detailed in Table 4.1.

Table 4.1: Weights of selected criteria for the TOPSIS analysis

Criterion	Weight
Topography of penstock line	0.55
Potential power	0.16
Type of land covering	0.09
Distance from the grid	0.06
LCOS	0.06
Area of the site	0.05
Distance from the coastline	0.03

4.2. Ranking The Feasible Sites

Following determining parameter weights through the AHP, the analysis advances to the TOPSIS analysis, which is the next crucial step. This comprehensive approach involves several distinct steps, each contributing to the systematic classification and ranking of the potential SPHS sites. The TOPSIS method includes the following steps:

1. **Creating the Decision Matrix (D):** The decision matrix is formed by organising the gathered data into a structured format. Each row in the matrix corresponds to a potential PHES site, while each column corresponds to a specific criterion. The data values in the matrix represent the performance or characteristics of each site about each criterion. Consequently, the size of the matrix depends on the number of sites and evaluation criteria.

$$D = \begin{matrix} & w_1 & w_1 & \cdots & w_n \\ \begin{matrix} A_1 \\ A_2 \\ \vdots \\ A_m \end{matrix} & \begin{bmatrix} x_{11} & x_{12} & \cdots & x_{1n} \\ x_{21} & x_{22} & \cdots & x_{2n} \\ \vdots & \vdots & \ddots & \vdots \\ x_{m1} & x_{m2} & \cdots & x_{mn} \end{bmatrix} \end{matrix} \quad (4.1)$$

2. **Normalisation of Criteria (R):** The next step is to normalise the evaluation criteria (R). Normalisation guarantees that all decision-making criteria are on the same scale and have equal weight. This step aids in the elimination of potential biases caused by differences in measurement units or scales.

$$R = r_{ijmn} \quad (4.2)$$

$$r_{ij} = \frac{x_{ij}}{\sqrt{\sum_{i=1}^m x_{ij}^2}}$$

3. **Weight Assignment (V):** In this phase, weights are assigned to each criterion to reflect their relative importance in decision-making. Those criteria deemed more important are assigned greater weights, while those considered less critical are assigned smaller weights.

$$V = v_{ijm \times n} \quad (4.3)$$

$$v_{ij} = w_j * r_{ij}$$

4. **Determination of Positive Ideal Solutions (PIS) and Negative Ideal Solutions (NIS):** The ideal solution represents the most desirable values for each criterion, whereas the negative ideal solution represents the most undesirable values. These solutions are determined based on the specified criteria and their respective weights. For each criterion, the ideal solution is denoted by the maximum value, whereas the minimum value denotes the negative ideal solution.

$$\begin{aligned} PIS : A : v_1, \cdots, v_j, \cdots, v_n, & \quad v_j = \max v_{ij} \\ NIS : A^- : v_1^-, \cdots, v_j^-, \cdots, v_n^-, & \quad v_j^- = \min v_{ij} \end{aligned} \quad (4.4)$$

5. **Calculation of Similarity Scores (S):** Similarity scores, referred to as proximity measures, are computed to determine the similarity between each alternative and the optimal solution. These

scores are calculated based on the weighted normalised values of the criteria for both the positive and negative ideal solutions.

$$\begin{aligned} S_i &= \sqrt{\sum_{j=1}^n v_{ij} - v_j^2} \\ S_i^- &= \sqrt{\sum_{j=1}^n v_{ij}^- - v_j^{-2}} \end{aligned} \quad (4.5)$$

6. **Calculating Relative Closeness to Ideal Solution (CP):** Each alternative's proximity to the optimal solution is determined by comparing its similarity scores to optimal and negative ideal solutions. Potential PHEs with greater relative proximity values are deemed preferable and ranked higher.

$$CP_i = \frac{S_i^-}{S_i + S_i^-} \quad (4.6)$$

7. **Ranking:** The potential PHEs are arranged in descending order based on relative closeness values. The alternative with the highest relative closeness value is deemed the most appropriate or preferred option.

Using TOPSIS to rank feasible sites for PHE installations enables a systematic evaluation of potential locations based on various criteria shown in Table 4.1. Considering these criteria and their respective weights, the method identifies the most suitable sites that align with the project's objectives and constraints, facilitating informed decisions in planning renewable energy projects.

4.3. Classification

In this study, the classification of identified potential SPHS locations employs a Relative Closeness to the Ideal Solution (CP) distribution from the TOPSIS analysis result. This classification is based on calculating average values (μ) and standard deviations (σ). The identified potential SPHS sites are categorised into ten classes, with the Relative Closeness to the Ideal Solution (CP) of each potential site serving as the criterion for classification, as outlined in Table 4.2.

Table 4.2: Classification criteria

Class	Closeness Index (CP_i)	
	Min	Max
1	$>\mu + 0.8\sigma$	
2	$>\mu + 0.6\sigma$	$\leq \mu + 0.8\sigma$
3	$>\mu + 0.4\sigma$	$\leq \mu + 0.6\sigma$
4	$>\mu + 0.2\sigma$	$\leq \mu + 0.4\sigma$
5	$>\mu$	$\leq \mu + 0.2\sigma$
6	$>\mu - 0.2\sigma$	$\leq \mu$
7	$>\mu - 0.4\sigma$	$\leq \mu - 0.2\sigma$
8	$>\mu - 0.6\sigma$	$\leq \mu - 0.4\sigma$
9	$>\mu - 0.8\sigma$	$\leq \mu - 0.6\sigma$
10		$\leq \mu - 0.8\sigma$

Technical and Economical Potential of Seawater Pumped Hydro Storage

This chapter examines the technical and economic potential of SPHS in Indonesia. In terms of the technical aspect, it examines the system's capacity for power regeneration and energy supply and potential sites categorised for their suitability. On the economic front, the chapter examines several aspects, including the LCOS, initial investment requirements, and a comparative analysis concerning other energy storage systems.

5.1. Technical Potential

Following the execution of the PyQGIS model explained in Chapter 3, a thorough evaluation revealed 682 potential SPHS sites dispersed across nearly all of Indonesia's major islands except Kalimantan Island. However, 73 of these potential SPHS sites were located within protected natural areas. Given the conservation objectives and environmental sensitivity of these regions, the construction of large-scale infrastructure, such as SPHS, is strictly prohibited. Finally, 609 feasible sites of SPHS have been found. Figure 5.1 visually depicts these potential SPHS sites and their geographical distribution, indicated by red dots.

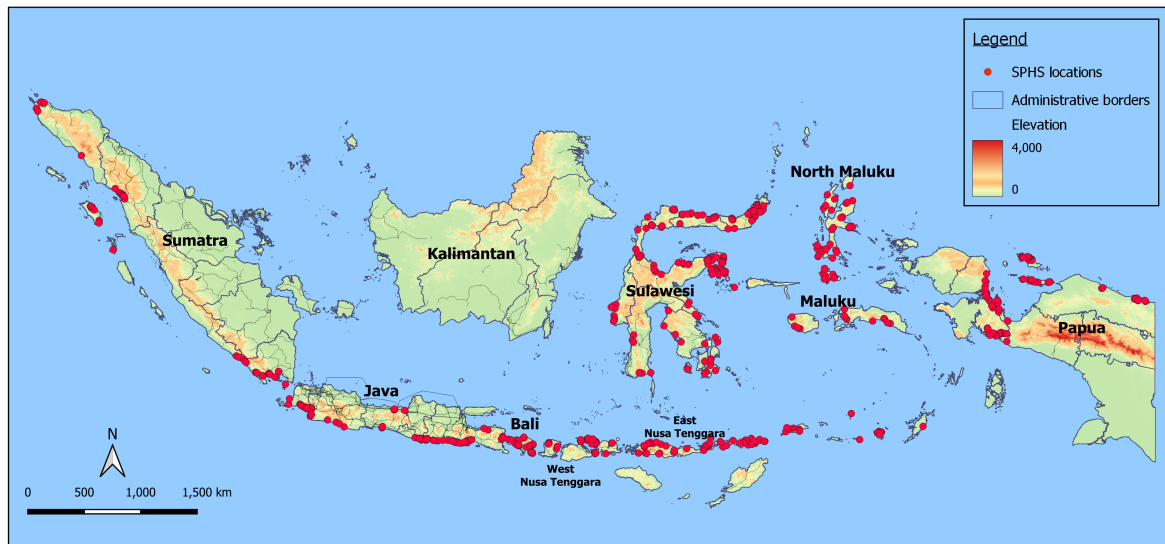


Figure 5.1: Distribution of 609 identified SPHS sites in Indonesia.

The absence of identified SPHS sites in Kalimantan and the eastern coast of Sumatra can be attributed to the geographical characteristics of these regions. In Kalimantan, such a head differential is not prominent, making it unsuitable for SPHS development. Similarly, the eastern coast of Sumatra faces a similar limitation due to a lack of significant head differences in the terrain. As for the western coast of Sumatra, the topography consists of extremely steep hills and narrow valleys, which presents challenges in constructing ideal reservoirs for SPHS systems. These geographical factors play a pivotal role in determining the feasibility and suitability of SPHS development in different regions of Indonesia.

5.1.1. SPHS Potential on National and Grid System Level

Leaving aside the potential locations in the nature reserve areas, 609 noteworthy sites were identified as prime possible sites for constructing SPHS facilities following an evaluation utilising the developed model. This evaluation included many factors and considerations, such as minimum power that can be regenerated, maximum distance from coastline, and minimum elevation, to ensure that these locations met the criteria, ensuring their viability and potential for successful SPHS implementation. These selected sites exhibit a wide range of geographical and topographical characteristics, demonstrating the adaptability of SPHS as an energy storage system to various terrains and landscapes. The peak power generation capability, as explained in Subsection 3.2.2, across these 609 locations varies widely, spanning from 15 to 316 MWp for each site.

Figure 5.2 represents the distribution among the identified SPHS sites, categorised by the power they can provide. This data provides insights into the prevalence of SPHS sites across different power ranges. Notably, a substantial portion of the identified sites falls within the 15 to 45 MW range, with 420 locations falling into this category. On the other hand, SPHS sites that can deliver more than 200 MW represent a smaller population in comparison.

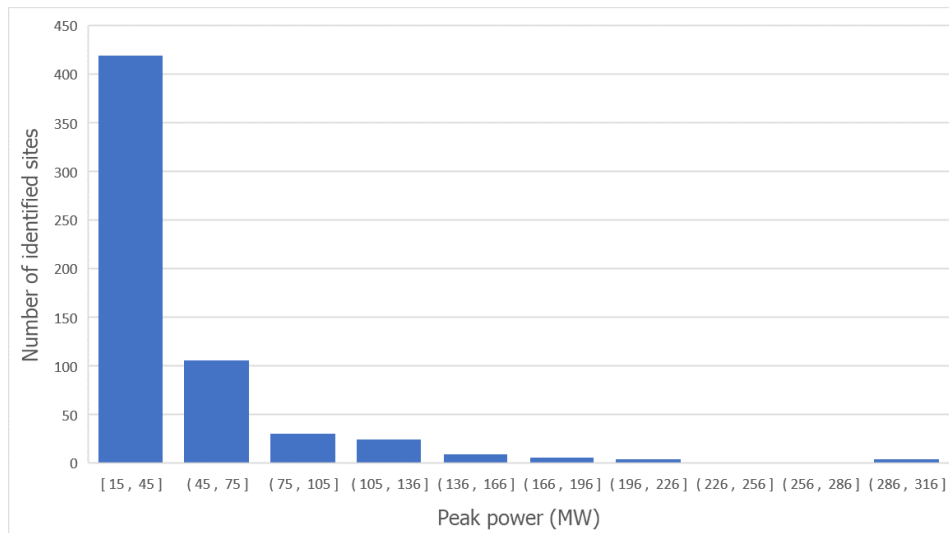


Figure 5.2: Distribution of SPHS sites per peak power classification.

The cumulative peak power potential that can be regenerated across all 609 sites is 29 Gigawatt-peak (GWp), 37% of projected peak power demand in 2030 on a national scale (77 GWp [18]). This substantial power regeneration seems to potentially contribute to Indonesia’s energy needs, supporting the nation’s growing demand for dependable and sustainable power sources. These SPHS sites could collectively store and regenerate approximately 48 TWh of electricity annually, almost 10% of annual energy demand nationwide (500 TWh). Furthermore, these SPHS systems are poised to support the effective integration of intermittent energy sources into the nation’s energy grid. Their ability to store excess energy during periods of surplus and discharge it during high-demand periods ensures a consistent and reliable energy supply, contributing to Indonesia’s energy ecosystem’s overall resilience and sustainability. The comparison at the national level between the potential energy storage and power generation of SPHS and the predicted energy consumption in 2030, serving as a benchmark year, is presented in Table 5.1.

Table 5.1: Comparison of annual energy and daily peak power between demand and SPHS

	Seawater-pumped hydro storage	Projected consumption 2030
Annual energy production/consumption (TWh)	48	500
Daily peak power generation/consumption (GWp)	29	77

At the national level, the potential energy harnessed from SPHS presents a notable percentage compared to the overall energy demand. Based on its technical potential, SPHS is expected to play a role in stabilising the energy production landscape, particularly with the increasing integration of intermittent renewable energy sources into the grid. The detailed information regarding SPHS sites properties can be found in Appendix A. However, a deeper dive into the grid system level reveals a more nuanced picture.

Take, for instance, the highly populated islands of Sumatra and Java, where energy demand is notably higher than the energy that SPHS systems could provide. These regions represent significant energy hubs, and while SPHS contributes to the energy mix, it may only partially cover the energy needs. This highlights the need for a diversified energy portfolio and enhanced infrastructure to ensure

a stable and uninterrupted power supply to these populated areas.

In contrast, there is a remarkable surplus of energy supplied by SPHS compared to local demand on other islands. This disparity between energy supply and demand highlights the need for a strategic and well-integrated approach to energy planning and infrastructure development, taking into account the unique energy landscapes of the different regions of the archipelago. Figure 5.3 presents the detailed findings of SPHS potential in every electrical grid.

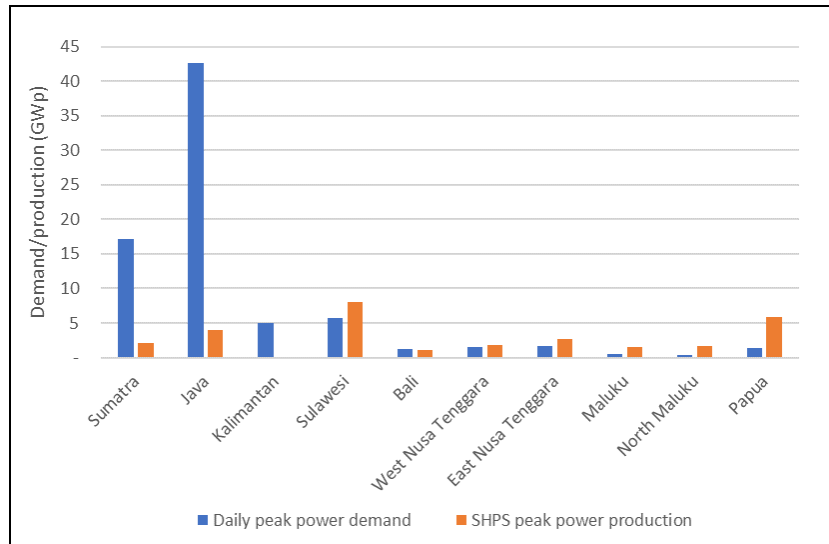


Figure 5.3: Electricity demand and SPHS power production per electrical grid.

5.1.2. Classification of The Potential SPHS Sites

Given the economic constraint regarding investment in the infrastructure and energy dynamics across Indonesia's electrical grids, it becomes essential to prioritise the potential sites for SPHS. This prioritisation is a factor to be considered for effective energy planning and resource allocation. Building upon the conditions and criteria outlined in Chapter 4, as well as the corresponding weightings assigned to these criteria through AHP analysis, the study employs the TOPSIS method to carry out this classification.

Each of the 609 potential sites identified through the study was assigned a unique rank ranging from 1 to 609. Once all sites were ranked, they were classified into ten distinct classes based on their relative closeness values calculated through the TOPSIS analysis, as explained in Subsection 4.3. Each class represents a cluster of sites that exhibit similar characteristics and meet specific criteria for suitability and feasibility in hosting SPHS installations. For instance, Class 1 represents the highest priority potential sites for SPHS, while Class 10 includes the least favourable sites regarding suitability and feasibility.

Figure 5.4 illustrates two distinct examples of identified sites with varying characteristics. The first example, as seen in Figure 5.4a, represents Class 1 of the classification, situated in West Nusa Tenggara province. This site boasts a substantial peak power capacity of 116 MWp. Notably, the topography of the shortest penstock line exhibits a favourable attribute with a uniform slope, enhancing its suitability. Furthermore, the predominant land cover in this area consists of shrubland.

In contrast, the second example, as seen in Figure 5.4b, in Aceh province, represents Class 10. This site has a relatively lower peak power capacity of 27 MWp. Moreover, it is important to note that the topography of the shortest penstock line in this location is less ideal due to a significant difference in elevation between the site and the coastline, which presents engineering challenges for implementation.

While there is potential for constructing the penstock underneath the ground using a tunnel, this study considers penstock lines built above ground level. The decision to exclude underground penstock options is a deliberate choice, and as a result, the topography of the penstock line becomes an essential aspect of consideration.

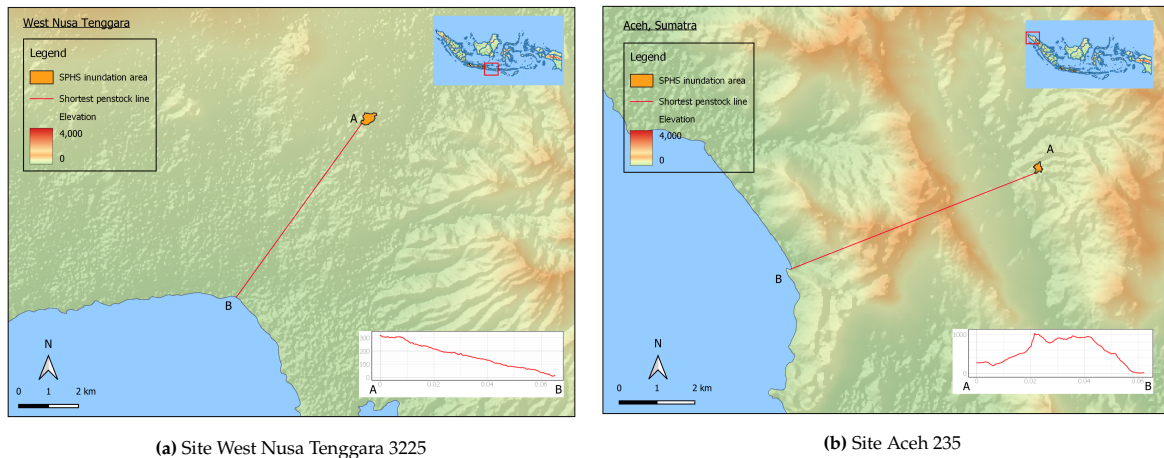


Figure 5.4: Example of the SPHS sites

From the TOPSIS analysis explained in Chapter 4, it becomes evident that Class 1 sites, representing the most promising locations under the multicriteria analysis (TOPSIS analysis), exhibit the highest peak power production among all classes. It is noteworthy that even though Class 1 sites provide substantial peak power, they still fall short of meeting the energy demand within most grid systems, except for the Papua grid system. This observation underscores the need for strategic site selection and the potential for SPHS to play a role in specific regional energy solutions. Table 5.2 presented below shows SPHS peak power production across different electrical grid systems, categorised by their respective classes.

Table 5.2: SPHS peak power production on each electrical grid system per class

Grid system	Demand (GWp)	SPHS (GWp)	SPHS power per class (GWp)										Number of sites	
			1	2	3	4	5	6	7	8	9	10		
Sumatra	17	2	0.2	-	-	-	-	-	-	-	-	0.6	1.4	56
Java	42	4	0.3	0.4	1.4	0.8	0.6	0.1	0.1	0.2	0.1	-	-	109
Kalimantan	5	-	-	-	-	-	-	-	-	-	-	-	-	-
Sulawesi	6	8	2.2	0.5	0.5	0.5	1.4	0.7	0.6	0.3	0.3	1.0	152	
Bali	1	1	0.2	0.4	0.2	0.1	-	0.1	0.0	0.0	0.0	0.4	28	
West NT	2	2	0.7	0.4	0.1	0.1	0.2	0.2	0.0	-	-	-	36	
East NT	2	3	0.5	0.2	0.3	0.2	0.7	0.2	0.1	0.1	0.1	0.2	54	
Maluku	0.5	1	0.5	0.2	0.2	0.2	0.0	0.1	0.0	-	0.0	0.3	33	
N. Maluku	0.5	2	0.3	0.2	0.3	0.4	0.2	0.1	0.1	-	0.1	0.1	43	
Papua	1	6	2.1	0.2	0.4	0.8	0.3	0.5	0.2	0.0	0.2	1.0	98	
Total	77	29	6.9	2.6	3.4	3.1	3.4	2.0	1.2	0.7	1.4	4.1	609	

Figure 5.5 through Figure 5.14 provide visual representations of these sites, organised according to their respective classes. These figures offer insights into the geographic diversity of SPHS potential in Indonesia, shedding light on how these sites are dispersed across different regions and their classification within the ten distinct classes.

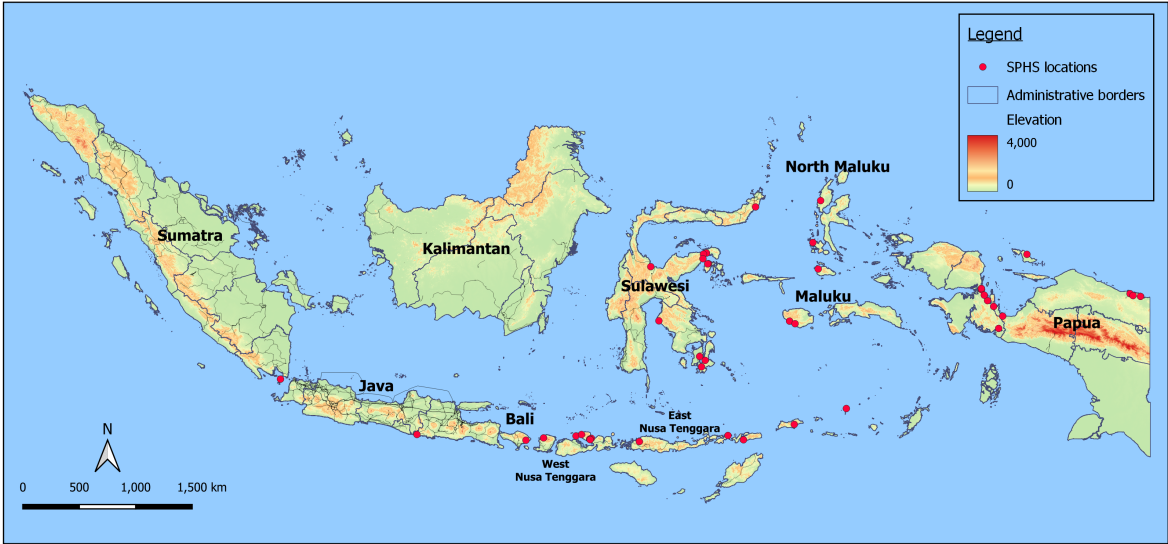


Figure 5.5: Distribution of class 1 SPHS sites.

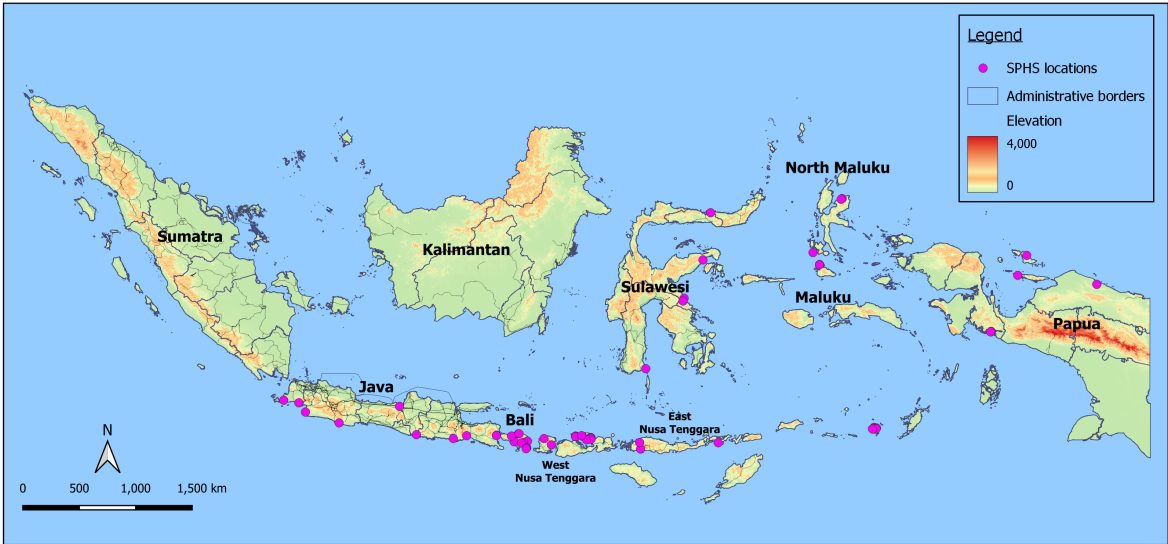


Figure 5.6: Distribution of class 2 SPHS sites.



Figure 5.7: Distribution of class 3 SPHS sites.



Figure 5.8: Distribution of class 4 SPHS sites.

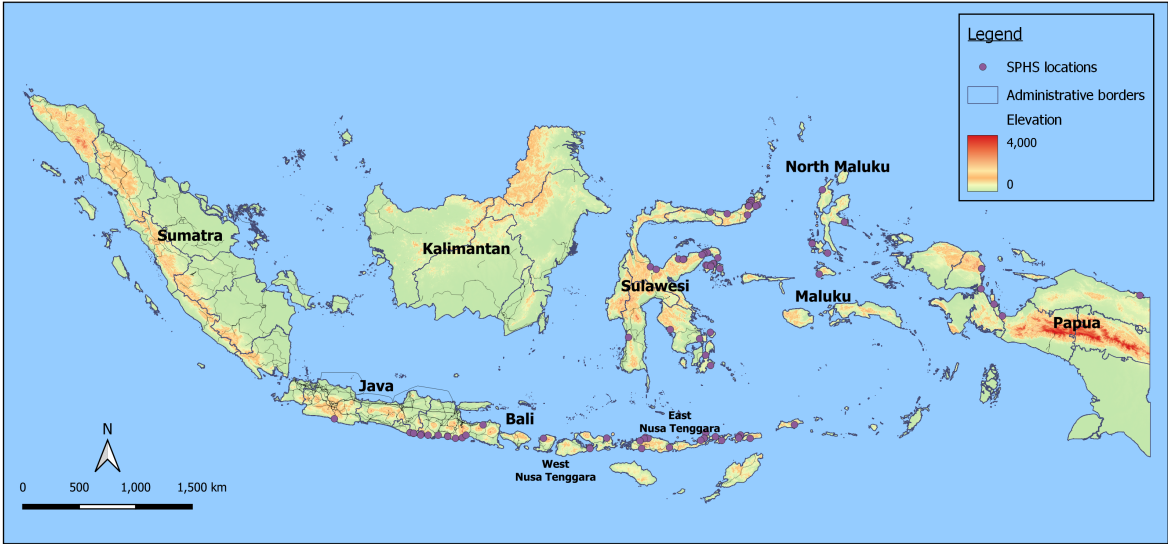


Figure 5.9: Distribution of class 5 SPHS sites.

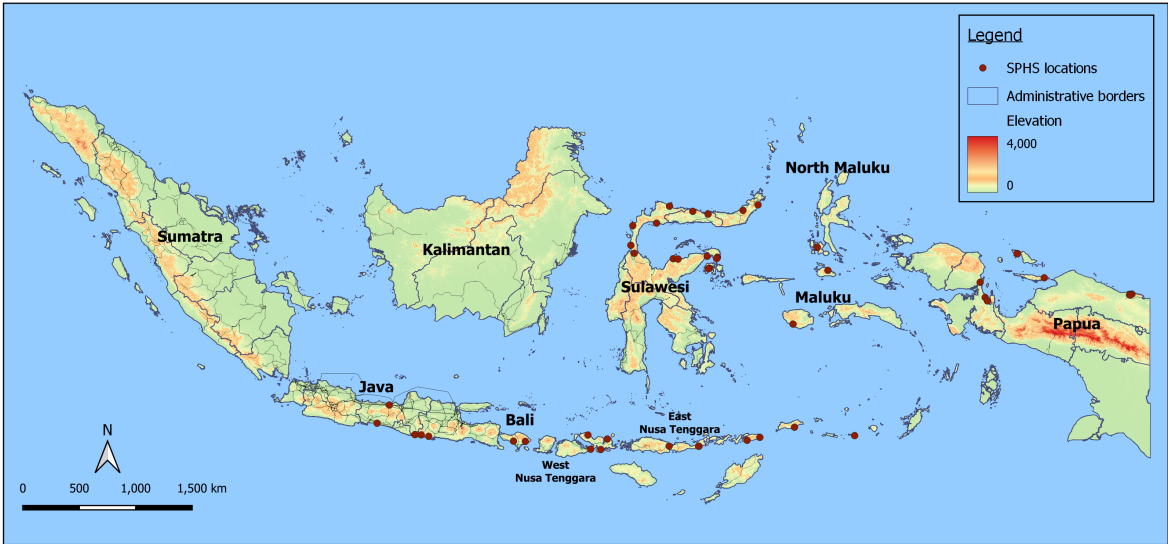


Figure 5.10: Distribution of class 6 SPHS sites.



Figure 5.11: Distribution of class 7 SPHS sites.



Figure 5.12: Distribution of class 8 SPHS sites.



Figure 5.13: Distribution of class 9 SPHS sites.

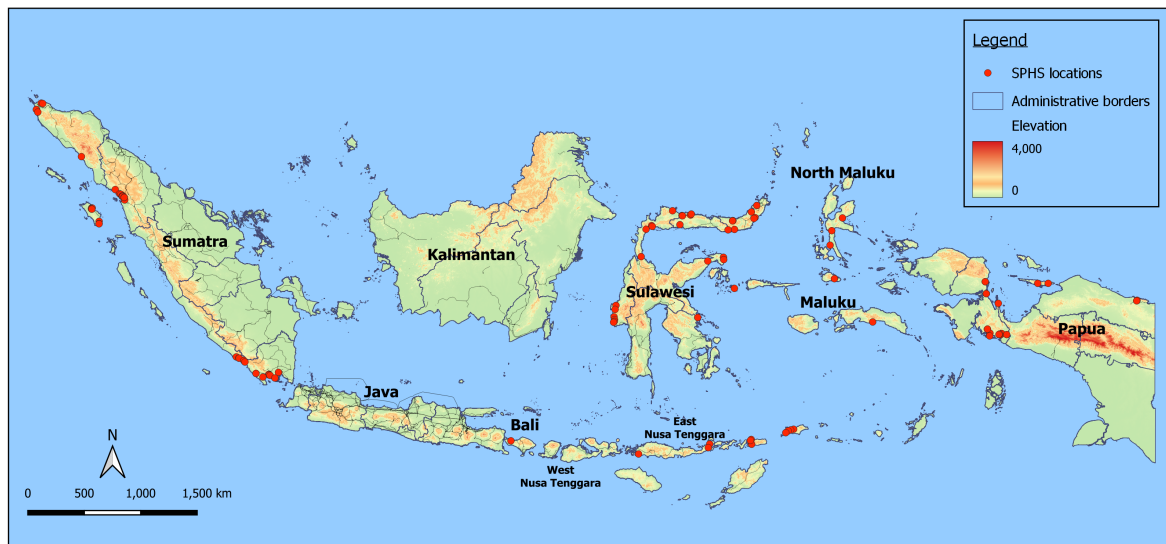


Figure 5.14: Distribution of class 10 SPHS sites.

Figure 5.5 shows that the Class 1 priority classification consists of 44 SPHS sites, primarily concentrated in eastern Indonesia. This distribution is influenced mainly by ideal heads and suitable topographical conditions in these areas. In contrast, the SPHS sites identified in Java Island are classified as lower priority, falling mainly within Class 2 to 5. This categorisation is primarily because power produced by SPHS systems identified in Java is lower than Class 1.

The SPHS sites identified in Sumatra are predominantly classified as Class 9 and 10. This classification is attributed to the challenging topography observed along the penstock lines in Sumatra, which is more demanding than other islands. The rugged terrain and geographical characteristics in this region make it less suitable for SPHS development, resulting in a lower priority classification. The SPHS sites identified in Sulawesi, Maluku, Nusa Tenggara, and Papua display a broader distribution across various priority classes, ranging from Class 1 to Class 10. Unlike some other regions where the classification tended to be concentrated in a few specific classes, these areas in eastern Indonesia exhibit a more

balanced distribution of SPHS sites across different priority levels. This suggests that these regions' topography and geographical conditions allow for a wider range of SPHS development possibilities. The detailed classification of identified SPHS sites can be seen in Appendix B.

Table 5.3 below summarises the peak power and annual energy production potential for the identified SPHS sites. This information underscores the contribution that SPHS can make to the nation's energy landscape. However, it's important to remember that harnessing this potential effectively will require careful planning and consideration of various factors, including grid integration.

Table 5.3: Power and energy provided by identified SPHS systems

Class	Number of sites	Power		Annual energy	
		Average per site (MW)	Total (GW)	Average per site (GWh)	Total (TWh)
1	44	157	7	243	11
2	57	46	3	77	4
3	89	39	3	66	6
4	87	35	3	60	5
5	81	42	4	70	6
6	50	41	2	69	3
7	40	31	1	54	2
8	20	34	1	59	1
9	37	37	1	63	2
10	104	40	4	66	7
Total	609		29		48

5.2. Economical Potential

The assessment of the economic potential of SPHS in Indonesia involves an analysis of the comparison of electricity prices in Indonesia with the total LCOS associated with SPHS and the average Levelised Cost of Electricity (LCOE) related to renewable energy sources in Indonesia, as calculated by existing studies. LCOS represents the cost of storing energy over the system's lifetime, considering factors such as initial capital expenditure, operation and maintenance costs, and the discount rate.

The goal is to assess whether SPHS can offer competitive pricing for energy storage while supporting the integration of intermittent renewable energy sources. By comparing electricity prices and the total LCOS and LCOE values, this analysis aids in understanding the cost-effectiveness and economic feasibility of implementing SPHS in the Indonesian energy landscape.

5.2.1. Levelised Cost of Storage (LCOS)

The LCOS for SPHS in Indonesia exhibit a range from approximately 3 cents €/kWh to 10.14 cents €/kWh, with an average value of approximately 6.25 cents €/kWh, consider 6% discount rate and 50 years lifetime of the project. The average CAPEX per site is 56.8 million euros, while the average OPEX is 1 million euros per site per year. Interestingly, as can be seen in Figure 5.15, the LCOS trend shows that as the power capacity of the SPHS system increases, the LCOS tends to decrease, indicating a potential economy of scale. However, a notable exception exists for SPHS systems with a power range of 195-255 MW, where the LCOS appears to increase. This phenomenon suggests that while power significantly determines LCOS, other factors such as distance to the coastline, land acquisition costs, material expenses, and other site-specific variables influence the final LCOS figure.

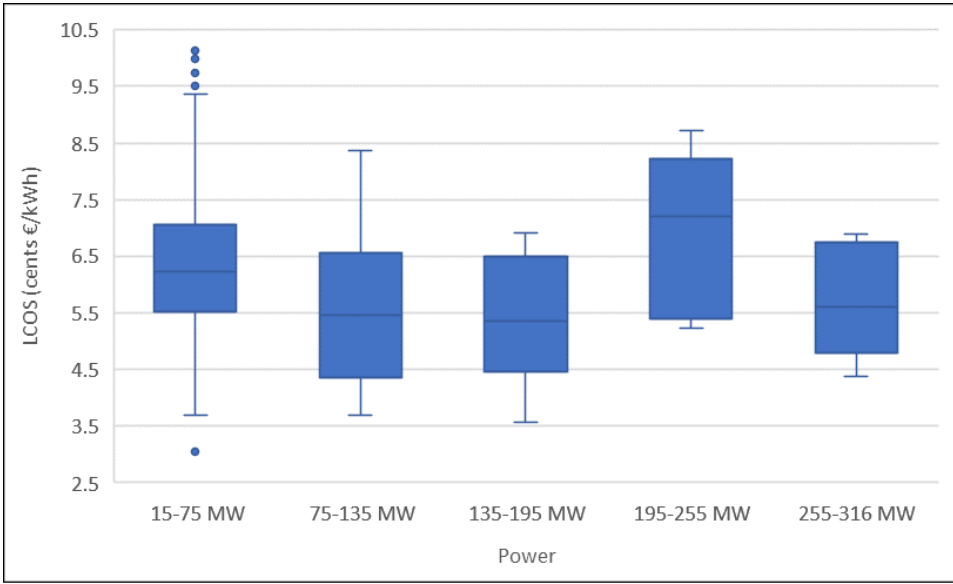


Figure 5.15: LCOS statistics.

In addition to analysing LCOS based on power production, exploring LCOS variations across different regions is equally intriguing to gain insights into localised economic and geographical factors that may influence the cost dynamics of SPHS deployment. By considering regional variations in factors like land acquisition costs, construction expenses, and other economic variables, stakeholders can make more informed decisions regarding the feasibility and prioritisation of SPHS development in specific areas of Indonesia. Figure 5.16 shows the LCOS's statistics in each region.

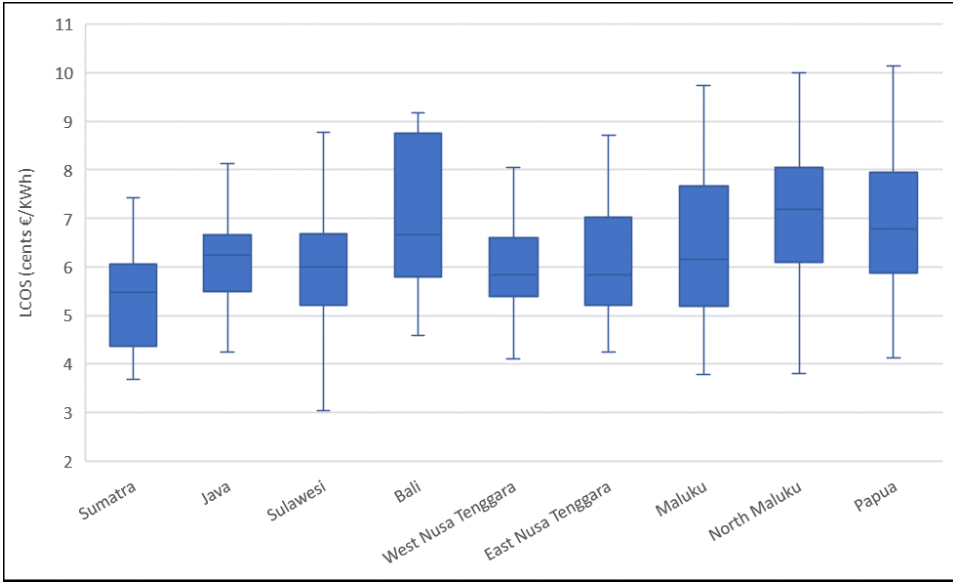


Figure 5.16: Distribution of LCOS per region.

Analysing the LCOS on a regional or grid system basis provides valuable insights into the economic feasibility of SPHS across different parts of Indonesia. One notable observation is that LCOS slight differences from region to region exist. Even though there are slight variations, these distinctions are instrumental in understanding the localised economic dynamics that can impact the viability of SPHS projects.

For instance, LCOS in Bali, an island known for its tourism and relatively high land prices, emerges as the highest among the regions studied. This higher LCOS in Bali can be attributed, at least partially, to the relatively elevated land acquisition costs in this tourist destination. The need to secure suitable land for constructing SPHS infrastructure contributes to the overall project expenses, impacting this region's LCOS.

Conversely, regions like Java and Sumatra present relatively lower LCOS figures compared to the other areas in Indonesia. Several factors may contribute to this cost advantage, including more favourable land acquisition conditions, proximity to suitable coastal areas for reservoirs, and other site-specific attributes that positively impact the overall cost-effectiveness of SPHS development. In contrast, in Papua, the relatively higher cost of civil works can be attributed to potentially elevated material prices in the region, which may impact the overall expenses associated with SPHS infrastructure development. Figure 5.17 below shows each region's average investment cost composition for a SPHS project.

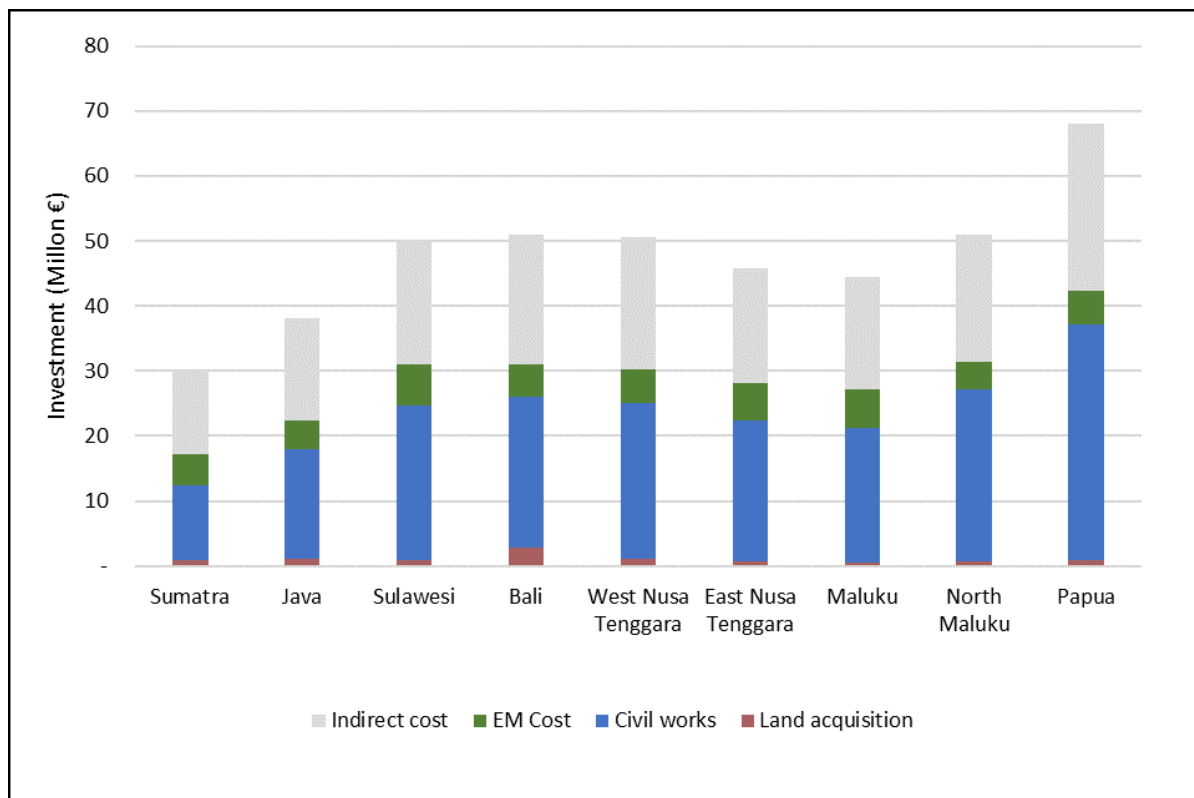


Figure 5.17: Average investment per site.

To summarise the distribution of LCOS, Figure 5.18 below illustrates the disparity in LCOS between various regions of Indonesia. The data demonstrates a similarity and consistency in the range of LCOS across these diverse regions. While the overall range of LCOS remains comparable, this observation emphasises the significance of contemplating regional nuances within a national context. Although LCOS may not vary substantially from region to region, other crucial factors, such as energy demand, available resources, and grid integration capabilities, may vary significantly and must be carefully considered during the SPHS deployment decision-making process.

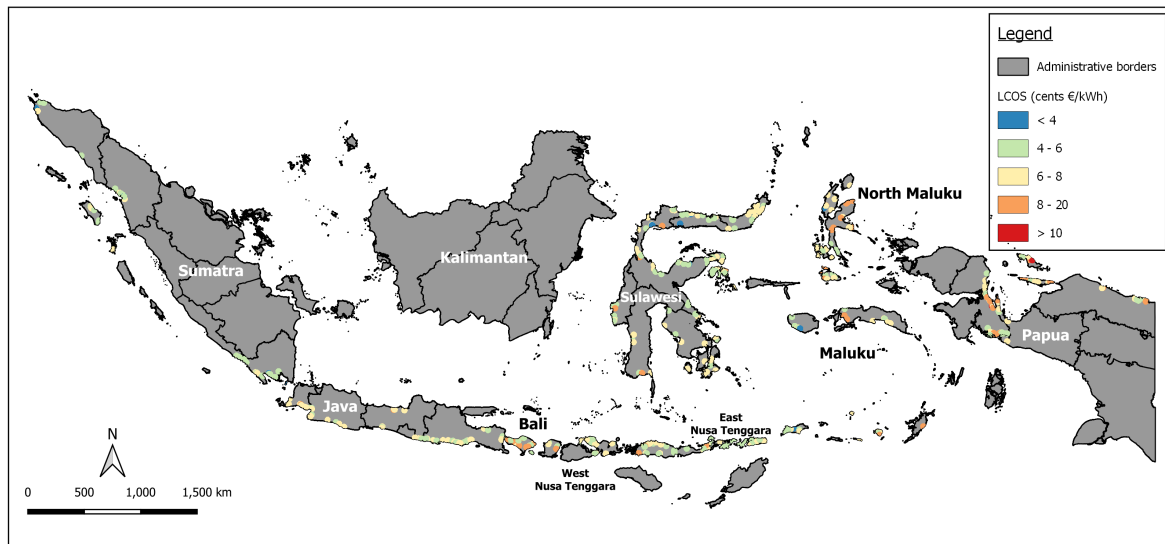


Figure 5.18: Map of SHPS' LCOS.

5.2.2. Economical Feasibility

The economic potential of SPHS in Indonesia is assessed through a comparative analysis that takes into account the LCOS and the LCOE associated with intermittent energy sources, specifically wind and solar energy. A combination of 50% wind and 50% solar energy generation is considered to derive these costs. According to research by the Institute for Essential Services Reform (IESR), the LCOE for wind energy is projected to be approximately 5.8 cents €/kWh, while for solar energy, it is estimated to be around 5.7 cents €/kWh in 2030 [67]. These costs are then compared to the projected electricity ceiling prices in 2030. The baseline for these future ceiling prices is set based on the current ceiling prices established in the Ministry of Energy and Mineral Resources Decree number 169/2021, which vary by region [68], with an added consideration of a 6% interest rate. Consequently, the economic potential of SPHS varies across different regions in Indonesia due to variations in electricity pricing and resource availability.

Out of the 609 analysed SPHS sites, it's important to note that only 297 of them exhibit both total LCOS and LCOE values that fall below the existing ceiling price for electricity. These 297 SPHS sites can collectively regenerate the power of 15 GWp. This finding underscores an economic consideration. While numerous SPHS sites have been identified in this study, not all of them are economically viable within the electricity pricing framework. Therefore, the economic feasibility of these SPHS projects is contingent upon potential adjustments to the ceiling price or other economic factors that could enhance their viability in the future. Figure 5.19 below illustrates the locations of SPHS sites, distinguishing between economically feasible and not.

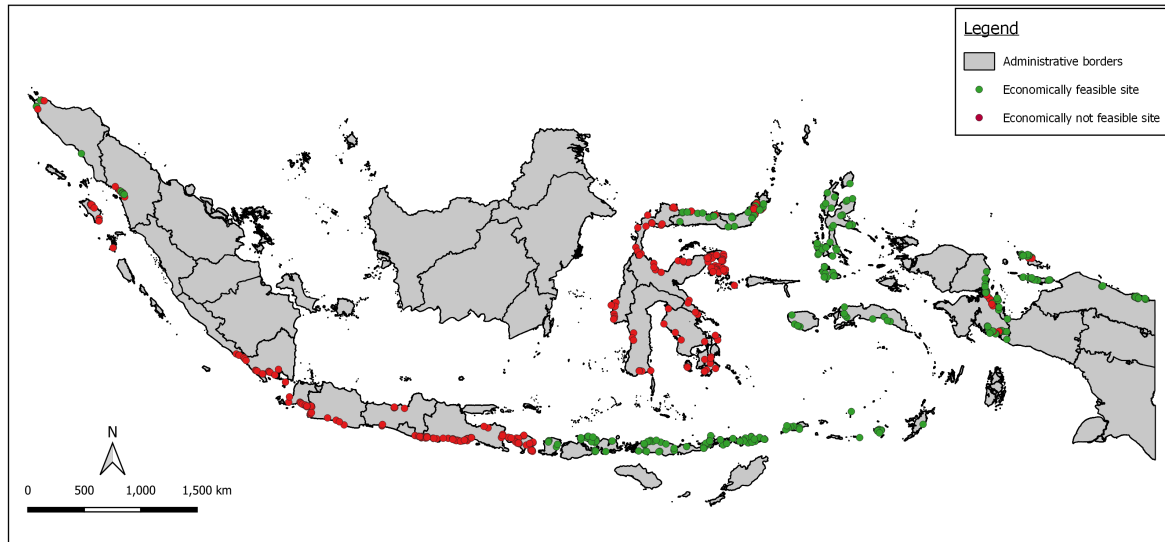


Figure 5.19: Economically feasible location of SPHS in Indonesia.

Many of the SPHS sites in the eastern part of Indonesia are economically feasible, while potential locations in Java and Bali do not meet the economic criteria. This discrepancy can be attributed to the ceiling electricity price regulations, where the more densely populated islands like Java and Bali tend to have lower electricity prices than other regions.

Table 5.4: Comparison between electricity ceiling price and total LCOE/LCOS per region

Region	Estimated ceiling price 2030 (cents €/kWh)	LCOS + LCOE (cents €/kWh)		
		Minimum	Maximum	Average
Sumatra	11.0	9.4	13.2	11.1
Java	7.4	10.0	14.6	11.9
Sulawesi	12.6	8.8	14.7	11.7
Bali	7.4	10.3	14.9	12.7
West Nusa Tenggara	14.0	9.8	13.8	11.7
East Nusa Tenggara	15.1	10.0	14.5	11.8
Maluku	19.7	9.5	15.5	12.1
North Maluku	17.9	9.5	15.7	12.9
Papua	14.7	9.9	15.9	12.6

The analysis results presented in Table 5.4 reveal some subtle variations in the average values of total LCOE and LCOS across different regions in Indonesia. However, the most critical factor determining project feasibility within each region is undeniably the ceiling price. Notably, the ceiling prices in Java and Bali are significantly lower compared to other regions. This discrepancy renders SPHS projects economically unfeasible in these areas. Therefore, there is a compelling need to reevaluate and adjust the ceiling prices in Java and Bali to ensure that SPHS projects become economically viable and contribute to Indonesia’s sustainable energy future. The discrepancy between the technical and economic potential of SPHS becomes apparent when examining the results for each region, as illustrated in 5.20 below.

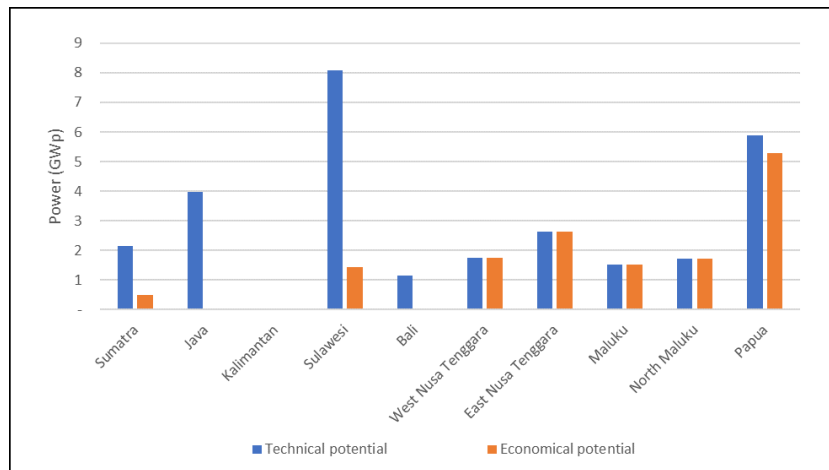


Figure 5.20: Comparison between technical and economical potential

The transition from the technical potential of 29 GWp power to the economical potential of 15 GWp highlights a significant reduction in feasible SPHS sites. Intriguingly, all the identified sites in the highly populated regions of Java and Bali do not align with economic feasibility criteria. Meanwhile, only a quarter of the identified locations in Sumatra and Sulawesi meet the economic viability.

5.2.3. Comparison with Other Energy Storage System

To put the result of the LCOS analysis conducted in this study into context, comparisons were made with LCOS values from previous studies on various energy storage systems. For instance, Mugyema et al. (2023) investigated battery and flywheel energy storage for a small-scale energy storage system (ESS) with a capacity of 10 MW [69]. Their research revealed significantly higher LCOS values of 28.8 cents \$/kWh for batteries and 11.5 cents \$/kWh for flywheels, underscoring the favourable LCOS of SPHS found in this study.

Cristea et al. (2022) assessed battery LCOS in Romania [70], while Martinez de Leon et al. (2023) focused on LCOS for hydrogen storage systems [71]. The LCOS values from these studies were generally higher than the LCOS of SPHS presented in this research. Moreover, a 2023 report from the Institute for Essential Services Reform (IESR) in Indonesia examined the LCOS of both PHES and batteries with a capacity of 100 MW. This report also indicated that the LCOS for these systems was higher than that of SPHS, reinforcing the economic competitiveness of SPHS as an energy storage solution in Indonesia. Table 5.5 presents the comparison of LCOS values obtained from this study and previous research.

Table 5.5: Comparison of LCOS Values - This Study vs. Previous Studies

ESS	This study	Mugyema, et.al (2023)	Cristea et.al (2022)	Martinez de Leon, et.al (2023)	IESR (2023)
SPHS/PHES	3 - 10.14 cents €/kWh				7.7 cents \$/kWh
Battery		28.8 cents \$/kWh	28 - 36.9 cents €/kWh		21.8 cents \$/kWh
Hydrogen				13.8 cents €/kWh	
Flywheel		11.5 cents \$/kWh			

5.2.4. Sensitivity Analysis

Sensitivity analysis is a tool for assessing the economic potential of SPHS in Indonesia. It involves the evaluation of variables such as CAPEX, OPEX, interest rates, infrastructure lifespan, and ceiling prices to understand their impact on the LCOS and, consequently, the economic feasibility of SPHS projects. This analysis helps identify which variables significantly enhance the economic potential of SPHS in Indonesia. Additionally, it aids in pinpointing support schemes or policy adjustments that can improve the economic viability of SPHS initiatives in the country. The LCOS and economic potential were assessed by varying each parameter within a $\pm 20\%$ range relative to the base LCOS value, which stands at 6.25 cents €/kWh, determined based on the average LCOS result. Similarly, the base value is 15 GWp for the economic potential. Figure 5.21 and Figure 5.22 show the sensitivity analysis results.

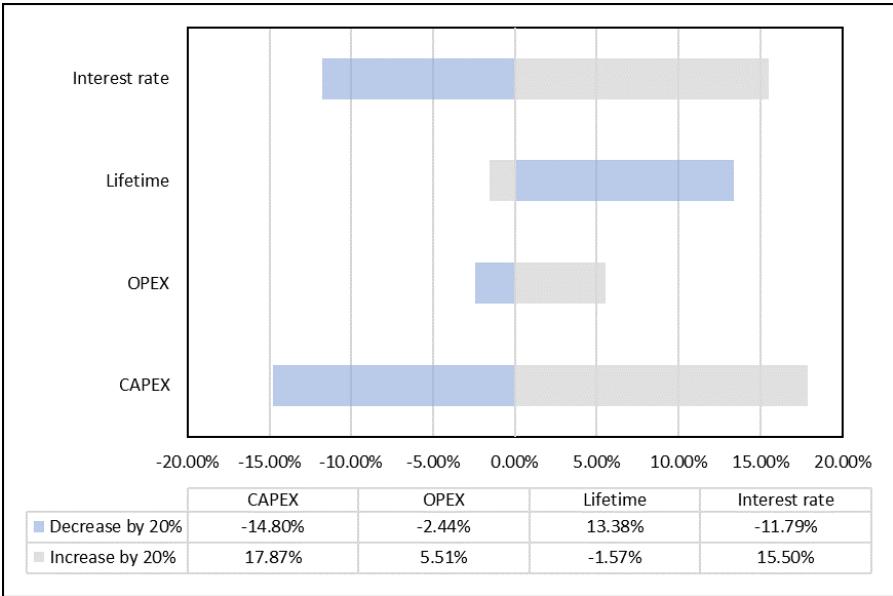


Figure 5.21: Sensitivity analysis of LCOS

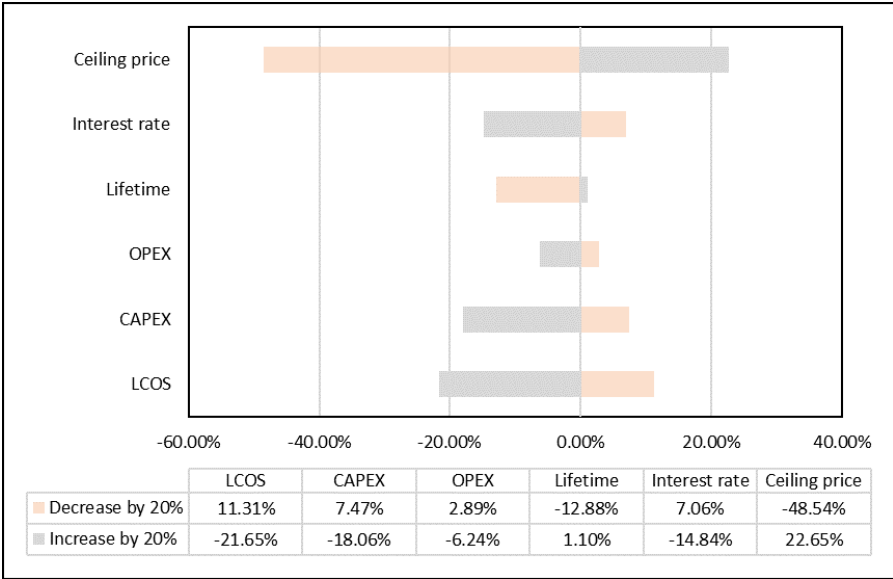


Figure 5.22: Sensitivity analysis of potential sites

The sensitivity analysis revealed that CAPEX has the most substantial impact on LCOS, followed by interest rate, infrastructure lifespan, and OPEX in descending order of significance. When CAPEX is reduced by 20%, LCOS can be decreased by around 15%. Conversely, a 20% increase in CAPEX leads to an LCOS increase of more than 17%.

The sensitivity analysis result also indicates that while changes in LCOS, CAPEX, OPEX, interest rate, and infrastructure lifespan have a limited impact on the economic feasibility of SPHS, increasing the ceiling price by 20% has a more pronounced effect. Specifically, raising the ceiling price by 20% can enhance the economic feasibility of SPHS by 23%. In contrast, a 20% reduction in the ceiling price leads to a substantial decrease in economic feasibility, amounting to a 48% reduction. This underscores the pivotal role of ceiling price adjustments in determining the economic viability of SPHS projects in Indonesia.

Environmental Impact

Chapter 6 delves into an examination of the environmental impact of SPHS development in Indonesia. As we continue our exploration of this energy storage solution, it is necessary to assess its environmental effects. This chapter offers a balanced perspective, discussing the positive contributions of SPHS in mitigating carbon emissions and the potential challenges and negative impacts.

6.1. Carbon Emission Reduction

In Indonesia, electricity generation still heavily relies on fossil fuels, particularly coal. Coal-fired power plants are a prominent part of the energy mix, contributing 61% to the nation’s electricity generation capacity [2]. Meanwhile, coal is one of the most carbon-intensive energy sources, emitting a substantial amount of carbon dioxide (CO₂) per unit of electricity generated. As shown in Figure 6.1, the carbon emissions associated with coal-fired power plants are estimated to be around 820 grams of CO₂ per kilowatt-hour (gCO₂/kWh) of electricity produced [23]. However, Indonesia aims to cut carbon emissions by 29% by 2030, with a focus on reducing coal-based electricity generation. By combining renewable energy sources, such as wind and solar, with SPHS, carbon emissions can be significantly reduced to meet the climate goals and maintain reliable energy production.

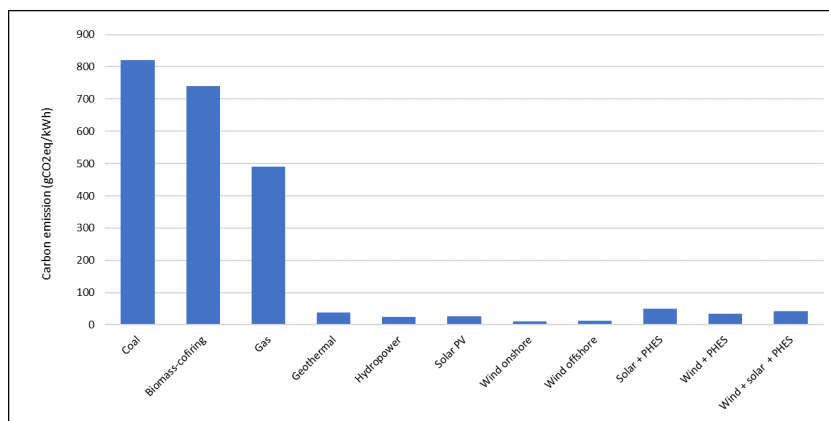


Figure 6.1: Carbon emission of various electricity generation

The technical and economical potential of SPHS become the foundation for calculating carbon emission reductions. In the scenario based on these potentials, SPHS generates a substantial amount of

electricity, replacing coal-fired production. Specifically, the 47 TWh of electricity produced by coal-fired power plants produce 39 million tons of CO₂ emissions. In contrast, the combination of wind, solar, and SPHS, which generates 47 TWh of energy in the technical potential scenario, emits only 2 million tons of CO₂. Similarly, the production of 24 TWh of electricity through coal-fired means contributes 20 million tons of CO₂, while the same amount generated through the combined renewable and SPHS system in the economical potential scenario results in just 1 million ton of CO₂ emissions. Table 6.1 below compares carbon emission produced by coal-fired power generation and SPHS system for every scenario.

According to the Electricity Supply Business Plan for 2021-2030, the carbon emissions from Indonesia's electricity sector are projected to reach 335 million tons in 2030 [2]. To meet the target of reducing carbon emissions by 29% in 2030, a substantial reduction of 97 million tons of CO₂ is required. The technical potential of SPHS offers a promising solution, as it has the potential to reduce carbon emissions by 37 million tons of CO₂, equivalent to 11% of the total carbon emissions, or around 38% of the target, aligning with Indonesia's emissions reduction objectives. Moreover, the economical potential of SPHS presents a reduction of 19 million tons of CO₂, which accounts for 6% of the total carbon emissions in 2030, or around 20% of the carbon reduction target.

Table 6.1: Carbon reduction per year

Scenario	Energy production per year (TWh)	Carbon emission per year (million ton CO ₂)		Carbon reduction per year (million ton CO ₂)
		Coal-fired	SPHS systems	
Technical potential	48	39	2	37
Class 1	11	9	1	8
Class 2	4	4	1	3
Class 3	6	5	1	4
Class 4	6	5	1	4
Class 5	6	5	1	4
Class 6	3	3	0.1	3
Class 7	2	2	0.1	2
Class 8	1	1	0.1	1
Class 9	2	2	0.1	2
Class 10	7	6	0.3	6
Economical potential	24	19.9	0.9	19

The distribution of SPHS sites and their energy potential, both in terms of technical and economic feasibility, leads to varying levels of carbon emission reduction across different grid systems within the nation. To visualise this discrepancy, Figures 6.2 and Figure 6.3 present the distribution of carbon emission reduction under the technical potential and economic potential scenarios, respectively. These figures provide valuable insights into how SPHS implementation can contribute to carbon emission reduction on a regional scale.

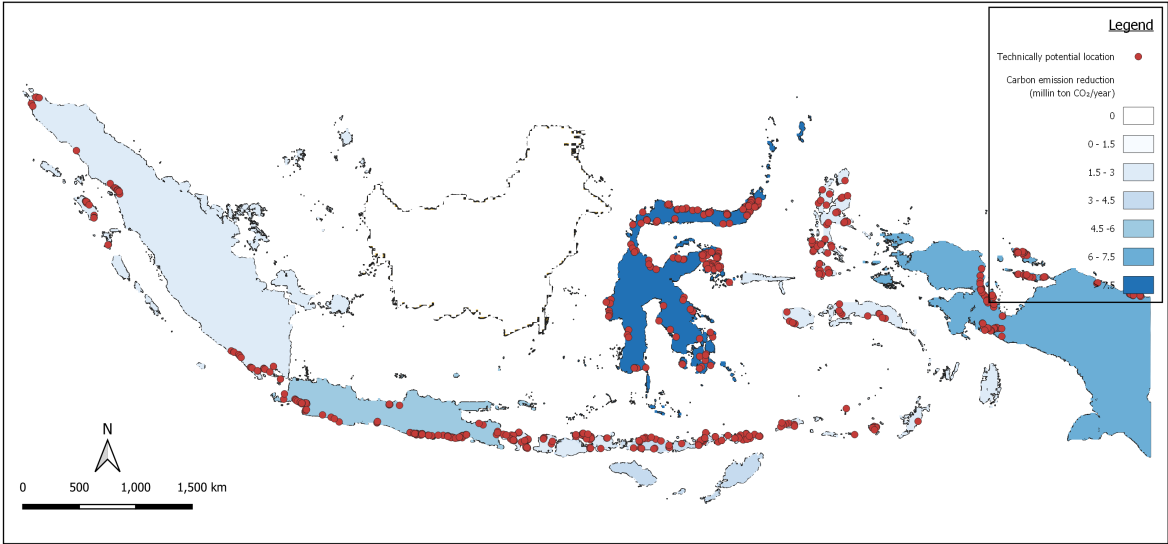


Figure 6.2: The reduction of carbon emission production per year based on the SHPS technical potential in every electrical grid.

Sulawesi emerges as the region with the most substantial technical potential for SPHS, capable of reducing 10 million tons of carbon emissions production per year if all technically feasible SPHS systems are developed within the region. Papua and Java follow, with the potential to reduce carbon emissions production by 7 million tons and 5 million tons of CO₂ per year, respectively. Sumatra, despite its substantial SPHS potential, is expected to contribute to a lower degree of carbon emission reduction compared to Java and Papua, with a reduction of 3 million tons of CO₂ per year. Smaller regions such as Bali, West Nusa Tenggara, East Nusa Tenggara, Maluku, and North Maluku also show notable carbon emission reduction potential, ranging from 1.5 to 3 million tons of CO₂ annually. These figures highlight the varied opportunities for carbon reduction across different regions of Indonesia through SPHS development.

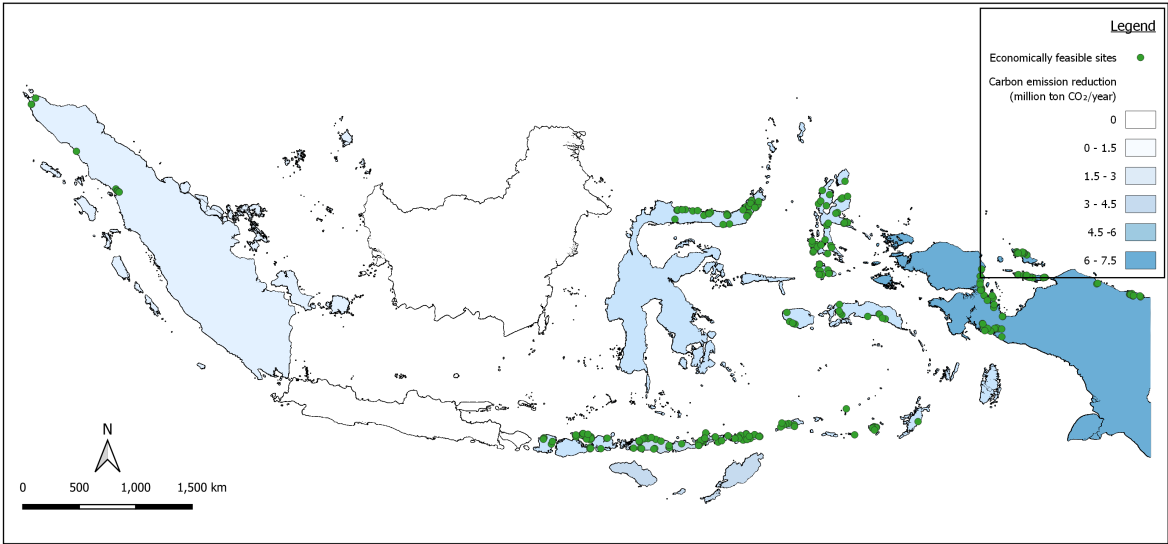


Figure 6.3: The reduction of carbon emission production per year based on the SHPS economical potential in every electrical grid.

Compared to its technical potential, the reduced economic feasibility of SPHS leads to a lower carbon

emission reduction potential, particularly in regions with significantly lower economic potential. In Java and Bali, the reduced economic viability renders SPHS incapable of contributing to carbon emission reduction. Similarly, the potential for carbon reduction in Sumatra and Sulawesi, while still at 0.6 and 2 million tons of CO₂ per year, respectively, falls far short of their technical potential, which could achieve a much greater reduction of 3 and 10 million tons per year, respectively. It must be noted that the economic potential of SPHS can increase in the future due to economic growth and the expected rise in the ceiling price of electricity more than predicted in this research. As the overall economy grows and electricity costs are anticipated to rise, the feasibility of SPHS projects may become more favourable.

6.2. Local Environment Impact

The development of SPHS systems presents certain environmental risks, predominantly associated with using seawater near or in the freshwater ecosystem. Seawater intrusion into groundwater is a possible environmental hazard. Seawater intrusion occurs when the draining and storage of seawater displaces or mixes fresh water in underground aquifers, leading to saltwater infiltration into freshwater sources. This phenomenon can have significant effects on ecosystems, agriculture, and the availability of potable water.

Seawater Intrusion

The risk of seawater intrusion into the SPHS system occurs predominantly during the pumping and storage of seawater in the reservoir. The porosity of the soil, the profundity of the groundwater table, and other technical parameters all contribute to this risk—seawater intrusion results from the displacement of freshwater by seawater in underground aquifers. When seawater is pumped into a reservoir, its higher specific gravity than fresh water causes the groundwater table to sink progressively. The impact of saltwater intrusion can be long-term and detrimental. It can lead to a gradual increase in salinity in local freshwater aquifers, affecting groundwater quality. This can impact ecosystems, agriculture, and drinking water supplies. The duration of the impact may be sustained if not mitigated effectively.

Several strategies can be implemented to reduce the risk of seawater intrusion in SPHS systems. A crucial stage is using impermeable materials, such as geomembranes, to line and isolate the reservoir from the surrounding soil, thereby reducing the probability of intrusion. The use of geomembranes has been included in the investment cost calculations in this study. Figure 6.4 shows the implementation of geomembrane in a reservoir. In addition, implementing physical barriers such as slurry walls or impermeable liners around the SPHS site can provide an additional layer of defence against seawater infiltration. To assure the efficacy of these mitigation measures, real-time, continuous monitoring systems of groundwater levels and salinity should be established. Detecting an intrusion as soon as possible is essential for prompt action. When an increase in the salinity of freshwater is detected, the protective coating system should be promptly maintained. In addition, risk considerations must be incorporated into the standard operating procedures for system maintenance and operation to manage and reduce the risk of seawater intrusion effectively.



Figure 6.4: Example of geomembrane installation in a reservoir [72]

Corrosion

The use of seawater in SPHS systems poses a significant corrosion risk to various components, including civil works such as penstocks, intake structures, and electromechanical equipment. The corrosive nature of seawater is due to its ability to degrade metal surfaces and encourage corrosion formation. This elevated risk of corrosion is a crucial factor in selecting materials for SPHS construction. Due to its corrosion resistance, GRP penstock material is preferred in this study over steel penstock. By utilising less susceptible materials to seawater's corrosive effects, SPHS systems can extend their operational lifetime and reduce the costs associated with corrosion-related damage.

Beyond these economic concerns, the rust caused by corrosion poses environmental dangers. When these rust particles decompose in water, they can potentially release harmful substances into the surrounding environment, contaminating the delicate marine ecosystem [73]. Furthermore, poor water quality may lead to the decline of fish populations. For the long-term effect, some corrosive byproducts can infiltrate the food chain through bioaccumulation, where toxins become concentrated as they move up the food chain. This can endanger the health of humans who ingest seafood from contaminated waters [74].

Several strategies can be employed to mitigate this risk. First and foremost, the selection of materials is crucial. Using non-corrosive materials, such as Glass Reinforced Plastic (GRP), for penstocks, intake structures, and other components in direct contact with seawater can substantially reduce corrosion-related risks. In addition, applying high-quality anti-corrosion coatings on non-replaceable metal components, such as pump-generator enclosures, can provide an additional layer of protection.

Furthermore, it is essential to implement routine inspection and maintenance protocols. Regularly examining all components for signs of corrosion, erosion, or damage enables prompt detection and repair. By applying corrosion-resistant coatings to vulnerable areas, the corrosion risk can be avoided. Monitoring systems that monitor salinity levels and the condition of metal surfaces can provide data in real-time to continuously evaluate the system's integrity. When corrosion is detected, prompt maintenance or replacement of affected elements is required to prevent additional damage. In addition, designing SPHS facilities with redundancy and backup systems can assure continuous operation and reduce the risk of unscheduled downtime due to corrosion-related failures. In conclusion, a combination of material selection, maintenance practices, and monitoring systems is necessary to mitigate corrosion risk effectively.

Conclusion and Recommendations

In this chapter, the thesis delves into the conclusions drawn to address the primary research questions and related subquestions, a reflection on the research's limitations, and a set of recommendations for future investigations.

7.1. Conclusion

The methodologies employed in this research have been instrumental in identifying potential locations for SPHS in the coastal regions of Indonesia. As Indonesia strives to integrate renewable energy into its power grid, the intermittent nature of sources like wind and solar can pose a challenge. As an alternative to the energy storage system needs, SPHS offers the ability to store and utilise this intermittent energy, contributing to a more stable and sustainable energy ecosystem. Each sub-question in this study was designed to address particular facets of the research, and the findings from these sub-questions collectively contribute to addressing the main research question.

SQ1: Where are the potential sites for seawater-pumped hydro storage in Indonesia?

The investigation into potential sites for SPHS in Indonesia using the PyQGIS algorithm developed in this research has identified a list of 682 locations. However, it is essential to note that 73 of these sites are located in protected natural areas where the construction of such infrastructure is prohibited. As a result, 609 feasible SPHS sites are dispersed across nearly all of Indonesia's main islands, except Kalimantan, due to its relatively flat terrain near the coast.

The potential sites are dispersed widely, considering Indonesia's diverse geography and coastlines. Sulawesi, renowned for its lengthy coastline, boasts the highest number of potential SPHS locations, totalling 152 sites. Java features 109 potential sites, Papua boasts 98 locations, and Sumatra offers 56 potential SPHS sites. The smaller island regions, including Bali, West Nusa Tenggara, East Nusa Tenggara, Maluku, and North Maluku, collectively house 194 potential SPHS locations. This distribution underlines the rich diversity and potential for seawater-pumped hydro storage throughout the Indonesian archipelago.

SQ2: What is the technical potential of seawater-pumped hydro storage in Indonesia?

609 identified SPHS systems could collectively regenerate a peak power output of 29 GWp from the energy stored in the systems from intermittent energy sources. This peak power production is equivalent to 37% of the projected peak power demand across the nation by 2030. The peak power production of

each potential SPHS site falls within a broad range, spanning from 15 to 316 MWp. Furthermore, the annual energy that can be stored and regenerated from these SPHS systems is 48 TWh of electricity. This annual energy production, amounting to 10% of the projected national energy demand in Indonesia for the year 2030.

SQ3: What is the economical potential of seawater-pumped hydro storage in Indonesia?

The LCOS for SPHS in the country exhibits a range, with values falling between 3 to 10.14 cents €/kWh. To determine the economic feasibility of each SPHS system, an analysis involving the comparison of LCOS and related LCOE with the ceiling price in the respective region was carried out. Among the 609 initially identified technically potential sites, only 297 were found to be economically viable. These sites collectively possess a peak power regeneration potential of 15 GWp and an annual stored and regenerated energy of 24 TWh. It is worth noting that no economically potential sites were identified in Java and Bali due to the relatively low ceiling prices in those regions. Conversely, the economically potential SPHS sites predominantly lie in the eastern regions of Indonesia, as these areas feature higher ceiling prices compared to the western part of the country.

SQ4: How much carbon reduction can be achieved by developing seawater-pumped hydro storage in Indonesia?

The impact of developing SPHS in Indonesia on carbon emissions is in line with the nation's commitment to reducing its carbon footprint. The technical potential of SPHS is particularly promising, potentially reducing carbon emissions by 37 million tons of CO₂ per year. This remarkable reduction constitutes 11% of Indonesia's annual total carbon emissions in the energy sector in 2030.

Furthermore, the economical potential of SPHS presents a noteworthy reduction in carbon emissions, amounting to 19 million tons of CO₂ per year. This reduction contributes to 6% of the total carbon emissions projected for 2030. These findings provide compelling evidence that the development of SPHS aligns harmoniously with Indonesia's goal of achieving a 29% reduction in carbon emissions by 2030.

Main Question: What is the potential for seawater pumped hydro storage in coastal areas of Indonesia?

In summary, this study has identified 609 potential locations for SPHS with a total power capacity regeneration of 29 GWp. Among these sites, 297 have been determined to be economically feasible, resulting in a combined power capacity regeneration of 15 GWp. When evaluating the technological potential scenario, it is evident that these sites could contribute to carbon reduction, with the potential to achieve a reduction of 38% of the 2030 target in carbon emissions reduction. Moreover, within the context of economic potential, these locations can potentially facilitate a carbon reduction of 21% towards the 2030 target.

7.2. Limitations of The Research

While this research has yielded insights and outcomes in capturing SPHS potential in Indonesia, it is necessary to acknowledge its limitations to provide a more comprehensive view of its scope and potential areas for further improvement. The utilisation of high-resolution DEM data from DEMNAS, boasting a resolution of 0.27 arc-seconds (equivalent to 8x8 meters), significantly impacted the research. While this dataset facilitated an in-depth analysis, the computational demands associated with such high-resolution data translated into prolonged processing times for the algorithm. This time-consuming

element hindered the ability to delve into other aspects requiring more attention, such as the geology condition of the site and local environmental issues.

Due to resource and time constraints, the research primarily focused on assessing the topographical features of the potential sites. Regrettably, the geological conditions of the sites and the specifics of the penstock line, which could substantially influence the feasibility of each site, were not taken into account. This limitation is a consideration for future studies aiming to provide a more comprehensive evaluation of SPHS sites.

In LCOS assessment, a simplified methodology was employed for estimating CAPEX and OPEX. While this simplified approach offered practicality in this context, it may not always provide the most precise calculations for SPHS projects. The uniqueness and variability of SPHS projects need more customised and accurate financial assessments.

Another limitation of this study is the exclusion of natural hazard considerations, such as earthquakes and tsunamis, from the site selection and evaluation process. Given Indonesia's geographic location, which is prone to seismic activity and tsunamis, further studies should explore the integration of disaster risk assessment and mitigation strategies to ensure the long-term resilience and safety of SPHS project.

7.3. Recommendations

This study has provided the technical and economical potential of SPHS at the national level in Indonesia. However, several key recommendations can be put forward to further advance the practical implementation of this technology.

While this research has identified potential SPHS sites across the nation and provides the picture of SPHS' role at a nationwide level, conducting in-depth assessments on a regional level would be instrumental for the next step of SPHS application. These smaller-level studies should consider the technical and geographical aspects and incorporate precise calculations, including geological conditions, penstock lines, and variations in electricity demand, so that the SPHS projects can be implemented.

Moreover, further studies should aim to refine the economic assessment by employing more tailored financial models. SPHS projects are unique, and a one-size-fits-all approach may not provide the most accurate results. Therefore, a customised financial modelling approach should be explored to ensure the economic feasibility of SPHS projects in each specific site.

Another aspect that can be improved is that future research endeavours should emphasise environmental impact assessments and mitigation strategies. Given the potential risks of seawater intrusion and corrosion associated with SPHS systems, studies focusing on minimising these environmental impacts will be essential. Developing effective mitigation strategies and monitoring systems can safeguard the delicate coastal ecosystems and the longevity of SPHS infrastructure.

Finally, the energy sector in Indonesia faces a challenge to meet the ambitious target of reducing carbon emissions. A steadfast commitment to incorporating more renewable energy into the national grid is necessary. To overcome the obstacles posed by the intermittent nature of renewable energy sources, implementing an efficient energy storage system becomes paramount, and SPHS emerges as an alternative technology that can work in line with other energy storage systems. By embracing SPHS and similar energy storage system innovations, Indonesia can move forward to ensure a resilient and sustainable energy future and make major progress toward its carbon reduction targets.

References

- [1] N. Reyseliani, A. Hidayatno, and W. W. Purwanto, "Implication of the Paris agreement target on Indonesia electricity sector transition to 2050 using TIMES model," en, *Energy Policy*, vol. 169, p. 113 184, Oct. 2022, ISSN: 03014215. DOI: 10.1016/j.enpo1.2022.113184. [Online]. Available: <https://linkinghub.elsevier.com/retrieve/pii/S0301421522004050>.
- [2] PLN, "Rencana Usaha Penyediaan Tenaga Listrik (RUPTL) PT PLN (Persero)," PT PLN Persero, Jakarta, Tech. Rep., 2021.
- [3] A. B. Setyowati, "Mitigating Energy Poverty: Mobilizing Climate Finance to Manage the Energy Trilemma in Indonesia," en, *Sustainability*, vol. 12, no. 4, p. 1603, Feb. 2020, ISSN: 2071-1050. DOI: 10.3390/su12041603. [Online]. Available: <https://www.mdpi.com/2071-1050/12/4/1603>.
- [4] IRENA, "Indonesia energy transition outlook," en, 2022.
- [5] L. P. Devkota, U. Bhattarai, P. Khatri, S. Marahatta, and D. Shrestha, "Resilience of hydropower plants to flow variation through the concept of flow elasticity of power: Theoretical development," en, *Renewable Energy*, vol. 184, pp. 920–932, Jan. 2022, ISSN: 09601481. DOI: 10.1016/j.renene.2021.11.051. [Online]. Available: <https://linkinghub.elsevier.com/retrieve/pii/S0960148121016335>.
- [6] D. de Vries, "Investigating the Potential Role of Pumped Hydro Storage in the Ethiopian Energy System using OSeMOSYS," M.S. thesis, Delft University of Technology, Delft, 2023.
- [7] M. Awang and S. S. Emamian, Eds., *Advances in Material Science and Engineering: Selected articles from ICMMPE 2020 (Lecture Notes in Mechanical Engineering)*, en. Singapore: Springer Singapore, 2021, ISBN: 9789811636400 9789811636417. DOI: 10.1007/978-981-16-3641-7. [Online]. Available: <https://link.springer.com/10.1007/978-981-16-3641-7>.
- [8] A. Blakers, M. Stocks, B. Lu, and C. Cheng, "A review of pumped hydro energy storage," en, *Progress in Energy*, vol. 3, no. 2, p. 022 003, Apr. 2021, ISSN: 2516-1083. DOI: 10.1088/2516-1083/abeb5b. [Online]. Available: <https://iopscience.iop.org/article/10.1088/2516-1083/abeb5b>.
- [9] J. D. Hunt, B. Zakeri, R. Lopes, et al., "Existing and new arrangements of pumped-hydro storage plants," en, *Renewable and Sustainable Energy Reviews*, vol. 129, p. 109 914, Sep. 2020, ISSN: 13640321. DOI: 10.1016/j.rser.2020.109914. [Online]. Available: <https://linkinghub.elsevier.com/retrieve/pii/S1364032120302057>.
- [10] G. Team, *The Importance of Energy Storage Systems for Sustainable Operations*, en-US, Dec. 2021. [Online]. Available: <https://galooli.com/blog/the-importance-of-energy-storage-systems-for-sustainable-operations/>.

- [11] Y. Wu, T. Zhang, C. Xu, *et al.*, "Location selection of seawater pumped hydro storage station in China based on multi-attribute decision making," en, *Renewable Energy*, vol. 139, pp. 410–425, Aug. 2019, ISSN: 09601481. DOI: 10.1016/j.renene.2019.02.091. [Online]. Available: <https://linkinghub.elsevier.com/retrieve/pii/S0960148119302459>.
- [12] A. Hiratsuka, T. Arai, and T. Yoshimura, "Seawater pumped-storage power plant in Okinawa island, Japan," en, *Engineering Geology*, vol. 35, no. 3-4, pp. 237–246, Oct. 1993, ISSN: 00137952. DOI: 10.1016/0013-7952(93)90012-2. [Online]. Available: <https://linkinghub.elsevier.com/retrieve/pii/0013795293900122>.
- [13] etakmaz, *Today and Future Pumped Hydro Energy Storage System in the US*, en, Oct. 2018. [Online]. Available: <https://las493energy.wordpress.com/2018/10/01/today-and-future-pumped-hydro-energy-storage-system-in-the-us/>.
- [14] N. Ghorbani, H. Makian, and C. Breyer, "A GIS-based method to identify potential sites for pumped hydro energy storage - Case of Iran," en, *Energy*, vol. 169, pp. 854–867, Feb. 2019, ISSN: 03605442. DOI: 10.1016/j.energy.2018.12.073. [Online]. Available: <https://linkinghub.elsevier.com/retrieve/pii/S0360544218324393>.
- [15] J. Jiménez Capilla, J. A. Carrión, and E. Alameda-Hernandez, "Optimal site selection for upper reservoirs in pump-back systems, using geographical information systems and multicriteria analysis," en, *Renewable Energy*, vol. 86, pp. 429–440, Feb. 2016, ISSN: 09601481. DOI: 10.1016/j.renene.2015.08.035. [Online]. Available: <https://linkinghub.elsevier.com/retrieve/pii/S0960148115302354>.
- [16] A. Pradhan, M. Marencé, and M. J. Franca, "The adoption of Seawater Pump Storage Hydropower Systems increases the share of renewable energy production in Small Island Developing States," en, *Renewable Energy*, vol. 177, pp. 448–460, Nov. 2021, ISSN: 09601481. DOI: 10.1016/j.renene.2021.05.151. [Online]. Available: <https://linkinghub.elsevier.com/retrieve/pii/S096014812100834X>.
- [17] Worldometer, *Indonesia Population (2023) - Worldometer*. [Online]. Available: <https://www.worldometers.info/world-population/indonesia-population/>.
- [18] M. A. McNeil, N. Karali, and V. Letschert, "Forecasting Indonesia's electricity load through 2030 and peak demand reductions from appliance and lighting efficiency," en, *Energy for Sustainable Development*, vol. 49, pp. 65–77, Apr. 2019, ISSN: 09730826. DOI: 10.1016/j.esd.2019.01.001. [Online]. Available: <https://linkinghub.elsevier.com/retrieve/pii/S0973082618312559>.
- [19] M. of Energy and Mineral Resources Republic of Indonesia, "Handbook of Energy and Economic Statistics of Indonesia 2021," Ministry of Energy and Mineral Resources Republic of Indonesia, Jakarta, Tech. Rep., 2021.
- [20] A. Sodri and I. Garniwa, "The Effect of Urbanization on Road Energy Consumption and CO2 Emissions in Emerging Megacity of Jakarta, Indonesia," en, *Procedia - Social and Behavioral Sciences*, vol. 227, pp. 728–737, Jul. 2016, ISSN: 18770428. DOI: 10.1016/j.sbspro.2016.06.139. [Online]. Available: <https://linkinghub.elsevier.com/retrieve/pii/S1877042816308254>.
- [21] N. Reyseliani and W. W. Purwanto, "Pathway towards 100% renewable energy in Indonesia power system by 2050," en, *Renewable Energy*, vol. 176, pp. 305–321, Oct. 2021, ISSN: 09601481. DOI: 10.1016/j.renene.2021.05.118. [Online]. Available: <https://linkinghub.elsevier.com/retrieve/pii/S0960148121008016>.

- [22] M. Maulidia, P. Dargusch, P. Ashworth, and F. Ardiansyah, "Rethinking renewable energy targets and electricity sector reform in Indonesia: A private sector perspective," en, *Renewable and Sustainable Energy Reviews*, vol. 101, pp. 231–247, Mar. 2019, issn: 13640321. doi: 10.1016/j.rser.2018.11.005. [Online]. Available: <https://linkinghub.elsevier.com/retrieve/pii/S1364032118307378>.
- [23] S. Schlömer, G. Hänsel, D. de Jager, and M. Neelis, "Technology-specific Cost and Performance Parameters," en, 2014.
- [24] H.-x. Wen, P.-y. Nie, M. Liu, *et al.*, "Multi-health effects of clean residential heating: Evidences from rural China's coal-to-gas/electricity project," en, *Energy for Sustainable Development*, vol. 73, pp. 66–75, Apr. 2023, issn: 09730826. doi: 10.1016/j.esd.2023.01.013. [Online]. Available: <https://linkinghub.elsevier.com/retrieve/pii/S097308262300011X>.
- [25] C. S. Permata, "Hydropower Potential in Indonesia: Assessment of the theoretical and economical potential of hydropower," M.S. thesis, Delft University of Technology, Delft, 2022.
- [26] Nasruddin, M. Idrus Alhamid, Y. Daud, *et al.*, "Potential of geothermal energy for electricity generation in Indonesia: A review," en, *Renewable and Sustainable Energy Reviews*, vol. 53, pp. 733–740, Jan. 2016, issn: 13640321. doi: 10.1016/j.rser.2015.09.032. [Online]. Available: <https://linkinghub.elsevier.com/retrieve/pii/S1364032115010023>.
- [27] D. F. Silalahi, A. Blakers, M. Stocks, B. Lu, C. Cheng, and L. Hayes, "Indonesia's Vast Solar Energy Potential," en, *Energies*, vol. 14, no. 17, p. 5424, Aug. 2021, issn: 1996-1073. doi: 10.3390/en14175424. [Online]. Available: <https://www.mdpi.com/1996-1073/14/17/5424>.
- [28] M. Rumbayan, A. Abudureyimu, and K. Nagasaka, "Mapping of solar energy potential in Indonesia using artificial neural network and geographical information system," en, *Renewable and Sustainable Energy Reviews*, vol. 16, no. 3, pp. 1437–1449, Apr. 2012, issn: 13640321. doi: 10.1016/j.rser.2011.11.024. [Online]. Available: <https://linkinghub.elsevier.com/retrieve/pii/S1364032111005703>.
- [29] F. Maghdavi, "Mapping of Floating Solar PV Technical and Economic Potential in Indonesia," M.S. thesis, Delft University of Technology, Delft, 2023.
- [30] P. (PWC), "Power In Indonesia: Investment and Taxation Guide," PricewaterhouseCoopers International Limited, Jakarta, Tech. Rep. 6th Edition, 2018. [Online]. Available: <https://www.pwc.com/id/en/publications/assets/eumpublications/utilities/power-guide-2018.pdf>.
- [31] R. Suryaningsih and Irhas, "Bioenergy Plants in Indonesia: Sorghum for Producing Bioethanol as an Alternative Energy Substitute of Fossil Fuels," en, *Energy Procedia*, vol. 47, pp. 211–216, 2014, issn: 18766102. doi: 10.1016/j.egypro.2014.01.216. [Online]. Available: <https://linkinghub.elsevier.com/retrieve/pii/S187661021400232X>.
- [32] S. Yana, M. Nizar, Irhamni, and D. Mulyati, "Biomass waste as a renewable energy in developing bio-based economies in Indonesia: A review," en, *Renewable and Sustainable Energy Reviews*, vol. 160, p. 112268, May 2022, issn: 13640321. doi: 10.1016/j.rser.2022.112268. [Online]. Available: <https://linkinghub.elsevier.com/retrieve/pii/S1364032122001897>.
- [33] C. Zhao, P. B. Andersen, C. Træholt, and S. Hashemi, "Grid-connected battery energy storage system: A review on application and integration," en, *Renewable and Sustainable Energy Reviews*, vol. 182, p. 113400, Aug. 2023, issn: 13640321. doi: 10.1016/j.rser.2023.113400. [Online]. Available: <https://linkinghub.elsevier.com/retrieve/pii/S1364032123002575>.

- [34] S. A. Memon, D. S. Upadhyay, and R. N. Patel, "Optimal configuration of solar and wind-based hybrid renewable energy system with and without energy storage including environmental and social criteria: A case study," en, *Journal of Energy Storage*, vol. 44, p. 103 446, Dec. 2021, ISSN: 2352152X. DOI: 10.1016/j.est.2021.103446. [Online]. Available: <https://linkinghub.elsevier.com/retrieve/pii/S2352152X21011300>.
- [35] M. Mahmoud, M. Ramadan, A.-G. Olabi, K. Pullen, and S. Naher, "A review of mechanical energy storage systems combined with wind and solar applications," en, *Energy Conversion and Management*, vol. 210, p. 112 670, Apr. 2020, ISSN: 01968904. DOI: 10.1016/j.enconman.2020.112670. [Online]. Available: <https://linkinghub.elsevier.com/retrieve/pii/S0196890420302089>.
- [36] J. Y. Lee, A. Ramasamy, K. H. Ong, R. Verayiah, H. Mokhlis, and M. Marsadek, "Energy storage systems: A review of its progress and outlook, potential benefits, barriers and solutions within the Malaysian distribution network," en, *Journal of Energy Storage*, vol. 72, p. 108 360, Nov. 2023, ISSN: 2352152X. DOI: 10.1016/j.est.2023.108360. [Online]. Available: <https://linkinghub.elsevier.com/retrieve/pii/S2352152X23017577>.
- [37] S. Ali, R. A. Stewart, and O. Sahin, "Drivers and barriers to the deployment of pumped hydro energy storage applications: Systematic literature review," en, *Cleaner Engineering and Technology*, vol. 5, p. 100 281, Dec. 2021, ISSN: 26667908. DOI: 10.1016/j.clet.2021.100281. [Online]. Available: <https://linkinghub.elsevier.com/retrieve/pii/S266679082100241X>.
- [38] J. Deane, B. Ó Gallachóir, and E. McKeogh, "Techno-economic review of existing and new pumped hydro energy storage plant," en, *Renewable and Sustainable Energy Reviews*, vol. 14, no. 4, pp. 1293–1302, May 2010, ISSN: 13640321. DOI: 10.1016/j.rser.2009.11.015. [Online]. Available: <https://linkinghub.elsevier.com/retrieve/pii/S1364032109002779>.
- [39] S. Rehman, L. M. Al-Hadhrami, and M. M. Alam, "Pumped hydro energy storage system: A technological review," en, *Renewable and Sustainable Energy Reviews*, vol. 44, pp. 586–598, Apr. 2015, ISSN: 13640321. DOI: 10.1016/j.rser.2014.12.040. [Online]. Available: <https://linkinghub.elsevier.com/retrieve/pii/S1364032115000106>.
- [40] E. McLean and D. Kearney, "An Evaluation of Seawater Pumped Hydro Storage for Regulating the Export of Renewable Energy to the National Grid," en, *Energy Procedia*, vol. 46, pp. 152–160, 2014, ISSN: 18766102. DOI: 10.1016/j.egypro.2014.01.168. [Online]. Available: <https://linkinghub.elsevier.com/retrieve/pii/S1876610214001842>.
- [41] Z. Lu, Y. Gao, and W. Zhao, "A TODIM-based approach for environmental impact assessment of pumped hydro energy storage plant," en, *Journal of Cleaner Production*, vol. 248, p. 119 265, Mar. 2020, ISSN: 09596526. DOI: 10.1016/j.jclepro.2019.119265. [Online]. Available: <https://linkinghub.elsevier.com/retrieve/pii/S0959652619341356>.
- [42] T. Ma, H. Yang, and L. Lu, "Feasibility study and economic analysis of pumped hydro storage and battery storage for a renewable energy powered island," en, *Energy Conversion and Management*, vol. 79, pp. 387–397, Mar. 2014, ISSN: 01968904. DOI: 10.1016/j.enconman.2013.12.047. [Online]. Available: <https://linkinghub.elsevier.com/retrieve/pii/S0196890413008236>.
- [43] C. R. Jones, P. Hilpert, J. Gaede, and I. H. Rowlands, "Batteries, compressed air, flywheels, or pumped hydro? Exploring public attitudes towards grid-scale energy storage technologies in Canada and the United Kingdom," en, *Energy Research & Social Science*, vol. 80, p. 102 228, Oct. 2021, ISSN: 22146296. DOI: 10.1016/j.erss.2021.102228. [Online]. Available: <https://linkinghub.elsevier.com/retrieve/pii/S2214629621003212>.

- [44] *Learnings — Grid Integration of Renewables* | by Mudit Maheshwari | Medium. [Online]. Available: <https://electricalsafety.medium.com/learnings-grid-integration-of-renewables-891ca304752>.
- [45] R. Ltd, *Pumped hydro ‘crucial to avoid blackouts’*, en-US, Sep. 2021. [Online]. Available: <https://renews.biz/72312/pumped-hydro-crucial-to-avoid-blackouts/>.
- [46] ATCO, *ATCO unveils 325MW pumped hydro storage project in NSW*, en-AU, Feb. 2021. [Online]. Available: <https://www.atco.com/en-au/about-us/stories/atco-pumped-hydro-storage-nsw.html>.
- [47] D. A. Katsaprakakis and D. G. Christakis, “Seawater pumped storage systems and offshore wind parks in islands with low onshore wind potential. A fundamental case study,” en, *Energy*, vol. 66, pp. 470–486, Mar. 2014, issn: 03605442. doi: 10.1016/j.energy.2014.01.021. [Online]. Available: <https://linkinghub.elsevier.com/retrieve/pii/S0360544214000280>.
- [48] K. Oshima, J. Kawai, S. Otsuka, T. Wada, and H. Imano, “Development of Pump-Turbine for Seawater Pumped Storage Power Plant,” EN, pp. 1–6, Apr. 2012, Publisher: American Society of Civil Engineers. doi: 10.1061/40440(1999)67. [Online]. Available: <https://ascelibrary.org/doi/10.1061/40440%281999%2967>.
- [49] C. E. Corporation, *CMS Energy Corporation - About - Consumers Energy*, Jan. 2020. [Online]. Available: <https://www.cmsenergy.com/about-cms-energy/consumers-energy/default.aspx>.
- [50] W. Bank, *Indonesia’s First Pumped Storage Hydropower Plant to Support Energy Transition*, en, Text/HTML, Sep. 2021. doi: 10/indonesia-s-first-pumped-storage-hydropower-plant-to-support-energy-transition. [Online]. Available: <https://www.worldbank.org/en/news/press-release/2021/09/10/indonesia-s-first-pumped-storage-hydropower-plant-to-support-energy-transition>.
- [51] B. I. Geospasial, *Indonesia Geospatial Portal*, 2023. [Online]. Available: <https://tanahair.indonesia.go.id/portal-web>.
- [52] D. Company, *Solcast | Solar Api and Solar Weather Forecasting Tool*, en, 2023. [Online]. Available: <https://solcast.com.au>.
- [53] A. International, *D3517: Standard Specification for “Fiberglass” (Glass-Fiber-Reinforced Thermosetting-Resin) Pressure Pipe*, Feb. 2020.
- [54] P. Halder, A. T. Doppalapudi, A. K. Azad, and M. Khan, “Efficient hydroenergy conversion technologies, challenges, and policy implication,” en, in *Advances in Clean Energy Technologies*, Elsevier, 2021, pp. 295–318, isbn: 978-0-12-821221-9. doi: 10.1016/B978-0-12-821221-9.00007-4. [Online]. Available: <https://linkinghub.elsevier.com/retrieve/pii/B9780128212219000074>.
- [55] T. M. of Energy and Mineral Resources of the Republic of Indonesia, *Ketenagalistrikan*. [Online]. Available: <https://geoportal.esdm.go.id/ketenagalistrikan/>.
- [56] G. Al Zohbi, “Cost Models for Pumped Hydro Storage System,” en, in *Encyclopedia of Energy Storage*, Elsevier, 2022, pp. 157–163, isbn: 978-0-12-819730-1. doi: 10.1016/B978-0-12-819723-3.00139-6. [Online]. Available: <https://linkinghub.elsevier.com/retrieve/pii/B9780128197233001396>.

- [57] G. Cavazzini, A. Santolin, G. Pavesi, and G. Ardizzon, "Accurate estimation model for small and micro hydropower plants costs in hybrid energy systems modelling," en, *Energy*, vol. 103, pp. 746–757, May 2016, issn: 03605442. doi: 10.1016/j.energy.2016.03.024. [Online]. Available: <https://linkinghub.elsevier.com/retrieve/pii/S0360544216302687>.
- [58] G. Alzohbi, "The cost of electromechanical equipment in a small hydro power storage plant," en, *Journal of Energy Systems*, vol. 2, no. 4, pp. 238–259, Dec. 2018, issn: 2602-2052. doi: 10.30521/jes.457288. [Online]. Available: <http://dergipark.org.tr/en/doi/10.30521/jes.457288>.
- [59] Q. F. (Zhang, B. Smith, and W. Zhang, "Small Hydropower Cost Reference Model Final Project Report," en, Oct. 2012.
- [60] S. M. K., "Optimum Design of Penstock for Hydro Projects," en, *International Journal of Energy and Power Engineering*, vol. 4, no. 4, p. 216, 2015, issn: 2326-957X. doi: 10.11648/j.ijepe.20150404.14. [Online]. Available: <http://www.sciencepublishinggroup.com/journal/paperinfo?journalid=164&doi=10.11648/j.ijepe.20150404.14>.
- [61] S. Singal and R. Saini, "Analytical approach for development of correlations for cost of canal-based SHP schemes," en, *Renewable Energy*, vol. 33, no. 12, pp. 2549–2558, Dec. 2008, issn: 09601481. doi: 10.1016/j.renene.2008.02.010. [Online]. Available: <https://linkinghub.elsevier.com/retrieve/pii/S0960148108000712>.
- [62] MISO, "Transmission Cost Estimation Guide: MTEP19," Midcontinent Independent System Operator (MISO), Tech. Rep., Apr. 2019.
- [63] D. de Jager, C. Klessmann, E. Stricker, T. Winkel, E. de Visser, and M. Koper, "Financing Renewable Energy in the European Energy Market," en, *Ecofys*, Tech. Rep., Jan. 2011.
- [64] F. Klumpp, "Comparison of pumped hydro, hydrogen storage and compressed air energy storage for integrating high shares of renewable energies—Potential, cost-comparison and ranking," en, *Journal of Energy Storage*, vol. 8, pp. 119–128, Nov. 2016, issn: 2352152X. doi: 10.1016/j.est.2016.09.012. [Online]. Available: <https://linkinghub.elsevier.com/retrieve/pii/S2352152X16301712>.
- [65] F. Zoma and M. Sawadogo, "A multicriteria approach for biomass availability assessment and selection for energy production in Burkina Faso: A hybrid AHP-TOPSIS approach," en, *Heliyon*, e20999, Oct. 2023, issn: 24058440. doi: 10.1016/j.heliyon.2023.e20999. [Online]. Available: <https://linkinghub.elsevier.com/retrieve/pii/S2405844023082075>.
- [66] P. Raja Shekar and A. Mathew, "Assessing groundwater potential zones and artificial recharge sites in the monsoon-fed Murredu river basin, India: An integrated approach using GIS, AHP, and Fuzzy-AHP," en, *Groundwater for Sustainable Development*, vol. 23, p. 100994, Nov. 2023, issn: 2352801X. doi: 10.1016/j.gsd.2023.100994. [Online]. Available: <https://linkinghub.elsevier.com/retrieve/pii/S2352801X23000942>.
- [67] H. M. Bintang, "A 2023's Update on The Levelized Cost of Electricity and Levelized Cost of Storage in Indonesia," Institute for Essential Services Reform (IESR), Tech. Rep., Mar. 2023. [Online]. Available: <https://iesr.or.id/wp-content/uploads/2023/03/IESR-2023-Making-Energy-Transition-Succeed-A-2023s-Update-on-The-Levelized-Cost-of-Electricity-and-Storage-LCOE-LCOS-1.pdf>.

- [68] K. E. dan Sumber Daya Mineral, *Keputusan Menteri Energi dan Sumber Daya Mineral Nomor 169.K/HK.02/MEM.N/2021 tentang Besaran Biaya Pokok Pembangunan PT Perusahaan Listrik Negara (Persero) Tahun 2020*, 2021. [Online]. Available: <https://jdih.esdm.go.id/storage/document/Kepmen%20No.%20169.K.HK.02.MEM.M.2021.pdf>.
- [69] M. Mogyema, C. Botha, M. Kamper, R.-J. Wang, and A. Sebitosi, "Levelised cost of storage comparison of energy storage systems for use in primary response application," en, *Journal of Energy Storage*, vol. 59, p. 106573, Mar. 2023, ISSN: 2352152X. DOI: 10.1016/j.est.2022.106573. [Online]. Available: <https://linkinghub.elsevier.com/retrieve/pii/S2352152X22025622>.
- [70] M. Cristea, R.-A. Tîrnovan, C. Cristea, and C. Făgărășan, "Levelized cost of storage (LCOS) analysis of BESSs in Romania," en, *Sustainable Energy Technologies and Assessments*, vol. 53, p. 102633, Oct. 2022, ISSN: 22131388. DOI: 10.1016/j.seta.2022.102633. [Online]. Available: <https://linkinghub.elsevier.com/retrieve/pii/S221313882200683X>.
- [71] C. Martínez De León, C. Ríos, P. Molina, and J. Brey, "Levelized Cost of Storage (LCOS) for a hydrogen system," en, *International Journal of Hydrogen Energy*, S0360319923037485, Aug. 2023, ISSN: 03603199. DOI: 10.1016/j.ijhydene.2023.07.239. [Online]. Available: <https://linkinghub.elsevier.com/retrieve/pii/S0360319923037485>.
- [72] Earthshield, *Construction Process of Anti-Seepage Geomembrane for Reservoir Dam Liner*, zh-CN, Jul. 2021. [Online]. Available: <https://www.earthshields.com/construction-process-of-anti-seepage-geomembrane-for-reservoir-dam-liner/>.
- [73] D. Bi, Y. Chang, H. Luo, *et al.*, "Corrosion behavior and passive film characteristics of AlNbTiZrSix high-entropy alloys in simulated seawater environment," en, *Corrosion Science*, vol. 224, p. 111530, Nov. 2023, ISSN: 0010938X. DOI: 10.1016/j.corsci.2023.111530. [Online]. Available: <https://linkinghub.elsevier.com/retrieve/pii/S0010938X23005723>.
- [74] M. Haseeb-ur-Rehman, A. B. Munshi, U. Atique, and S. Kalsoom, "Metal pollution and potential human health risk assessment in major seafood items (fish, crustaceans, and cephalopods)," en, *Marine Pollution Bulletin*, vol. 188, p. 114581, Mar. 2023, ISSN: 0025326X. DOI: 10.1016/j.marpolbul.2023.114581. [Online]. Available: <https://linkinghub.elsevier.com/retrieve/pii/S0025326X23000127>.

Appendix **A**

SPHS Sites Properties

Detailed information about the properties and characteristics of the identified Seawater Pumped Hydro Storage (SPHS) sites can be found on the following pages of this report.

Appendix **B**

SPHS Classification

The information about the identified Seawater Pumped Hydro Storage (SPHS) classification can be found on the following pages of this report.

Preprocessing Python Script

Listing C.1: The preprocessing python script

```

1 """
2 Model exported as python.
3 Name : 01_preprocessing
4 Group :
5 With QGIS : 32810
6 """
7
8 from qgis.core import QgsProcessing
9 from qgis.core import QgsProcessingAlgorithm
10 from qgis.core import QgsProcessingMultiStepFeedback
11 from qgis.core import QgsProcessingParameterExtent
12 from qgis.core import QgsProcessingParameterVectorLayer
13 from qgis.core import QgsProcessingParameterCrs
14 from qgis.core import QgsProcessingParameterRasterLayer
15 from qgis.core import QgsProcessingParameterFile
16 from qgis.core import QgsProcessingParameterString
17 import processing
18 import os
19 from operator import itemgetter
20 import csv
21 from pcraster import*
22
23 class preprocessing(QgsProcessingAlgorithm):
24
25     def initAlgorithm(self, config=None):
26         self.addParameter(QgsProcessingParameterExtent('extent', 'Extent', defaultValue
27             =None))
28         self.addParameter(QgsProcessingParameterVectorLayer('input_coastline_shp_file',
29             'Input_coastline_SHP_file', types=[QgsProcessing.TypeVectorLine],
30             defaultValue=None))
31         self.addParameter(QgsProcessingParameterCrs('input_crs', 'Input_CRS',
32             defaultValue='EPSG:4326'))
33         self.addParameter(QgsProcessingParameterRasterLayer('input_dem', 'Input_DEM',
34             defaultValue=None))
35         self.addParameter(QgsProcessingParameterFile('working_directory', 'Working_
36             directory', behavior=QgsProcessingParameterFile.Folder, fileFilter='All_
37             files_(*.*)', defaultValue=None))

```

```

31     self.addParameter(QgsProcessingParameterString('regional', 'Regional',
32         multiLine=False, defaultValue='Indonesia'))
33
34     def processAlgorithm(self, parameters, context, model_feedback):
35         # Use a multi-step feedback, so that individual child algorithm progress
36         # reports are adjusted for the
37         # overall progress through the model
38         feedback = QgsProcessingMultiStepFeedback(23, model_feedback)
39         results = {}
40         outputs = {}
41         os.chdir(parameters['working_directory'])
42
43         # Reproject layer
44         alg_params = {
45             'INPUT': parameters['input_coastline_shp_file'],
46             'OPERATION': '',
47             'TARGET_CRS': parameters['input_crs'],
48             'OUTPUT': 'temp_projected'}
49         outputs['ReprojectLayer'] = processing.run('native:reprojectlayer', alg_params,
50             context=context, feedback=feedback, is_child_algorithm=True)
51
52         feedback.setCurrentStep(1)
53         if feedback.isCanceled():
54             return {}
55
56         # Buffer with 200 meters distance from coastline
57         fn_buffer = "buffer_" + parameters['regional'] + ".shp"
58         alg_params = {
59             'DISSOLVE': True,
60             'DISTANCE': 0.08, #in degree
61             'END_CAP_STYLE': 0, # Round
62             'INPUT': parameters['input_coastline_shp_file'],
63             'JOIN_STYLE': 0, # Round
64             'MITER_LIMIT': 1,
65             'OUTPUT': fn_buffer,
66             'SEGMENTS': 100,
67             'OUTPUT': fn_buffer}
68         outputs['Buffer'] = processing.run('native:buffer', alg_params, context=context
69             , feedback=feedback, is_child_algorithm=True)
70
71         feedback.setCurrentStep(2)
72         if feedback.isCanceled():
73             return {}
74
75         # line to polygon the coastline shp
76         fn_poly = "poly_" + parameters['regional'] + ".shp"
77         fn_poly_fixed = "poly_fixed_" + parameters['regional'] + ".shp"
78         outputs['Poly'] = processing.run("qgis:linestopolygons", {'INPUT':parameters['
79             input_coastline_shp_file'],'OUTPUT':fn_poly})
80         outputs['Poly_fixed'] = processing.run("native:fixgeometries", {'INPUT':outputs
81             ['Poly']['OUTPUT'],'METHOD':1,'OUTPUT':fn_poly_fixed})
82
83         feedback.setCurrentStep(3)
84         if feedback.isCanceled():
85             return {}
86
87         # Rename layer

```



```

82     name1 = "DEM_" + parameters['regional']
83     alg_params = {
84         'INPUT': parameters['input_dem'],
85         'NAME': name1}
86     outputs['RenameLayer'] = processing.run('native:renamelayer', alg_params,
87         context=context, feedback=feedback, is_child_algorithm=True)
88
89     feedback.setCurrentStep(4)
90     if feedback.isCanceled():
91         return {}
92
93     # Raster calculator to eliminate area with elevation < 200 meters
94     expression1 = "" + "'" + name1 + "@1" + "'" + ">=200" ""
95     alg_params = {
96         'CELLSIZE': 0,
97         'CRS': parameters['input_crs'],
98         'EXPRESSION': expression1,
99         'EXTENT': parameters['extent'],
100        'LAYERS': parameters['input_dem'],
101        'OUTPUT': 'temp_raster_calculator1.tif'}
102    outputs['RasterCalculator'] = processing.run('qgis:rastercalculator',
103        alg_params, context=context, feedback=feedback, is_child_algorithm=True)
104
105    feedback.setCurrentStep(5)
106    if feedback.isCanceled():
107        return {}
108
109    # Polygonize (raster to vector) the study area
110    alg_params = {
111        'BAND': 1,
112        'EIGHT_CONNECTEDNESS': False,
113        'EXTRA': '',
114        'FIELD': 'DN',
115        'INPUT': outputs['RasterCalculator']['OUTPUT'],
116        'OUTPUT': 'temp_polygonize1.shp'}
117    outputs['PolygonizeRasterToVector'] = processing.run('gdal:polygonize',
118        alg_params, context=context, feedback=feedback, is_child_algorithm=True)
119
120    feedback.setCurrentStep(6)
121    if feedback.isCanceled():
122        return {}
123
124    # Select and delete DN, remain the study area into a shp file
125    fn_elev = "elev_200_" + parameters['regional'] + ".shp"
126    alg_params = {
127        'Extract': fn_elev,
128        'Input_vector': outputs['PolygonizeRasterToVector']['OUTPUT'],
129        'Select_DN_to_retain': '1',
130        'Extract': fn_elev}
131    outputs['SelectAndDeleteDn'] = processing.run('script:Select_and_delete_DN',
132        alg_params, context=context, feedback=feedback, is_child_algorithm=True)
133
134    feedback.setCurrentStep(7)
135    if feedback.isCanceled():
136        return {}
137
138    #make a shp file of the study area boundary

```

```

135     fn_clip1 = 'clip1.shp'
136     alg_params = {
137         'INPUT': outputs['Poly_fixed']['OUTPUT'],
138         'OVERLAY': outputs['Buffer']['OUTPUT'],
139         'OUTPUT': fn_clip1}
140     outputs['clip1'] = processing.run("native:clip", alg_params)
141
142     feedback.setCurrentStep(8)
143     if feedback.isCanceled():
144         return {}
145
146     fn_clip2 = 'clip2.shp'
147     alg_params = {
148         'INPUT': outputs['clip1']['OUTPUT'],
149         'OVERLAY': outputs['SelectAndDeleteDn']['Extract'],
150         'OUTPUT': fn_clip2}
151     outputs['clip2'] = processing.run("native:clip", alg_params)
152
153     feedback.setCurrentStep(9)
154     if feedback.isCanceled():
155         return {}
156
157     # Clip raster by mask layer, cut DEM into study area step 1
158     alg_params = {
159         'ALPHA_BAND': False,
160         'CROP_TO_OUTLINE': True,
161         'DATA_TYPE': 0, # Use Input Layer Data Type
162         'EXTRA': '',
163         'INPUT': parameters['input_dem'],
164         'KEEP_RESOLUTION': True,
165         'MASK': outputs['clip2']['OUTPUT'],
166         'MULTITHREADING': False,
167         'NODATA': -999999999,
168         'OPTIONS': '',
169         'SET_RESOLUTION': False,
170         'SOURCE_CRS': parameters['input_crs'],
171         'TARGET_CRS': parameters['input_crs'],
172         'TARGET_EXTENT': parameters['extent'],
173         'X_RESOLUTION': None,
174         'Y_RESOLUTION': None,
175         'OUTPUT': 'temp_clipped.tif'}
176     outputs['ClipRasterByMaskLayer'] = processing.run('gdal:cliprasterbymasklayer',
177         alg_params, context=context, feedback=feedback, is_child_algorithm=True)
178
179     feedback.setCurrentStep(10)
180     if feedback.isCanceled():
181         return {}
182
183     # Convert to PCRaster Format
184     fn_map = "study_area_" + parameters['regional'] + ".map"
185     alg_params = {
186         'INPUT': outputs['ClipRasterByMaskLayer']['OUTPUT'],
187         'INPUT2': 3, # Scalar
188         'OUTPUT': fn_map,
189         'OUTPUT': fn_map}
190     outputs['ConvertToPcrasterFormat'] = processing.run('pcraster:
191         converttopcrasterformat', alg_params, context=context, feedback=feedback,

```

```

        is_child_algorithm=True)
190
191     feedback.setCurrentStep(11)
192     if feedback.isCanceled():
193         return {}
194
195     # Load DEM in PCRaster format layer into project
196     alg_params = {
197         'INPUT': fn_map,
198         'NAME': 'study_area_' + parameters['regional']}
199     outputs['LoadLayerIntoProject'] = processing.run('native:loadlayer', alg_params
        , context=context, feedback=feedback, is_child_algorithm=True)
200
201     feedback.setCurrentStep(12)
202     if feedback.isCanceled():
203         return {}
204
205     #Create LDD map for calculation in PCRaster
206     fn_ldd = "ldd_" + parameters['regional'] + ".map"
207     alg_params = {
208         'INPUT': outputs['ConvertToPcrasterFormat']['OUTPUT'],
209         'INPUT0': 0, # No
210         'INPUT1': 0, # Map units
211         'INPUT2': 9999999,
212         'INPUT3': 9999999,
213         'INPUT4': 9999999,
214         'INPUT5': 9999999,
215         'OUTPUT': fn_ldd,
216         'OUTPUT': fn_ldd}
217     outputs['Lddcreate'] = processing.run('pcraster:lddcreate', alg_params, context
        =context, feedback=feedback, is_child_algorithm=True)
218
219     feedback.setCurrentStep(13)
220     if feedback.isCanceled():
221         return {}
222
223     # Load LDD layer into project
224     alg_params = {
225         'INPUT': fn_ldd,
226         'NAME': 'ldd_' + parameters['regional']}
227     outputs['LoadLayerIntoProject'] = processing.run('native:loadlayer', alg_params
        , context=context, feedback=feedback, is_child_algorithm=True)
228
229     feedback.setCurrentStep(14)
230     if feedback.isCanceled():
231         return {}
232
233     # streamorder
234     fn_so = "streamorder_" + parameters['regional'] + ".map"
235     alg_params = {
236         'INPUT': outputs['Lddcreate']['OUTPUT'],
237         'OUTPUT': fn_so}
238     outputs['Streamorder'] = processing.run('pcraster:streamorder', alg_params,
        context=context, feedback=feedback, is_child_algorithm=True)
239
240     feedback.setCurrentStep(15)
241     if feedback.isCanceled():

```

```

242     return {}
243
244     # spatial
245     alg_params = {
246         'INPUT': 5,
247         'INPUT1': 2, # Ordinal
248         'INPUT2': outputs['Streamorder']['OUTPUT'],
249         'OUTPUT': 'temp_spatial.map'}
250     outputs['Spatial'] = processing.run('pcraster:spatial', alg_params, context=
        context, feedback=feedback, is_child_algorithm=True)
251
252     feedback.setCurrentStep(16)
253     if feedback.isCanceled():
254         return {}
255
256     # comparison operators
257     alg_params = {
258         'INPUT': outputs['Streamorder']['OUTPUT'],
259         'INPUT1': 0, # ==
260         'INPUT2': outputs['Spatial']['OUTPUT'],
261         'OUTPUT': 'temp_comparison.map'}
262     outputs['ComparisonOperators'] = processing.run('pcraster:comparisonoperators',
        alg_params, context=context, feedback=feedback, is_child_algorithm=True)
263
264     feedback.setCurrentStep(17)
265     if feedback.isCanceled():
266         return {}
267
268     # if then
269     alg_params = {
270         'INPUT': outputs['ComparisonOperators']['OUTPUT'],
271         'INPUT1': outputs['Streamorder']['OUTPUT'],
272         'OUTPUT': 'temp_ifthen.map'}
273     outputs['IfThen'] = processing.run('pcraster:ifthen', alg_params, context=
        context, feedback=feedback, is_child_algorithm=True)
274
275     feedback.setCurrentStep(18)
276     if feedback.isCanceled():
277         return {}
278
279     # clump
280     fn_gc = "group_channel_" + parameters['regional'] + ".map"
281     alg_params = {
282         'INPUT': outputs['IfThen']['OUTPUT'],
283         'INPUT1': 0, # Diagonal (8 cell)
284         'OUTPUT': fn_gc,
285         'OUTPUT': fn_gc}
286     outputs['Clump'] = processing.run('pcraster:clump', alg_params, context=context
        , feedback=feedback, is_child_algorithm=True)
287
288     feedback.setCurrentStep(19)
289     if feedback.isCanceled():
290         return {}
291
292     # Load channel (clumped) layer into project
293     alg_params = {
294         'INPUT': fn_gc,

```

```

295     'NAME': 'group_channel_' + parameters['regional']]
296 outputs['LoadLayerIntoProject2'] = processing.run('native:loadlayer',
297     alg_params, context=context, feedback=feedback, is_child_algorithm=True)
298
299 feedback.setCurrentStep(20)
300 if feedback.isCanceled():
301     return {}
302
303 # Hillshade
304 fn_hillshade = "hillshade_" + parameters['regional'] + ".tif"
305 alg_params = {
306     'INPUT': parameters['input_dem'],
307     'BAND': 1,
308     'Z_FACTOR': 1,
309     'SCALE': 1,
310     'AZIMUTH': 315,
311     'ALTITUDE': 45,
312     'COMPUTE_EDGES': False,
313     'ZEVENBERGEN': False,
314     'COMBINED': False,
315     'MULTIDIRECTIONAL': False,
316     'OPTIONS': '',
317     'EXTRA': '',
318     'OUTPUT': fn_hillshade}
319 outputs['Hillshade'] = processing.run("gdal:hillshade", alg_params)
320
321 feedback.setCurrentStep(21)
322 if feedback.isCanceled():
323     return {}
324
325 # Load hillshade layer into project
326 alg_params = {
327     'INPUT': fn_hillshade,
328     'NAME': 'hillshade_' + parameters['regional']}
329 outputs['LoadLayerIntoProject1'] = processing.run('native:loadlayer',
330     alg_params, context=context, feedback=feedback, is_child_algorithm=True)
331
332 feedback.setCurrentStep(22)
333 if feedback.isCanceled():
334     return {}
335
336 # map2col channel
337 expression3 = '"map2col_' + fn_gc + '_' + 'channel_' + parameters['regional'] +
338     '.txt"'
339 os.system(expression3)
340
341 return results
342 os.remove('temp_ifthen.map')
343 os.remove('temp_raster_calculator1')
344 os.remove('temp_comparison.map')
345
346 def name(self):
347     return '01_preprocessing'
348
349 def displayName(self):
350     return '01_preprocessing'

```

```
349     def group(self):
350         return ''
351
352     def groupId(self):
353         return ''
354
355     def createInstance(self):
356         return preprocessing()
```

Appendix D

Main Processing Python Script

Listing D.1: The mainprocessing python script

```
1 """
2 Model exported as python.
3 Name : 02_mainprocessing
4 Group :
5 With QGIS : 32810
6 """
7
8 from qgis.core import QgsProcessing
9 from qgis.core import QgsProcessingAlgorithm
10 from qgis.core import QgsProcessingParameterNumber
11 from qgis.core import QgsProcessingParameterRasterLayer
12 from qgis.core import QgsProcessingParameterVectorLayer
13 from qgis.core import QgsProcessingParameterFile
14 from qgis.core import QgsProcessingParameterString
15 from qgis.core import QgsVectorLayer
16 from qgis.core import QgsProject
17 import processing
18 import numpy as np
19 from pcraster import*
20 import os
21
22 class Model(QgsProcessingAlgorithm):
23
24     def initAlgorithm(self, config=None):
25         self.addParameter(QgsProcessingParameterFile('working_directory', 'Working_
26             directory', behavior=QgsProcessingParameterFile.Folder, fileFilter='All_
27             files_(*.*)', defaultValue=None))
28         self.addParameter(QgsProcessingParameterVectorLayer('input_coastline', 'Input_
29             coastline_SHP_file', types=[QgsProcessing.TypeVectorLine], defaultValue=
30             None))
31         self.addParameter(QgsProcessingParameterString('regional', 'Regional',
32             multiLine=False, defaultValue='Indonesia'))
33         self.addParameter(QgsProcessingParameterNumber('damheight', 'Dam_height_[meters]
34             ', type=QgsProcessingParameterNumber.Integer, minValue=1, maxValue=99,
35             defaultValue=15))
36         self.addParameter(QgsProcessingParameterNumber('cellsize', 'Cell_size_[meters]'
37             ', type=QgsProcessingParameterNumber.Integer, minValue=1, maxValue=99,
38             defaultValue=8.25))
```

```

30     self.addParameter(QgsProcessingParameterNumber('min_energy', 'Minimum energy [
        MWh]', type=QgsProcessingParameterNumber.Integer, minValue=1, maxValue
        =1000, defaultValue=140))
31     self.addParameter(QgsProcessingParameterNumber('duration', 'Duration of power
        generation [hours]', type=QgsProcessingParameterNumber.Integer, minValue=1,
        maxValue=24, defaultValue=8))
32
33     def processAlgorithm(self, parameters, context, model_feedback):
34         os.chdir(parameters['working_directory'])
35
36         #call the files needed
37         fn_map = "study_area_" + parameters['regional'] + ".map"
38         study_area_map = readmap(fn_map)
39         DEM = readmap(fn_map)
40         fn_gc = "group_channel_" + parameters['regional'] + ".map"
41         fn_gc_txt = "channel_" + parameters['regional'] + ".txt"
42         channel_all = readmap(fn_gc)
43         fn_ldd = "ldd_" + parameters['regional'] + ".map"
44         fn_outlet = 'gully_outlet_' + parameters['regional'] + '.txt'
45         fn_outlet_map = 'outlet_coord_' + parameters['regional'] + '.map'
46         fn_outlet_shp = 'outlet_coord_' + parameters['regional'] + '.shp'
47         fn_energy = 'DG_Vol_Energy_' + parameters['regional'] + '.txt'
48         fn_inundation_map = 'inundation_' + parameters['regional'] + ".map"
49         fn_inundation_txt = 'inundation_' + parameters['regional'] + ".txt"
50         fn_inundation_true_map = 'inundation_true_' + parameters['regional'] + ".map"
51         fn_sample_code = 'sample_code_ok_' + parameters['regional'] + '.txt'
52         fn_sample_code_notokay = 'sample_code_no_' + parameters['regional'] + '.txt'
53
54         outputs = {}
55         results = {}
56
57         #define parameters
58         damheight = parameters['damheight']
59         cellsize = parameters['cellsize']
60         min_energy = parameters['min_energy']
61
62         #make a list of sample location code
63         list1 = open(fn_gc_txt, 'r').readlines()
64         list2 = []
65         for n in range(len(list1)):
66             a = list1[n].split()[2].strip()
67             list2.append(float(a))
68         max_code = np.min(list2)
69         sample = np.linspace(1, max_code, max_code)
70
71         code_storage = open(fn_sample_code, 'w')
72         code_storage.write('channel_code_DG_volume_elev_DG_energy_power' + '\n')
73         code_storage_notokay = open(fn_sample_code_notokay, 'w')
74
75         for i in range(len(sample)):
76             #build a raster layer that represent the same channel code and store the
                data into a txt file
77             channel_code = int(sample[i])
78             fn_spatial = 'temp_chan_spatial_' + parameters['regional'] + '.map'
79             alg_params = {'INPUT':channel_code, 'INPUT1':1, 'INPUT2':fn_gc, 'OUTPUT':
                fn_spatial}
80             outputs['spatial'] = processing.run("pcraster:spatial", alg_params)

```



```

81     fn_channel_class_map = "channel_class_" + parameters['regional'] + ".map"
82     alg_params = {'INPUT':fn_spatial,'INPUT1':0,'INPUT2':fn_gc,'OUTPUT':
83         fn_channel_class_map}
84     processing.run("pcraster:comparisonoperators", alg_params)
85
86     fn_chan_shp1 = 'temp_chan1_' + parameters['regional'] + '_' + str(sample[i
87         ]) + '.gpkg'
88     alg_params = {'INPUT':fn_channel_class_map,'BAND':1,'FIELD':'DN','
89         EIGHT_CONNECTEDNESS':True,'EXTRA':'','OUTPUT':fn_chan_shp1}
90     outputs['Polygonize1'] = processing.run("gdal:polygonize", alg_params)
91
92     fn_chan_shp2 = 'temp_chan2_' + parameters['regional'] + '_' + str(sample[i
93         ]) + '.gpkg'
94     alg_params = {'EXPRESSION': f'DN={1}','INPUT': fn_chan_shp1,'OUTPUT':
95         fn_chan_shp2}
96     outputs['ExtractByExpression1'] = processing.run('native:
97         extractbyexpression', alg_params)
98
99     channel_layer = QgsVectorLayer(fn_chan_shp2, '', 'ogr')
100     ext = str(channel_layer.extent())
101     x1 = float(ext.split(' ')[1])
102     y1 = float(ext.split(' ')[2].split(',')[0])
103     x2 = float(ext.split(' ')[3])
104     y2 = float(ext.split(' ')[4].split('>')[0])
105     x1_new = x1 - 0.03
106     x2_new = x2 + 0.03
107     y1_new = y1 - 0.03
108     y2_new = y2 + 0.03
109     new_extent = str(x1_new) + "," + str(x2_new) + "," + str(y1_new) + "," +
110         str(y2_new) + "[EPSG:4326]"
111     QgsProject.instance().removeMapLayers([channel_layer.id()])
112     QgsProject.instance().removeMapLayers([channel_layer.id()])
113     channel_layer = None
114
115     fn_study_area_clipped = "study_area_clipped_" + parameters['regional'] + ".
116         map"
117     alg_params = {'INPUT':fn_map,'PROJWIN':new_extent,'OVERCRS':False,'NODATA'
118         :'-999999999.000000','OPTIONS':'','DATA_TYPE':0,'EXTRA':'','OUTPUT':
119         fn_study_area_clipped}
120     outputs['clipstudyarea'] = processing.run("gdal:cliprasterbyextent",
121         alg_params)
122
123     fn_channel_class_map_clipped = "channel_class_clipped_" + parameters['
124         regional'] + ".map"
125     alg_params = {'INPUT':fn_channel_class_map,'PROJWIN':new_extent,'OVERCRS':
126         False,'NODATA':-999999999.000000,'OPTIONS':'','DATA_TYPE':0,'EXTRA':'',
127         'OUTPUT':fn_channel_class_map_clipped}
128     outputs['clipchannel'] = processing.run("gdal:cliprasterbyextent",
129         alg_params)
130
131     fn_ldd_clipped = "ldd_clipped_" + parameters['regional'] + ".map"
132     alg_params = {'INPUT':fn_ldd,'PROJWIN':new_extent,'OVERCRS':False,'NODATA'
133         :'-999999999.000000','OPTIONS':'','DATA_TYPE':0,'EXTRA':'','OUTPUT':
134         fn_ldd_clipped}
135     outputs['clipldd'] = processing.run("gdal:cliprasterbyextent", alg_params)
136
137     channel_map_clipped = readmap(fn_channel_class_map_clipped)

```

```

121     study_area_map_clipped = readmap(fn_study_area_clipped)
122     group_name = 'class_map_' + parameters['regional'] + '.map'
123     outputs['ifthen'] = processing.run("pcraster:ifthen", {'INPUT':
        fn_channel_class_map_clipped, 'INPUT1':fn_study_area_clipped, 'OUTPUT':
        group_name})
124
125     group_text = 'class_' + parameters['regional'] + '.txt'
126     alg = 'map2col_' + group_name + '_' + group_text
127     os.system(alg)
128
129     #define the outlet coordinate of the channel
130     attribute = open(group_text, 'r').readlines()
131     elev = []
132     for n in range(len(attribute)):
133         el = attribute[n].split()[2].strip()
134         elev.append(float(el))
135     index = elev.index(np.min(elev))
136
137     gully_outlet_point = attribute[index]
138     x_outlet = gully_outlet_point.split()[0].strip()
139     y_outlet = gully_outlet_point.split()[1].strip()
140     elev_outlet = gully_outlet_point.split()[2].strip()
141     elev_float = float(elev_outlet)
142     list = str(x_outlet) + "_" + str(y_outlet) + "_" + str(1) + "\n"
143     outlet = open(fn_outlet, 'w')
144     outlet.write(list)
145     outlet.close()
146     outlet = open(fn_outlet, 'w')
147     outlet.write(list)
148     outlet.close()
149
150     #run the "catchment" feature from PCRaster to deliniate the catchment of
        the channel
151     alg = 'col2map_N_' + fn_outlet + '_' + fn_outlet_map + '_--clone_' +
        fn_ldd_clipped
152     os.system(alg)
153     alg_params = {'INPUT':fn_outlet_map, 'BAND':1, 'FIELD':'DN', '
        EIGHT_CONNECTEDNESS':False, 'EXTRA':'', 'OUTPUT':fn_outlet_shp}
154     outputs['polygonizeoutlet'] = processing.run("gdal:polygonize", alg_params)
155     outlet_coord = readmap(fn_outlet_map)
156     gullycatchment = catchment(fn_ldd_clipped, outlet_coord)
157     fn_catchment = 'gully_catchment_' + parameters['regional'] + ".map"
158     report(gullycatchment, fn_catchment)
159
160     #crop the DEM by the catcment
161     catchment1 = readmap(fn_catchment)
162     catch = catchment1 == 1
163     topo = ifthen(catch, study_area_map_clipped)
164     report(topo, 'temp_topo')
165
166     #crop the previous DEM with elevation more than elevation on the outlet +
        dam height
167     y = elev_float + damheight
168     cal_map = topo < y
169     is_cal_map = cal_map == 1
170     topo_cal_map = ifthen(is_cal_map, topo)
171     report(topo_cal_map, 'temp_topocal')

```

```

172
173     #make a map file of inundation
174     h = y - topo_cal_map
175     volume_cell = h * (cellsize**2)
176     report(volume_cell, fn_inundation_map)
177     alg = 'map2col' + fn_inundation_map + '_' + fn_inundation_txt
178     os.system(alg)
179
180     #calculate volume and energy in the storage (calculation is done per cell)
181     vol_lines = open(fn_inundation_txt, 'r').readlines()
182     vol_lines_sum = 0
183     for n in vol_lines:
184         if n.strip():
185             vol = n.split()[-1].strip()
186             vol_lines_sum += float(vol)
187     y_energy = elev_float + (damheight/2)
188     energy = (vol_lines_sum * y_energy * 9.81 * 1000 * 0.8) / (3600 * 1000000)
189     energy_float = float(energy)
190     list = str(channel_code) + '_' + str(x_outlet) + '_' + str(y_outlet) + '_'
191           + str(elev_float) + '_' + str(vol_lines_sum) + '_' + str(energy_float)
192           + '\n'
193     energy_save = open(fn_energy, 'w')
194     energy_save.write(list)
195     energy_save.close
196     energy_save = open(fn_energy, 'w')
197     energy_save.write(list)
198     energy_save.close
199
200     #create shp file(s) that represent the inundation, complete with the volume
201     and energy storage
202     read_energy = open(fn_energy, 'r').readlines()
203     if float(read_energy[0].split()[-1].strip()) >= min_energy:
204         DG_volume = float(read_energy[0].split()[4].strip())
205         DG_energy = float(read_energy[0].split()[5].strip())
206         water = readmap(fn_inundation_map)
207         inundation = water > 0
208         report(inundation, fn_inundation_true_map)
209
210     #calculate average discharge
211     discharge = DG_volume / 3600 / parameters['duration']
212
213     #make new shp files representing the gullies
214     fn_inundation_shp = 'DG_' + parameters['regional'] + '_' + str(
215         channel_code) + '.shp'
216     fn_inundation_temp1 = 'temp_DG1.shp'
217     fn_inundation_temp2 = 'temp_DG2.shp'
218
219     alg1 = {
220         'INPUT':fn_inundation_true_map,
221         'BAND':1,
222         'FIELD':'DN',
223         'EIGHT_CONNECTEDNESS':True,
224         'EXTRA':'',
225         'OUTPUT':fn_inundation_temp2}
226     outputs['inundation_temp'] = processing.run("gdal:polygonize", alg1)
227
228     #fix geometry

```

```

225     alg_fix = {
226         'INPUT':fn_inundation_temp2,
227         'METHOD':1,
228         'OUTPUT':fn_inundation_temp1}
229
230     outputs['inundation_temp1'] = processing.run("native:fixgeometries",
231         alg_fix)
232
233     #calculate shortest distance from coastline
234     fn_line = 'shortline_' + parameters['regional'] + '_' + str(
235         channel_code) + '.shp'
236     alg_line = {
237         'SOURCE':fn_outlet_shp,
238         'DESTINATION':parameters['input_coastline'],
239         'METHOD':0,
240         'NEIGHBORS':1,
241         'DISTANCE':None,
242         'OUTPUT':fn_line}
243     outputs['short_line'] = processing.run("native:shortestline", alg_line)
244
245     short_line = QgsVectorLayer(fn_line, '', 'ogr')
246     feat = short_line.getFeature(0)
247     distance_coastline = float(feat['distance']) * 111139 #convert from
248         degree to meters
249     slope = elev_float / distance_coastline #calculating slope
250     power = energy_float / parameters['duration'] #calculating power
251
252     #add attribute (DG code, volume, energy)
253     alg2 = {
254         'INPUT':fn_inundation_temp1,
255         'FIELD_NAME':'DG_Code',
256         'FIELD_TYPE':0,
257         'FIELD_LENGTH':4,
258         'FIELD_PRECISION':0,
259         'OUTPUT':fn_inundation_temp2}
260     outputs['inundation_temp2'] = processing.run("native:
261         addfieldtoattributetable", alg2)
262
263     alg3 = {
264         'INPUT':fn_inundation_temp2,
265         'FIELD_NAME':'Volume_m3',
266         'FIELD_TYPE':1,
267         'FIELD_LENGTH':10,
268         'FIELD_PRECISION':5,
269         'OUTPUT':fn_inundation_temp1}
270     outputs['inundation_temp3'] = processing.run("native:
271         addfieldtoattributetable", alg3)
272
273     alg3 = {
274         'INPUT':fn_inundation_temp1,
275         'FIELD_NAME':'Area_m2',
276         'FIELD_TYPE':1,
277         'FIELD_LENGTH':10,
278         'FIELD_PRECISION':5,
279         'OUTPUT':fn_inundation_temp2}
280     outputs['inundation_temp3'] = processing.run("native:
281         addfieldtoattributetable", alg3)

```

```

276
277     alg4 = {
278         'INPUT':fn_inundation_temp2,
279         'FIELD_NAME': 'Disc_m3/s',
280         'FIELD_TYPE':1,
281         'FIELD_LENGTH':10,
282         'FIELD_PRECISION':5,
283         'OUTPUT':fn_inundation_temp1}
284     outputs['inundation_temp3'] = processing.run("native:
        addfieldtoattributetable", alg4)
285
286     alg5 = {
287         'INPUT':fn_inundation_temp1,
288         'FIELD_NAME': 'Energy_MWh',
289         'FIELD_TYPE':1,
290         'FIELD_LENGTH':10,
291         'FIELD_PRECISION':5,
292         'OUTPUT':fn_inundation_temp2}
293     outputs['inundation_temp4'] = processing.run("native:
        addfieldtoattributetable", alg5)
294
295     alg6 = {
296         'INPUT':fn_inundation_temp2,
297         'FIELD_NAME': 'x_outlet',
298         'FIELD_TYPE':1,
299         'FIELD_LENGTH':10,
300         'FIELD_PRECISION':5,
301         'OUTPUT':fn_inundation_temp1}
302     outputs['inundation_temp5'] = processing.run("native:
        addfieldtoattributetable", alg6)
303
304     alg7 = {
305         'INPUT':fn_inundation_temp1,
306         'FIELD_NAME': 'y_outlet',
307         'FIELD_TYPE':1,
308         'FIELD_LENGTH':10,
309         'FIELD_PRECISION':5,
310         'OUTPUT':fn_inundation_temp2}
311     outputs['inundation_temp5'] = processing.run("native:
        addfieldtoattributetable", alg7)
312
313     alg8 = {
314         'INPUT':fn_inundation_temp2,
315         'FIELD_NAME': 'Elevation',
316         'FIELD_TYPE':1,
317         'FIELD_LENGTH':10,
318         'FIELD_PRECISION':5,
319         'OUTPUT':fn_inundation_temp1}
320     outputs['inundation_temp5'] = processing.run("native:
        addfieldtoattributetable", alg8)
321
322     alg9 = {
323         'INPUT':fn_inundation_temp1,
324         'FIELD_NAME': 'Dist_m',
325         'FIELD_TYPE':1,
326         'FIELD_LENGTH':10,
327         'FIELD_PRECISION':5,

```

```

328         'OUTPUT':fn_inundation_temp2}
329     outputs['inundation_temp6'] = processing.run("native:
330         addfieldtoattributetable", alg9)
331
332     alg10 = {
333         'INPUT':fn_inundation_temp2,
334         'FIELD_NAME': 'Slope',
335         'FIELD_TYPE':1,
336         'FIELD_LENGTH':10,
337         'FIELD_PRECISION':5,
338         'OUTPUT':fn_inundation_temp1}
339     outputs['inundation_temp7'] = processing.run("native:
340         addfieldtoattributetable", alg10)
341
342     alg11 = {
343         'INPUT':fn_inundation_temp1,
344         'FIELD_NAME': 'Loss',
345         'FIELD_TYPE':1,
346         'FIELD_LENGTH':10,
347         'FIELD_PRECISION':5,
348         'OUTPUT':fn_inundation_temp2}
349     outputs['inundation_temp8'] = processing.run("native:
350         addfieldtoattributetable", alg11)
351
352     alg12 = {
353         'INPUT':fn_inundation_temp2,
354         'FIELD_NAME': 'Eff_Energy',
355         'FIELD_TYPE':1,
356         'FIELD_LENGTH':10,
357         'FIELD_PRECISION':5,
358         'OUTPUT':fn_inundation_temp1}
359     outputs['inundation_temp9'] = processing.run("native:
360         addfieldtoattributetable", alg12)
361
362     alg13 = {
363         'INPUT':fn_inundation_temp1,
364         'FIELD_NAME': 'Power_MW',
365         'FIELD_TYPE':1,
366         'FIELD_LENGTH':10,
367         'FIELD_PRECISION':5,
368         'OUTPUT':fn_inundation_temp2}
369     outputs['inundation_shp'] = processing.run("native:
370         addfieldtoattributetable", alg13)
371
372     alg14 = {
373         'INPUT':fn_inundation_temp2,
374         'FIELD_NAME': 'Grid_dist',
375         'FIELD_TYPE':1,
376         'FIELD_LENGTH':10,
377         'FIELD_PRECISION':5,
378         'OUTPUT':fn_inundation_temp1}
379     outputs['inundation_shp'] = processing.run("native:
380         addfieldtoattributetable", alg14)
381
382     #calculate area
383     alg15 = {
384         'INPUT':fn_inundation_temp1,

```

```

379         'FIELD_NAME': 'Area_m2',
380         'FIELD_TYPE': 0,
381         'FIELD_LENGTH': 10,
382         'FIELD_PRECISION': 5,
383         'FORMULA': '□$area□',
384         'OUTPUT': fn_inundation_shp}
385     processing.run("native:fieldcalculator", alg15)
386
387     #store data for volume, energy, coordinate for outlet, minimum elevation
    and distance from coastline into shp field
388     layer = QgsVectorLayer(fn_inundation_shp, '', 'ogr')
389     prov = layer.dataProvider()
390     DG_code = layer.fields().lookupField('DG_Code')
391     vol = layer.fields().lookupField('Volume_m3')
392     disch = layer.fields().lookupField('Disc_m3/s')
393     en = layer.fields().lookupField('Energy_MWh')
394     xc = layer.fields().lookupField('x_outlet')
395     yc = layer.fields().lookupField('y_outlet')
396     min_elev = layer.fields().lookupField('Elevation')
397     distance = layer.fields().lookupField('Dist_m')
398     slope_att = layer.fields().lookupField('Slope')
399     power_att = layer.fields().lookupField('Power_MW')
400     atts = {DG_code: channel_code,
401            vol: DG_volume,
402            disch: discharge,
403            en: DG_energy,
404            xc: x_outlet,
405            yc: y_outlet,
406            min_elev: elev_float,
407            distance: distance_coastline,
408            slope_att: slope,
409            power_att: power}
410     feat = layer.getFeature(1)
411     prov.changeAttributeValues({feat.id(): atts})
412
413     DG_data = str(channel_code) + '□' + str(DG_volume) + '□' + str(
        elev_float) + '□' + str(DG_energy) + '□' + str(power) + '\n'
414     code_storage.write(DG_data) #save the gully code
415
416     os.remove(fn_inundation_temp1)
417     os.remove(fn_inundation_temp2)
418
419     else:
420         code_storage_notokay.write(str(channel_code) + '\n')
421
422     os.remove(fn_outlet_shp)
423     os.remove(fn_chan_shp1)
424     os.remove(fn_chan_shp2)
425
426     return results
427
428     def name(self):
429         return '02_mainprocessing'
430
431     def displayName(self):
432         return '02_mainprocessing'
433

```

```
434     def group(self):  
435         return ''  
436  
437     def groupId(self):  
438         return ''  
439  
440     def createInstance(self):  
441         return Model()
```